Universidad Autónoma de Madrid

Departamento de Bioquímica – Facultad de Medicina

Programa de Doctorado en Biociencias Moleculares

MEMORIA DE TESIS DOCTORAL

LXR transcription factors in the specialization of tissue resident macrophages and their role in iron homeostasis

Marta Celorio Orizaola

Madrid, 2019

Universidad Autónoma de Madrid

Departamento de Bioquímica

Facultad de Medicina

Instituto de Investigaciones Biomédicas "Alberto Sols"

CSIC / UAM

LXR transcription factors in the specialization of tissue resident macrophages and their role in iron homeostasis

Memoria de tesis para optar al grado de Doctor dentro del Programa Oficial de Posgrado en Biociencias Moleculares, presentada por la Graduada en Biología:

Marta Celorio Orizaola

Directores de tesis:

Dr. Antonio Castrillo Viguera

Dra. Susana Alemany de la Peña

Instituto de Investigaciones Biomédicas "Alberto Sols"

CSIC / UAM

El trabajo recogido en la presente Tesis Doctoral ha sido realizado en el marco de los Proyectos de Investigación a SAF2014-56819-R y SAF2017-83289-R financiados por el Ministerio de Economía, Industria y Competitividad con la ayuda de una beca-contrato de formación de personal investigador (FPI) BES-2015-075339.

You can't always get what you want,
but if you try, sometimes, you might just find
you get what you need.

The Rolling Stones

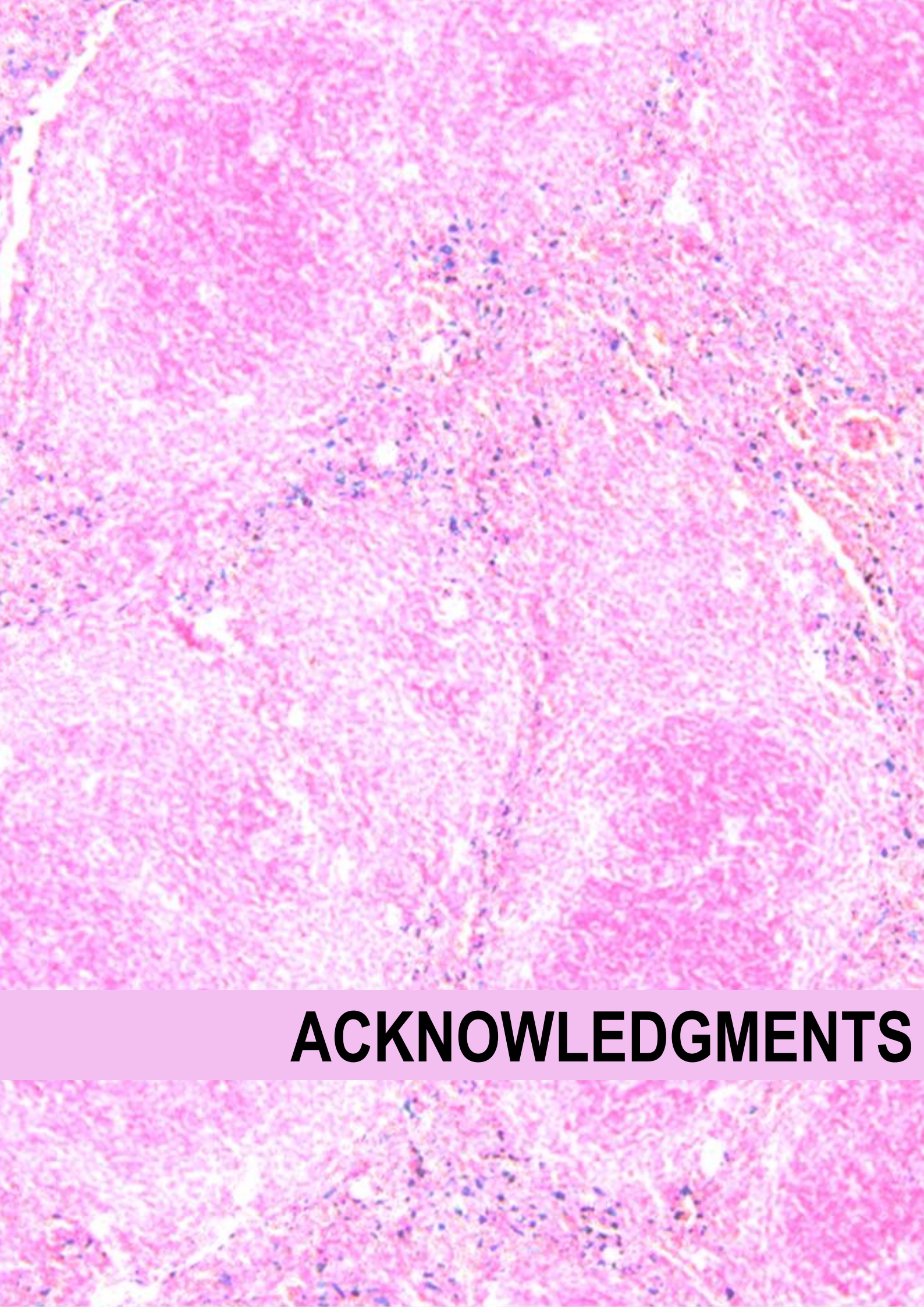

ACKNOWLEDGMENTS

Lo que no te cuentan cuando te matriculas el primer año de tesis es que, en proporción, de ciencia es de lo que menos vas a aprender. Tú, inquieto manojo de nervios, llegas el primer día al laboratorio pensando que si no sabes hacer bien un Western, si en tu vida has hecho una PCR o si nunca has compensado la fluorescencia de un citómetro, estás perdido. Pero no pasa nada, porque en seguida te das cuenta de que incluso el saber hacer las cosas, no significa que te vayan a salir bien. En la repetición está el éxito, pero también hay que tener un poco de suerte. Y paciencia.

Hace cuatro años, cuando llegué al B-15 a empezar mi tesis con todos los nervios que mencionaba antes, una compañera me dijo: 'relájate y disfrútalo, porque tu tesis no va a ser ni la mejor ni la peor. Sólo va a ser una tesis'. Acto seguido, como no me vio muy convencida (todavía no me conocía y no sabía lo neurótica que puedo llegar a ser), añadió: 'para hacer una buena tesis, lo más importante es tener un buen director. Si tienes un buen director, tienes la mitad de la tesis hecha'. Tenía mucha razón, por supuesto. A falta de un buen director, yo he tenido dos: Antonio y Susana, mil millones de gracias por todo. Por la oportunidad de aprender de vosotros, y con vosotros. A Antonio por hacerme un hueco en este proyecto tan increíble, y a Susana por hacérmelo en el laboratorio. Huelga decir que todo lo que haga a partir de ahora será gracias a esta oportunidad. Esto ha sido trabajo duro, pero con vosotros se ha hecho más fácil. Nos ha quedado una tesis bastante decente.

Tan importante es tener buenos directores como buenos compañeros. La ciencia, la buena ciencia, es una vocación, pero aún así las horas se hacen muy largas, y la buena compañía aligera la carga. Así que por todos los que están ahora y por los que estuvieron en algún momento, ahí va:

A esa compañera tan sabia (que ahora es un poquito más sabia que antes, porque ya es mamá), que sabe que a veces necesito un tirón de orejas que me espabile, porque si no se me van los dramas de las manos; y a mi compañero de piques, de bromas, de risas y quejas, de marrones compartidos y de partidos de pádel… Ángela y Diego, gracias por la paciencia infinita, y por bajarme los pies a la tierra y llamarme 'exagerada' en los momentos justos. Vaya donde vaya ahora, o vayáis donde vayáis vosotros, espero que sigáis llamándomelo, que me va a seguir haciendo falta. Fijo.

A Ana, que por desgracia llegó un poco tarde y se fue un poco rápido, pero estuvo tiempo suficiente para dejarme sus consejos y su amistad. Gracias por todo. Y siguiendo en orden creciente de numeración de laboratorio, gracias a Rafa, Natalia y Marta; Raúl; Pablo; Martina, Manu y Michela (ya sabes que siempre nos pasan cosas, pero como yo voy por delante, quizás podamos evitar que te pasen a ti las mismas que a mi).

Gracias a Laura Molero por compartir toda su experiencia, que es mucha, y su tiempo, que es poco. Se caería el servicio de Citometría sin ti, y gran parte de esta tesis no habría sido posible. A todo el personal de los servicios de microscopía y animalario, cuyo trabajo diario saca adelante todos los proyectos del centro.

A mi amiga Cris, por su apoyo incondicional y su franqueza. Estás a 600 kilómetros, pero siempre a mi lado. A Lucía, que me conoce tan bien y me lleva aguantando tanto tiempo, que es como si fuéramos familia. A Laura, por los reencuentros inesperados, y las amistades que sobreviven al paso de los años. A mis dos pollitos, Patri y Pei, que tanto echo de menos. Y a toda la familia UBAL. Por muchos más años de baloncesto juntos, aunque estemos tan separados.

A Guille, por cargar con todo el peso de mis nervios y mis agobios, y aprender a compaginarlos con los suyos. Porque tus primeras palabras son siempre 'qué necesitas, cómo te ayudo'. Por acompañarme en este viaje tan duro, y que nos ha traído hasta aquí, y por poder contar contigo para el siguiente.

En los agradecimientos de las tesis siempre se menciona lo último a la familia. Quizás es porque, en cualquier mensaje o comunicación, el último argumento es siempre el que más peso lleva. A mis hermanos, Ángela y Miguel, porque contra viento y marea siempre están ahí. A mi madre Elsa, porque no estaría donde estoy sin ella. Eres mi referente de mujer fuerte e independiente. Y a mis abuelos, Juan José y Elsa. Sois la abnegación y el cariño personificados y el respaldo de todos nosotros, y por ello, os dedico esta tesis. Gracias a todos. Os quiero.

A mis abuelos

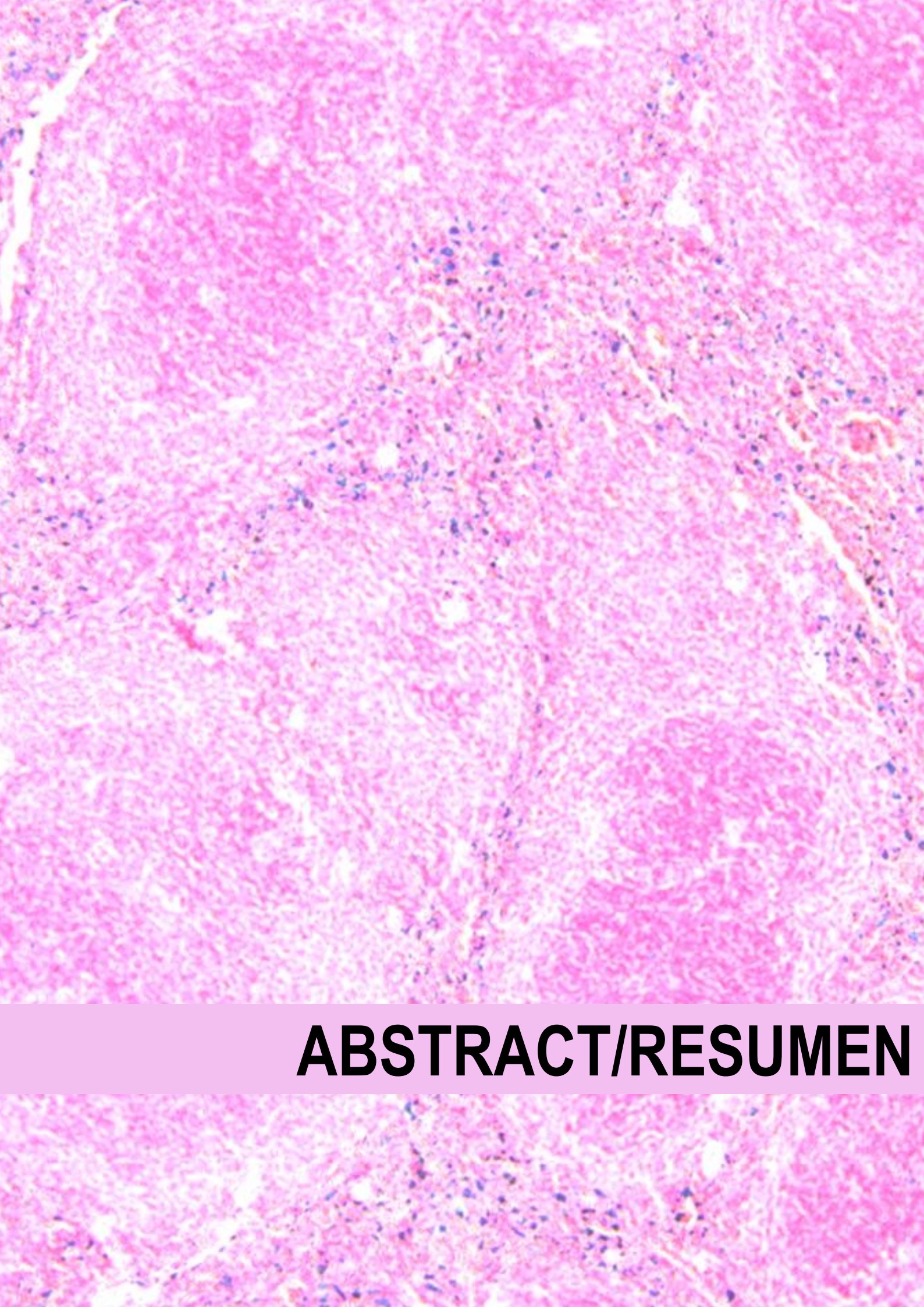

ABSTRACT/RESUMEN

Abstract/Resumen

The liver X receptors (LXRα and LXRβ) are members of the nuclear receptor superfamily of transcription factors. In macrophages, LXRs play essential roles in the coordination of both metabolic and immune responses, such as the transcriptional control of lipid metabolism or the modulation of innate and adaptive immune responses. Tissue resident macrophages are professional phagocytes that orchestrate innate immune responses, but also participate in the maintenance of tissue homeostasis by regulating different metabolic processes. Consequently, they acquire considerable genetic and phenotypic diversity at different anatomical locations. In the spleen, there are four different macrophage subpopulations, including white and red pulp macrophages (**WPM** and **RPM**), marginal metallophilic macrophages (**MMM**) and marginal zone macrophages (**MZM**), and all of them play specific roles in homeostasis and disease. Red pulp macrophages (**RPMs**, identified as $CD45^{+}CD11b^{lo}F4/80^{hi}VCAM^{hi}$ by flow cytometry) are specialized cells, important for the maintenance of iron homeostasis. They actively phagocytose injured and senescent red blood cells (**RBCs**), thus being critical for the recycling of hemoglobin iron. The iron recycled by these macrophages contributes to meet the iron requirements of the whole organism, like the generation of new erythrocytes in the bone marrow or the correct functioning of several enzymes in the cells. Previous reports established that LXRα is crucial for the differentiation of both splenic marginal zone macrophages. Here we now show the importance of this nuclear receptor in the correct development of the red pulp compartment of the spleen.

LXR-null mice present a markedly reduced RPM population, despite elevated proportion of resident monocytes, and transcriptional profiling of isolated RPMs showed that these mice presented defective expression of many genes associated with the identity of RPMs, including CD163, the hemoglobin scavenger receptor. Further flow cytometry analysis revealed the existence of two resident macrophage subpopulations within the red pulp of the spleen, defined by their expression of CD163 receptor. Strikingly, the cell reduction observed in the RPM compartment of LXR-deficient mice corresponded with the absence of the $CD163^{+}$ RPM subset. Presumably as a result of these alterations, iron handling is impaired in LXR-deficient mice, that accumulate RBCs and excessive iron in the splenic red pulp. Additionally, these mice presented a similar defect in the bone marrow resident macrophage population (**BMMs**), with a concomitant monocyte accumulation. Studies using $LXR\alpha^{-/-}$ and LXRα-GFP mouse models revealed that the absence of LXRα, and not LXRβ, was the cause for the RPM and BMM deficiency and the malfunctioning of the iron machinery in the spleen of these mice. These results indicate a novel role for LXRα in the regulation of iron homeostasis, possibly in part through the generation of an appropriate splenic RPM compartment.

Abstract/Resumen

Los receptores X hepáticos (LXRα y LXRβ) son factores de transcripción, miembros de la familia de los receptores nucleares. En los macrófagos, estos receptores juegan papeles esenciales en la coordinación de procesos metabólicos como la regulación transcripcional del metabolismo lipídico, o inmunes, como la modulación de las respuestas inmunes innatas y adaptativas. Los macrófagos residentes en los tejidos, además de controlar estas respuestas inmunes mediante su extraordinaria capacidad de fagocitar y procesar agentes extraños, participan en el mantenimiento de la homeostasis de los tejidos que habitan, regulando diferentes procesos metabólicos. En consecuencia, adquieren una marcada diversidad tanto genética como fenotípica para adaptarse a diferentes localizaciones anatómicas. En el bazo hay descritas cuatro poblaciones diferentes de macrófagos tisulares, incluyendo los macrófagos de las pulpas blanca (**WPM**, *white pulp macrophages*) y roja (**RPM**, *red pulp macrophages*), y los macrófagos de la zona marginal (**MMM**, *marginal metallophilic macrophages*; **MZM**, *marginal zone macrophages*), con funciones muy específicas tanto en la homeostasis como durante el desarrollo de enfermedades. Los RPM (caracterizados por citometría de flujo como $CD45^{+}CD11b^{lo}F4/80^{hi}VCAM^{hi}$) son células altamente especializadas, importantes en el mantenimiento de la homeostasis del hierro. Fagocitan activamente eritrocitos (**RBC**, *red blood cells*) dañados o envejecidos, siendo de esta forma imprescindibles para el reciclaje del hierro de la hemoglobina. El hierro reciclado por los macrófagos tisulares contribuye de manera importante a las necesidades de hierro generales del organismo, que son esenciales para la generación de nuevos eritrocitos en la medula ósea o para el funcionamiento de muchas enzimas de la célula. Estudios previos establecieron a LXRα como un factor de transcripción crucial en la formación de la zona marginal del bazo y la correcta diferenciación de sus dos subpoblaciones de macrófagos. En esta tesis, mostramos la importancia de este factor de transcripción en el correcto desarrollo de los macrófagos de la pulpa roja del bazo.

Los ratones deficientes en LXR presentan una población de macrófagos muy reducida en la pulpa roja, pero un elevado número de monocitos, y el análisis del perfil transcripcional de estos macrófagos aislados reveló la existencia de defectos en la expresión de varios genes importantes para la identidad de los RPM, como el receptor de la hemoglobina, CD163. Los análisis de citometría de flujo revelaron la existencia de dos subpoblaciones de macrófagos dentro de la pulpa roja del bazo de ratones de genotipo salvaje, muy bien diferenciados por la expresión o ausencia de CD163. Sorprendentemente, la reducción del número de RPM que observado en ratones deficientes en LXR se correlaciona con el número de macrófagos $CD163^{+}$ en el bazo de ratones WT control. Presumiblemente debido a este defecto, los ratones deficientes en LXR presentan fallos en el manejo y reciclaje del hierro en el bazo, y acumulan eritrocitos en la pulpa roja. Además, este defecto es también visible en la población de macrófagos residentes de la médula ósea de estos ratones (**BMM**, *bone marrow macrophages*), que también presentan un incremento en la población de monocitos medulares. Estudios realizados en ratones deficientes en LXRα, y en el modelo de ratón LXRα-GFP (con fluorescencia verde intrínseca en lugar de expresión de LXRα) revelaron que la ausencia de LXRα, y no de LXRβ, era la principal causante de los defectos en las poblaciones de RPM y BMM, así como del mal funcionamiento de la maquinaria de reciclaje de hierro en el bazo. Nuestros resultados indican un nuevo papel para LXRα en la regulación de la homeostasis del hierro, posiblemente mediante la generación apropiada de la población de macrófagos residentes de la pulpa roja.

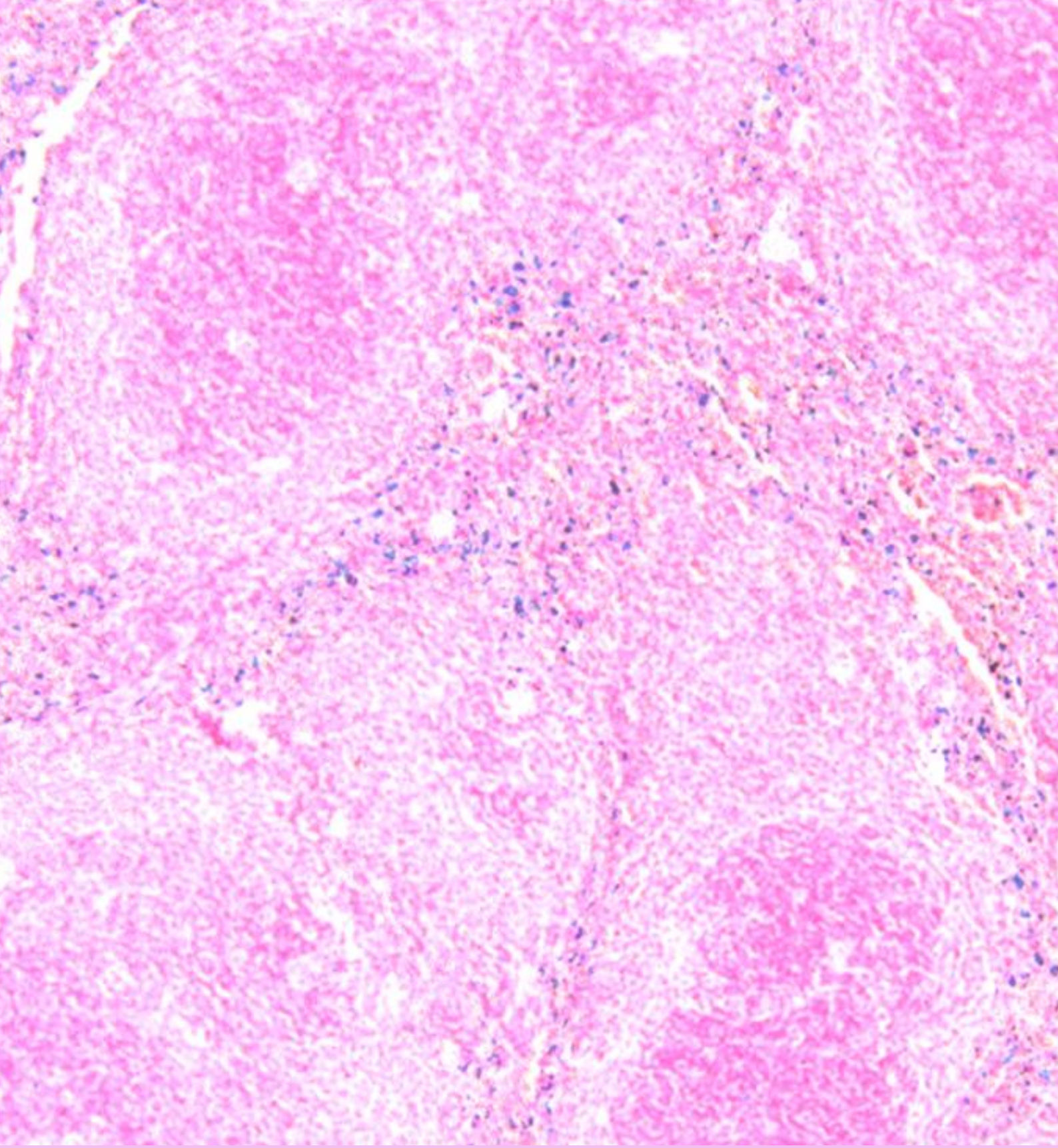

INDEX

Index

Abbreviation key……25

Introduction ……31

1. **The Macrophage**……33
   1.1. Macrophages in the immune system……33
      1.1.1. Macrophages and tolerance: apoptotic clearance……34
   1.2. Tissue resident macrophages……35
      1.2.1. Development of tissue resident macrophages……35
      1.2.2. From embryonic progenitor to tissue resident macrophage: who if whom?……37
      1.2.3. Tissue macrophage transcriptional program……38
   1.3. Spleen development and splenic tissue macrophages……39
      1.3.1. Splenic compartmentalization……39
   1.4. Red pulp macrophages in iron metabolism……40
      1.4.1. Elimination of unwanted red blood cells……41
      1.4.2. Iron recycling……41
      1.4.3. Regulation of iron metabolism……43
      1.4.4. Iron and inflammation……44
   1.5. Bone marrow and splenic resident macrophages in erythropoiesis……44
      1.5.1. Functions of the central 'nursing' macrophage……45
      1.5.2. Erythropoiesis regulation……47
   1.6. Red pulp macrophages in extramedullary erythropoiesis……47

2. **Liver X Receptors**……48
   2.1. Nuclear receptor superfamily……48
   2.2. Liver X Receptors……49
   2.3. LXRs in lipid metabolism……50

3. **LXRs in macrophages**……51
   3.1. LXR in atherosclerosis……51
   3.2. LXR in immunity and inflammation……51
   3.3. LXR in apoptotis……52
   3.4. LXRα in splenic macrophages……52

Objectives……53

Materials and Methods……57

Animals……59
Flow Cytometry……59
Cell Sorting……60
Transcriptional profiling and biological pathway analysis……60
Real time quantitative PCR analysis……61
Immunofluorescence analysis……61
Citospin and tissue iron staining……61

Index

Iron (Fe^{2+}) and hemoglobin quantification……..……..61
Statistical analysis……62

Results……...**69**

1. LXRα is highly expressed in macrophages from the marginal zone and red pulp splenic compartment ……..……71
2. LXRs control the frequency of $CD11b^{lo}F4/80^{hi}$ splenic resident macrophages……..…73
3. $LXR\alpha\beta^{-/-}$ mice present iron accumulation in the spleen and deregulation of iron related gene expression……..……..79
4. LXRs are essential for the regulation of red pulp macrophage transcriptional phenotype…..…....83
5. LXRα transcriptional program is required for the correct development of the red pulp macrophage compartment……...……88
6. Study of LXRα deficiency in macrophages *in vivo* CD64CRE;$LXR\alpha^{fl/fl}$ mice……..…..…….93
7. Transcriptional regulation by LXRα determinates the identity of $CD11b^{lo}F4/80^{hi}CD163^{+}TIM4^{+}$ macrophages in the spleen that are critical for iron handling……..……96

Discussion……..…….…… **99**

1. LXRα and LXRβ present differential roles in macrophages……..101
2. The identity of tissue resident macrophages is determined by a combination of origin and microenvironment……..…101
3. LXRs in the context of tissue macrophages differentiation……....…102
4. LXRs and the proper maintenance of the red pulp macrophage compartment in the spleen...…103
5. Loss of LXR alters the red pulp macrophage transcriptome…….....105
6. LXR activity in red pulp macrophages and the implications for iron metabolism…….....105
7. LXRs control the generation of a specific subset of CD163+ resident macrophages ……..……107
8. $CD11b^{lo}F4/80^{hi}CD163^{+}$ red pulp macrophages constitute a subpopulation with iron recycling functions……...……..108
9. Possible implications of LXR deficiency in bone marrow erythropoiesis…….110
   Concluding remarks……..110

Conclusions…….....…..**113**

Bibliography……...……...…….**119**

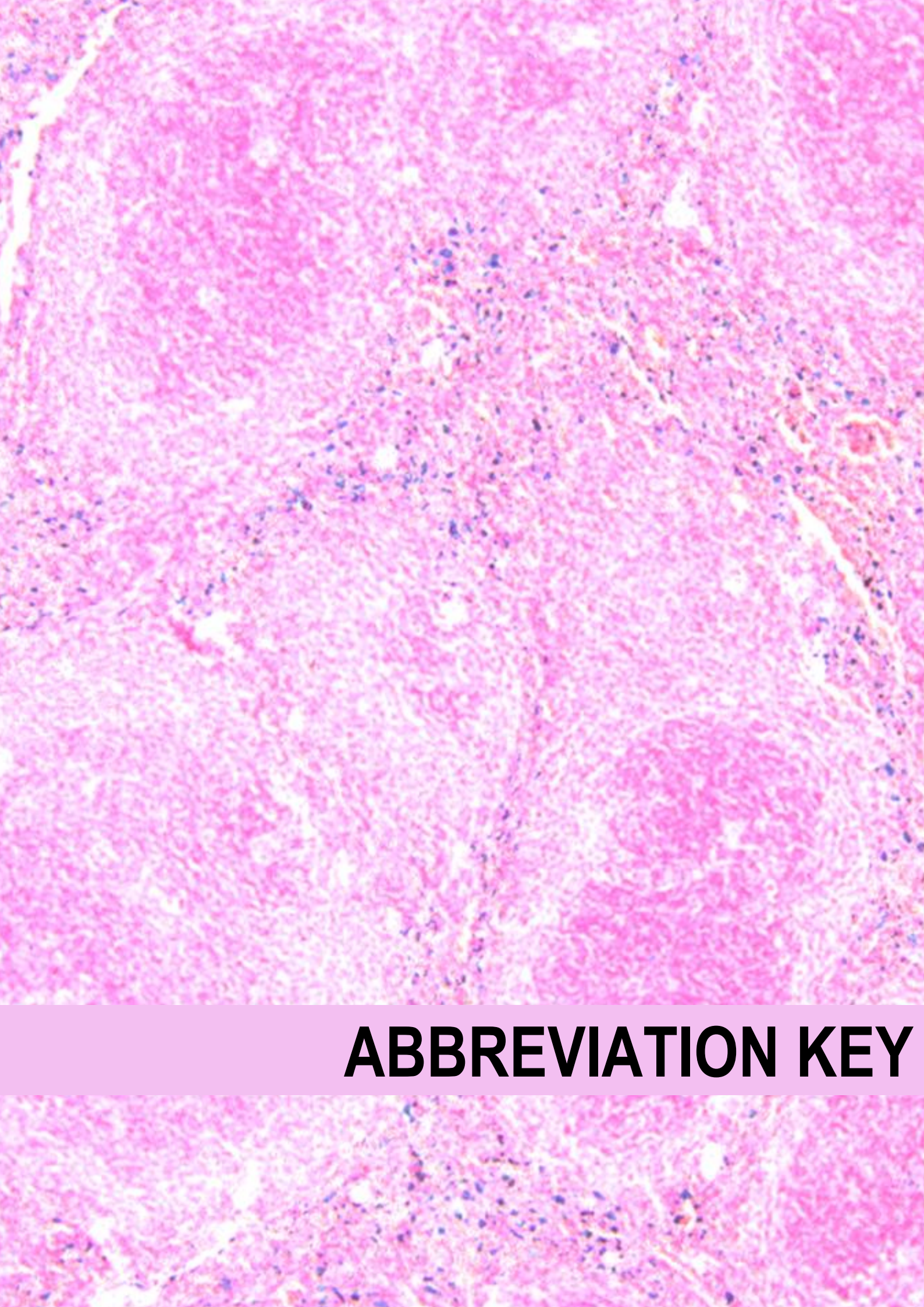

ABBREVIATION KEY

Abbreviation key

Ab Antibody

ABCA1/G1/G5/G8 ATP binding cassette A1/G1/G5/G8

ACC Acetyl CoA carboxylase

Aco1 Aconitase 1

AF-1/2 Activation function 1/2

Ag Antigen

AGM Aorta gonad mesonephros

ALAS (Alas1) 5-Aminolevulinate synthase

AP-1 Activator protein 1

APC Antigen presenting cells

APOC/E Apolipoprotein C/E

ATP Adenin triphosphate

AU Arbitrary unit

BACH-1 BTB and CNC homology 1

Blvra/b Biliverdin reductase A/B

BM Bone marrow

BMDM Bone marrow derived macrophages

BMM Bone marrow macrophage

BR-C Broad-Complex genes

BTB BR-C, TTK and BAB

C1q Complement subcomponent 1q

C2 Complement subcomponent 2

C6 Complement subcomponent 6

CD Cluster of differentiation

cDNA complementary DNA

CFU-e Colony forming unit-erythroid

ChIP-seq Chromatin Immunoprecipitation Sequencing

Clec9a C-type lectin domain, family 9, member A

CNC Segmentation protein cap`n´collar

COX-2 Ciclooxygenase 2

CRE Cre recombinase

CSF-1R Colony stimulating factor 1 receptor

Cx3cr C-X3-C motif chemokine receptor

Cyp7a1 Cytochrome =450, family 7, subfamily A, polypeptide 1

DAMP Damage-associated molecular pattern

DAPI 4´, 6-Diamidino-2-Phenylindole, Dihydrochloride

DBD DNA binding domain

DC Dendritic cell

dL deciliter

DMT-1 Divalent metal transporter 1

DNA Deoxyribonucleic acid

DR Direct repetitions

DsRed Discosoma sp. red fluorescent protein

DT Diphteria toxin

DTR Diphteria toxin receptor

EBI Erythroblastic island

EDTA Ethylene diamine tetra acetate

EGF Epidermal growth factor

EGFP Enhanced GFP

EMH Extramedullary erythropoiesis

EMP Erythromyeloid precursors

EPO Erythropoietin

EPOR Erythropoietin receptor

Ery A Basophilic erythroblast

Ery B Poly erythroblast

Ery C Ortho erythroblast

FACS Fluorescence-activated cell sorting

Fas Fatty acid synthase

FBS Fetal Bovine Serum

FC Functional connectivity

Fcgr1 High affinity immunoglobulin gamma Fc receptor I

FcR Fragment-crystallizable receptor

Fe^{2+} Ferric iron

fl/fl flox/flox

FLVCR1a Feline leukemia virus, subgroup C, cellular receptor 1

FPN-1 Ferroportin 1

FSC Forward Scatter

FTN Ferritin

Fwd Forward primer sequence (5`→3´)

Abbreviation key

FXR Farnesoid X Receptors

g Gram

GATA-1 Guanine, Adenine, Thymine, Adenine 1 (erythroid transcription factor)

Gata6 Guanine, Adenine, Thymine, Adenine 6

G-CSF Granulocyte colony stimulating factor

GFP Green fluorescent protein

GO term Gene ontology term

Hb Hemoglobin

HDL High density lipoprotein

Hebp1 Heme binding protein 1

HFE (Hfe) Hereditary hemochromatosis protein homolog

hHB-EGF Human heparin-binding EGF-like growth factor

Hi High expression

HIF1α/2α Hypoxia-inducible transcription factor 1α/2α

HO-1/2 (Hmox1/2) Heme oxygenase 1/2

Hp Haptoglobin

Hpx Hemopexin

HRE Hormone response element

HRG-1 Heme response gene 1

HSC Hematopoietic stem cell

ICAM-4 Intercellular adhesion molecule 4

Id3 Inhibitor of DNA Binding 3

IDOL Inducible degrader of low-density lipoprotein receptor

IFN-1/β/γ Interferon 1/β/γ

iGFP Inducible Green fluorescent protein

IHC Immunohistochemistry

IL Interleukin

IMMGEN Immunological Genome Project

iNOS Inducible Nitric oxide synthase

IRE Iron responsive element

Ireb2 Iron Responsive Element Binding Protein 2

IRF8 Interferon regulatory factor 8

IRP1/2 Iron regulatory protein 1/2

KC Kupffer Cell

LBD Ligand binding domain

LDL Low density lipoprotein

LDLR Low densitiy lipoprotein receptor

Lo Low expression

LPS Lipopolysaccharide

LRP Low density lipoprotein related protein

LTR Long term reconstitution

LXR Liver X receptor

LysM Lysozyme M

Ly6C Lymphocyte antigen 6 C

MAEA (Emp) Erythroblast macrophage protein

MARCO Macrophage receptor with collagenous structure

MERTK MER Proto-oncogene, tyrosine kinase

MFGE8 Milk fat globule-EGF factor 8 protein

MFI Mean fluorescence intensity

mg miligram

MHC-II Major histocompatibility complex II

mL mililiter

mM milimolar

MMM Marginal metallophilic macrophage

MPS Mononuclear phagocytic system

mRNA Messenger ribonucleic acid

MZ Marginal zone

MZ-B Marginal zone B cell

MZM Marginal zone macrophage

NCOA4 (Ncoa4) Nuclear Receptor Coactivator 4

NCoR Nuclear-receptor Co-Repressor

NF-κB Nuclear factor kappa-light-chain-enhacerof activated B cells

NK Natural killer

NO Nitric oxide

NR Nuclear receptor

Nr1h2/3 Nuclear Receptor Subfamily 1, Group H, Member 2/3

Abbreviation key

NRAMP-1/2 (Nramp1/2) Natural resistance-associated macrophage protein 1/2

OCT Optimal cutting temperature compound

OD Optical density

PAMP Pathogen-associated molecular pattern

PBS Phosphate buffered saline

PCA Principal component analysis

PCR Polymerase chain reaction

PFA Paraformaldehyde

PHZ Phenylhydrazine

PLTP Phospholipid transfer protein

pMAC Macrophage precursor

PPARγ (Pparg) Peroxisome proliferator activated receptor gamma

Pre-RPM Red pulp macrophage precursor

PRR Pathogen recognition receptors

P-Sp Para-aortic splanchnopleura

PtdSer Phosphatidylserine

qRT-PCR Quantitative real time polymerase chain reaction

RBC Red blood cell

RCT Reverse cholesterol transport

Rev Reverse primer sequence (5`→3´)

RNA Ribonucleic acid

ROS Reactive oxygen species

RP Red pulp

RPM Red pulp macrophage

rpm revolutions per minute

RPMI Roswell Park Memorial Institute culture medium

RUNX1/3(Runx1/3) Runt-related transcription factor 1/3

RXR Retinoic acid receptor

SEM Standard error mean

Siglec-1 Sialic acid binding Ig like lectin 1

SIGN-R1 CD209 antigen-like protein B

SIRP1-α (Sirpa) Signal regulatory protein alpha

Slc11a1 Solute carrier 11 a 1

Slc40a1 Solute carrier 40 a 1

Slc48a1 Solute carrier 48 a 1

Slc49a1 Solute carrier 49 a 1

SMRT Silencing mediator of retinoid acid and thyroid-hormone receptors

SRCR Scavenger receptor cysteine-rich

SREBP-1c Sterol regulatory element binding protein

SSC Side Scatter

STAT Signal transducer and activator of transcription

SUMO Small ubiquitin-like modifier

TAM Tyrosine kinase receptor family (Tyro3, Axl, Mer)

TBM Tingible body macrophage

Tf Transferrin

TfR Transferrin receptor

TGFβ Transforming growth factor β

TIM4 (Timd4) T-cell immunoglobulin and mucin domain containing 4

TLR Toll-like receptor

TNFα Tumor necrosis factor α

TRAIL Tumor necrosis factor ligand superfamily member (TNFSF10)

TRM Tissue resident macrophage

TTK Tramtrack genes

U.A. Umbilical artery

µg microgram

µL microliter

V.A. Vitelline artery

VCAM-1 (Vcam1) Vascular cell adhesion molecule 1

WP White pulp

WT Wild type

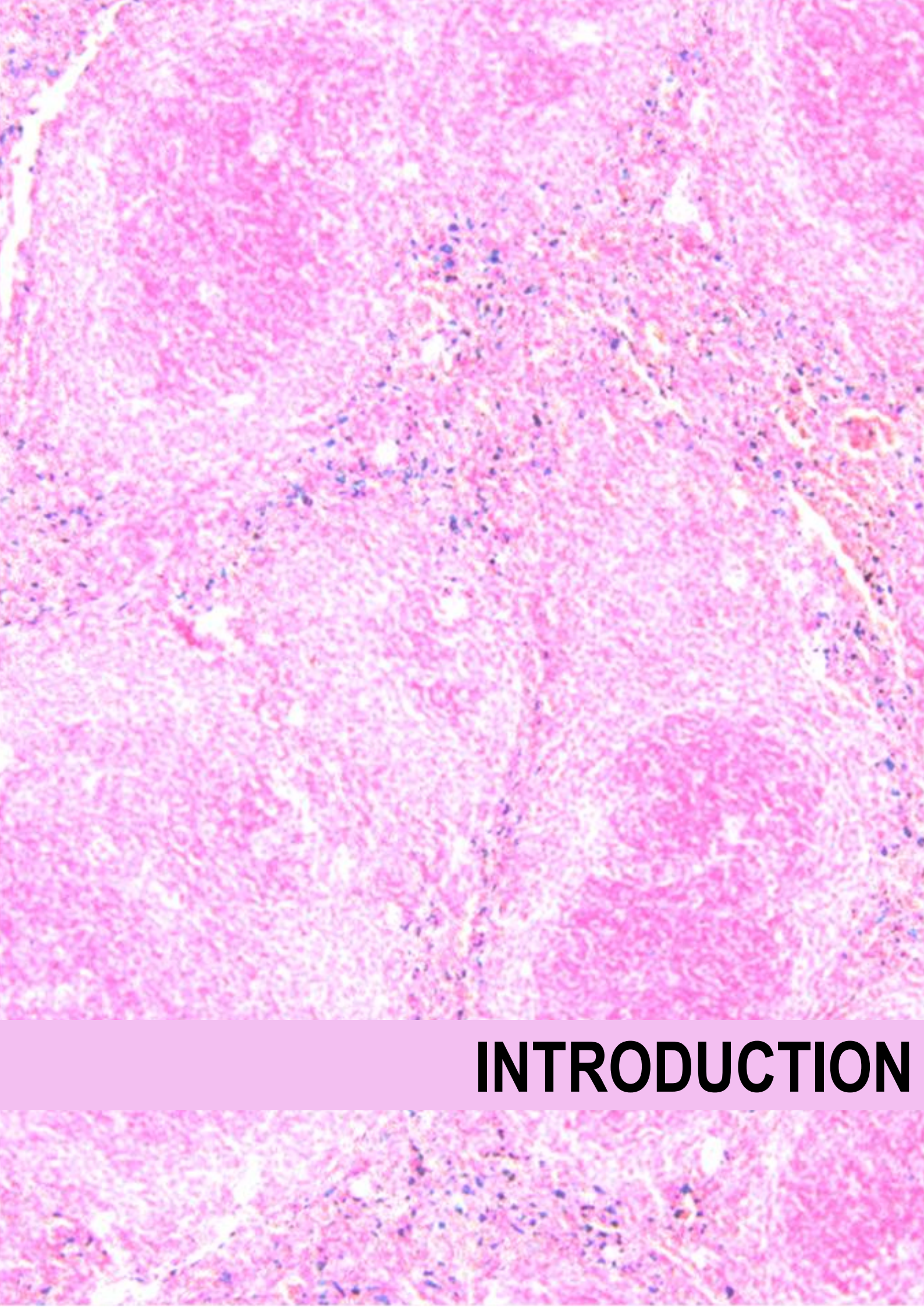

INTRODUCTION

1. THE MACROPHAGE

1.1 Macrophages in the immune system

The immune system is a sophisticated machinery constituted by different physical and biological components, that account for host defense against external threats. In order to do so, it has to be able to distinguish between self, and foreign agents, and coordinate an elaborated response that efficiently eliminates the threat without damaging own structures[1].

The **innate immune response** is the first line of defense, and provides immediate protection. It is present in the organism before the pathogen invasion. Innate immune cells recognize specific molecular patterns in the surface of microbial agents like lipopolysaccharide (LPS), flagellin or peptidoglicans, known as PAMPs (pathogen-associated molecular patterns) and tissue injury signals, called DAMPs (damage-associated molecular patterns) through specialized receptors, called PRRs (pathogen recognition receptors), like TLR (Toll-like receptors)[2]. This triggers an inflammatory reaction mediated by the secretion of different soluble factors (cytokines and chemokines) that recruit more immune cells, and ultimately cause the destruction of the pathogen[2]. The cellular components of the innate response include granulocyte lineage cells (neutrophils, basophils, eosinophils and mast cells), which contain cytotoxic granules filled with microbicidal substances, enzymes, and inflammatory mediators that expel to the extracellular medium; natural killer (NK) lymphocytes, whose high cytotoxicity drives the apoptosis of pathogen-infected cells; dendritic cells (DCs); and monocytes and macrophages[1].

The **adaptive immune response** is acquired during life and is the result of the continuous exposure to foreign antigens (Ag), which allows its components to develop immunological memory. This response is extremely specific, and guaranties the elimination of the infectious agent. More importantly, it endows the organism with the ability to recognize that particular pathogen in future infections, that way shortening the process of the immunological response[1]. It is mediated by the close interaction between B and T lymphocytes ($CD4^+$ T helper cells, and $CD8^+$ T cytotoxic cells), and small soluble molecules (antibodies, Ab). B cells circulate through the different lymphoid organs, acting as antigen presenting cells (APCs): they process foreign Ags and present them to T naïve cells through the major MHC-II (Major Histocompatibility Complex II) molecules in their surface, activating them, and initiating the response. Once the response is activated, B cells travel to the germinal centers in the lymph nodes and white pulp of the spleen, where they differentiate into plasmatic cells, specialized factories that produce enormous amounts of Abs, that recognize specific Ags, and remain in the organism at low amounts after the response is resolved, constituting the immunological memory[1].

Macrophages, along with circulating monocytes and DCs, are part of the **mononuclear phagocytic system (MPS)**, and participate in both innate and adaptive immune responses[1]. Due to their professional phagocytic capacity, they are in charge of the scavenging of pathogens, toxic materials, or even cellular debris and abnormal host components from the tissues. In the context of immunity, macrophages and DCs orchestrate inflammatory processes by the secretion of cytokines and chemokines, which recruit other immune cells to the site of infection. They are also able to act as APCs, and activate T naïve lymphocytes[1].

Macrophages are very heterogeneous and plastic cells, and express a wide range of surface, cytosolic, and vacuolar receptors that integrate different stimuli from the environment. Their different functions largely depend on the tissue they reside in, and the signals they receive. They can acquire two different states of activation, extensively described *in vitro*, based on the responses that they orchestrate: a **'classical activation'** (also known for years as **M1 state**), has a pro-inflammatory phenotype and promotes the development of the immune response, whereas an **'alternative activation'** (or **M2 state**) corresponds with a pro-repair, anti-inflammatory behavior and participates in wound healing and cellular debris clearance[3,4]. Each one has a characteristic cytokine secretion patterns. However, these two states are neither antagonistic nor static, but likely represent an oversimplification of the macrophage status. *In vitro* studies[5] hardly reproduce the complexity of the context of an *in vivo* system, where macrophage activation states must be subject to constant and dynamic change. In fact, M1 and M2 activation states have been described to coexist in tissues[3,4].

Apart from their defensive role, macrophages have important homeostatic functions. They ensure self-tolerance and immune suppression by the removal of apoptotic or damaged cells, promote tissue repair, and have a key role in the regulation of different metabolic pathways, such as lipid metabolism, that way ensuring a proper balance in the organism.

1.1.2. Macrophages and tolerance: apoptotic clearance

Under physiological conditions, a large amount of new born cells substitute the aged ones in every tissue on a daily basis. In order to maintain the homeostatic balance, the aged or defective cells suffer profound biochemical and physical changes that ultimately lead to cell-programmed death, **apoptosis**[6]. The clearance of apoptotic cells prevents abrupt rupture that would liberate a plethora of intracellular Ags to the external microenvironment, which could trigger an unnecessary immune response. Thus, macrophages effectively clear all this cellular debris by a process denominated **efferocytosis**, and ensure self-tolerance[6].

During apoptosis, cells lose membrane asymmetry, and display carbohydrates and lipids on the outer membrane that would normally be facing the cytosol, leading to their oxidation[6]. This is the case of phosphatidylserine (PtdSer), the more common marker for programmed cell death. These 'eat-me' signals will be recognized by specific receptors in the macrophage surface, including TIM4 (T-cell immunoglobulin and mucin domain containing 4), CD36, αvβ3-integrin, and the TAM family receptors (Tyro3, Axl and Mer)[6–8], which will establish interactions with the apoptotic cell with the help of different bridging molecules (such as GAS6, Protein S, MFGE8 or C1q) that facilitate phagocytosis[9–11]. The engulfment of cellular remnants triggers different tolerogenic pathways inside the macrophages that limit self-reactivity by the suppression of pro-inflammatory cytokines production (TNFα, IFN-1), and the release of anti-inflammatory mediators (TGFβ, IL-10), preventing unwanted immune reactions[12,13].

A defective withdrawal of the apoptotic materials from the environment could have pathological consequences. Their accumulation in the tissues could activate the immune system causing an inflammatory reaction, and ultimately provoking autoimmunity[6,14]. Different macrophage populations perform the clearance of apoptotic cells throughout the body. Two good examples are liver Kupffer cells (KC) and several splenic macrophage subpopulations, given that these two organs are in charge of filtering the blood, and scavenging for cell debris and blood-born pathogens[15].

1.2. Tissue resident macrophages

Unlike other phagocytic cells, like neutrophils, many different macrophage populations naturally reside in the tissues, and help maintain homeostasis by both phenotypically and transcriptionally adapting to its physiological needs[16]. They interact with their surroundings and establish cell-cell communications, developing a complex network of information that detects environmental changes, and responds appropriately, ensuring tissue integrity. This way, macrophages are key mediators of important processes like wound healing[17,18] and tissue development[19], and participate in almost every metabolic pathway.

1.2.1. Development of tissue resident macrophages

One of the classic dogmas of developmental immunology has always placed the origin of adult tissue resident macrophages (TRM) in the bone marrow, with the adult hematopoietic stem cell (HSC) as their progenitor, and the circulating monocyte as their undifferentiated stage. Macrophages were attributed non-proliferative capacity whatsoever, being constantly replaced by their monocytic intermediates when needed[20,21]. Even though during inflammation or tissue injury, circulating monocytes can, in fact, be chemotactically recruited and differentiate into mature macrophages to the tissues[22], the real contribution of these monocytes to the TRM pool at the steady state remained unclear.

With the emergence of new technologies, a different understanding of the TRM ontology paradigm has been enlightened. Several studies have shown that adult macrophage populations are able to self-maintain independently from the bone marrow. Epidermal Langerhans cells have been shown to resist high doses of irradiation, and be able to self-repopulate with time[23]. Parabiosis experimental models (with surgically joined blood circuit) obtained similar results in microglia[24,25] and alveolar macrophages[26,27], where peripheral precursors after congenic bone marrow transplant displayed up to a 40% of chimerism, but tissue macrophages presented a negligible chimerism level after several months of parabiosis. Hashimoto et al. (2013)[27] conditionally depleted the TRM pool using Cre-recombinase technology, and diphteria toxin (DT) directed depletion mouse models to confirm the intrinsic capacity of these cells to proliferate without any monocyte contribution at the steady state, or after a moderate inflammatory insult[27,28]. However, the infiltration of blood precursors is required in situations where the TRM compartment is severely affected and unable to recuperate, or when inflammation processes take place, in order to recover a normal cell count and overcome the inflammation[23,27,29,30].

The combination of all these data led to revisit the possibility of an alternative TRM ontology in mice. Even though the specifics of this complex process are still under meticulous scrutiny, today, the origin of the different TRM populations is strongly linked to early embryonic progenitors that seed the organs anlagen prior to birth[31–33], through a succession of three waves that arise from both extra and intra-embryonic locations, and maintain themselves locally in a HSC-independent manner under homeostatic conditions[34–36].

- FIRST WAVE/PRIMITIVE WAVE

At embryonic day E7,0-E7,25 progenitors arise from the extra-embryonic yolk sac blood islands, with potential to generate primitive megakaryocytes[37], erythroblasts and macrophages[38]. This initial hematopoiesis is rapidly replaced, and its main

functions are the proper oxygenation of the developing embryo through newly produced red blood cell progenitors, and the completion of the first pool of **primitive yolk sac macrophages**, with no monocytic intermediate stage described[32,39–41] (Fig. 1).

- SECOND WAVE/TRANSIENT DEFINITIVE WAVE

Between E8,0-E8,25, from the yolk sac hemogenic endothelium, appear hematopoietic progenitors with both erythroid and myeloid potential, called **erythro-myeloid precursors (EMPs)**[42] (Fig. 1). This second wave has been divided into two sheds: an 'early' EMP wave that starts at E7,5 with transient proliferative potential, and mostly produces primitive yolk sac macrophages and expresses CSF-1R (Colony stimulating factor 1 receptor) a signature of myeloid/macrophage commitment), and a second wave of 'late' EMPs, at E8,25, with expression of the transcription factor *Myb*[43,44], required for HSC development[45] (Fig. 1). Late EMPs are able to produce yolk sac macrophages locally, but the majority of them migrate to the fetal liver at E9,5, when blood circulation is established. In the fetal liver they expand, and generate CSF-1R$^+$ myeloid progenitors of all lineages, including fetal liver monocytes around E12,5, initiating the first phase of intra-embryonic hematopoiesis[35,46,47]. From this stage on, the fetal liver will transiently be the main hematopoietic organ where definitive hematopoiesis occurs. Fetal liver monocytes then spread to the developing tissues of the embryo, and differentiate into definitive macrophages, eventually outnumbering the primitive macrophages of the first wave, and with self-renewal capacity that will last through adulthood with no contribution from the adult bone marrow in the steady state[35] (Fig. 1).

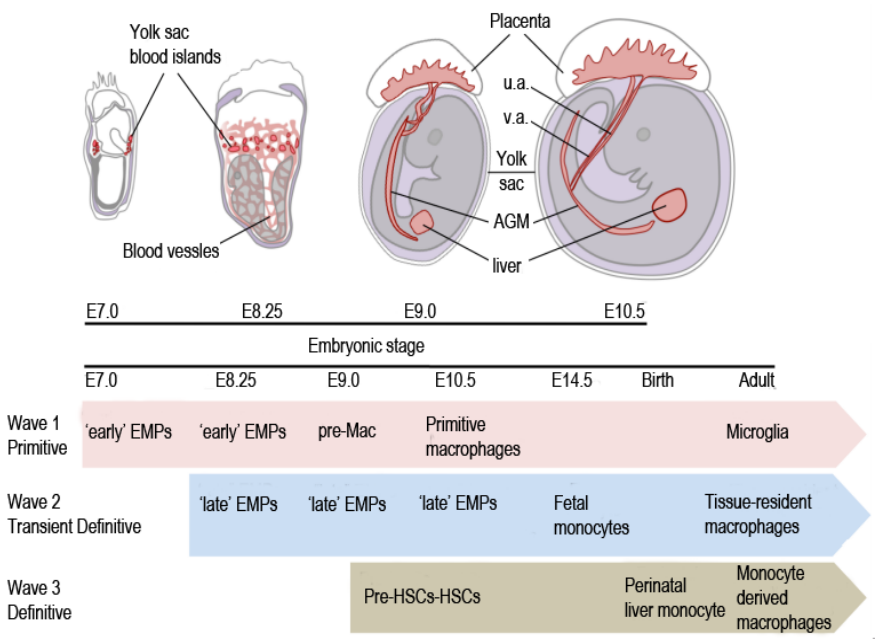

Figure 1. Extracted from Hoeffel and Ginhoux, 2018. Schematic representation of embryonic hematopoietic tissues (top); u.a. (umbilical artery); v.a. (vitelline artery); AGM (aorta-gonad-mesonephros). Three sequential waves of progenitors that give rise to TRMs (bottom).

- THIRD WAVE/DEFINITIVE WAVE

Concomitant with the formation of late EMPs at E8,5, another wave arises from the para-aortic splanchnopleura (P-Sp) of the yolk sac hemogenic endothelium, and generates immature HSCs. At E10,5 the aorta, gonads and mesonephros (AGM) region is formed from the P-Sp, and gives rise to **fetal HSCs**[35] (Fig. 1). Through blood circulation, both immature and fetal HSCs reach the fetal liver, and progenitors of all hematopoietic lineages arise[35]. It is in the fetal liver where fetal

HSCs acquire their long-term reconstitution (LTR) capacity in a final maturation step[48]. Eventually, fetal HSCs also seed the fetal bone marrow, where they will constitute adult bone marrow HSCs[35] (Fig. 1).

1.2.2. From embryonic progenitor to tissue resident macrophage: who is whom?

The identification of the particular progenitor that gives rise to each different macrophage population continues to be a challenge. To address this issue, several fate mapping strategies have been designed in the past few years. Samokhvalov et al. (2007)[49] used the Runt-related transcription factor 1 (RUNX1), whose expression is necessary for the sequential emergence of the EMPs and HSCs from the hemogenic endothelium of the yolk sac during embryonic hematopoiesis[50], to develop a very useful fate mapping mouse model. Still, there are several theories about the contribution of each wave to the different macrophage compartments.

- YOLK SAC MACROPHAGES

Ginhoux et al. (2010) combined the RUNX1 fate mapping mouse model combined with the tamoxifen inducible CRE recombination technique (Runx-Mer-Cre-Mer) to trace the embryonic provenance of the different progenitors through the first days of development, and discriminate the two waves of EMPs that emerged from the hemogenic endothelium almost at the same time[25]. They were able to identify microglia, as the only adult macrophage population that arises exclusively from RUNX1^{+} yolk sac progenitors at day E7,25[25]. However, other groups propose that these yolk sac macrophages constitute in fact the precursors of many TRM population in the adult mice, not just microglia[51]. Schulz et al. (2012) used a *Cx3cr1$^{gfp/+}$* reporter mouse and *Pu.1$^{-/-}$* and *Myb$^{-/-}$* mouse models to describe two different macrophage lineages[52]. The first one, PU.1-dependent, that arose from the yolk sac at embryonic day E9,5 and seeded the cephalic area, colonizing the rest of the tissues by E10,5. The second one, Myb-dependent, appeared in the fetal liver at E12,5[52]. Previous reports had established that PU.1 activity is required for the development of macrophages, but HSC develop normally in its absence[53], whereas Myb, is known to be dispensable for yolk sac proper myelopoiesis, but necessary for HSC development[45]. These studies pointed to the yolk sac PU.1-dependent macrophage lineage as the precursors for most TRM populations in adult mice, and to the Myb-dependent lineage as the progenitors for the rest of hematopoietic cells, including monocytes[52]. However, this data reported a lower macrophage frequency than normal in Myb-deficient adult mice[52]. This led Hoeffel et al. (2015) to speculate whether a compensatory mechanism, set in place by a Myb-independent wave of EMPs (early EMPs), was attempting to occupy an empty niche, that, in homeostatic conditions, would be fulfilled by a Myb-dependent wave of progenitors (late EMPs)[44]. This could implicate that, even though the TRM compartment seems to develop in the absence of Myb, in homeostasis, late EMPs could depend on this transcription factor to lead the proliferation of fetal monocytes, and the establishment of definite TRM populations[38,45,54].

- FETAL MONOCYTES/LATE EMPs

At E.8,5, late EMPs arise from the yolk sac and populate de fetal liver (E9,5) producing cells of many lineages, including fetal liver monocytes at E12,5. Eventually, these monocytes seed all the tissues, likely constituting the main precursors for the majority of the adult TRMs at E14,5[44], outcompeting the 'early' EMP macrophages everywhere but in the brain (Fig. 1).

It is unclear whether 'early' and 'late' EMPs are two different cell lineages, or rather one maturates into the other, but studies have shown different functionalities and phenotypes. For example, while early EMPs highly express CSF-1R, late EMPs do not express it at all[44]. The same observations have been made when comparing fetal and adult monocytes. Opposite to adult HSC-dependent monocytes, fetal monocytes do not require the expression of CSF-1R to properly differentiate into macrophages, and possess high proliferating capacity and low expression of immune-related genes[44,55].

- HEMATOPOIETIC STEM CELLS

Despite the proved embryonic origin and self-renewal capacity of adult macrophages, a few studies have shown that HSCs actually supply certain tissues with monocytes that differentiate into macrophages in order to sustain the turnover rate. However, not every organ has the same requirements, and this contribution increases with age[27]. Gomez-Perdiguero et al. (2015) observed that the alveolar macrophage compartment, which is normally virtually inaccessible for HSC-derived monocytes, could be progressively repopulated by HSCs in elder mice[51].

The reason for this is that some macrophage populations have a higher turnover rate, due to the nature of the different functions they develop, and need help from bone marrow progenitors to maintain homeostasis in the adult tissues, as would be the case of the intestinal lamina propia[56], the dermis[57], and the heart[58,59]. In these tissues, parabiotic mouse models showed different degrees of mixing within the macrophage compartment. Thus, Hoeffel et al. (2015) classified adult mice tissues in 'closed', with no steady-state monocyte recruitment (like the brain or the epidermis), 'open' with slow steady-state recruitment (like the heart) and 'open' with fast steady-state recruitment (the gut or the dermis)[44].

1.2.3. Tissue macrophage transcriptional program

Despite the newly established common embryonic origin for the different TRM populations, the observation of the wide variety and diversity that all these populations display in each location brought to light the question of whether these differentiated phenotypes were solely granted by their embryonic progenitors or rather by the tissue-specific environmental signals they are exposed to[60]. For example, both the proliferative potential and the survival advantage inherent to TRM have been proved to be linked to their embryonic provenance. Yolk sac-derived macrophages and fetal liver monocytes present high expression of proliferation genes, and thus adult macrophages that derived from them partially maintain that capacity[44,55,61]. In contrast, HSC-derived monocytes, whose transcriptional signature leans more towards inflammation and immune programs, are not normally able to engraft to the tissues they are recruited to after the inflammation resolves[24,27].

Mass et al. (2016) attempted to answer this issue, and conducted a comprehensive study of the expression of many different transcription factors in different progenitors and macrophage populations[62]. They proposed the existence of a macrophage immature progenitor, the pre-macrophage or 'pMac', that arises from EMPs and simultaneously populates the whole embryo at E9,5. This macrophage precursor would have an unspecialized transcriptional program (a core macrophage program) that would progressively be restricted upon tissue colonization at E10,5, thanks to tissue-specific cues and regulators, to meet the different homeostatic needs of each tissue[62]. For instance, other studies have reported that the deletion of a particular transcription factor severely affects a determined macrophage population, as is the case of *Nr1h3* and marginal zone macrophages[63], *Spic* and red pulp macrophages (RPMs)[64], *Pparg* for alveolar macrophages[65],

and *Id3* for KCs[62]. Lavin et al. (2014) described the potential of macrophage plasticity through the ability of tissue-specific influence to reprogram differentiated macrophages when relocated to another microenvironment[16]. In summary, all these data seem to indicate that both embryonic origin and niche environmental signals define tissue resident macrophage phenotypes. While embryonic progenitor transcriptional core programs account for the ability to self-maintain, different transcriptional regulators in each tissue are responsible for the heterogeneity and specificity resident macrophages display.

1.3. Spleen development and splenic tissue macrophages

The spleen is a secondary lymphoid organ with highly organized compartmentalization[66]. In mammals, it constitutes the largest filter in the organism, thanks to its complex internal circulatory system, through which blood constantly percolates. Within this organ, multiple hematopoietic cell types, with different immune and homeostatic functions, coexist in perfectly shaped microenvironments that conform between the third and fourth week of postnatal development[63,67,68].

1.3.1 Splenic compartmentalizacion

Four different tissue resident macrophages can be identified in the adult mice spleen, each one limited to a specific location[66,69] (Fig. 2). But at the neonatal stage, before the white and red pulp segregation is final, the primary spleen is a homogenous mix of primitive macrophages. At the first week after birth, the developing organ is populated by one sole red pulp-like macrophage subset, with high expression of F4/80. At week 2, appear other macrophage populations, but they will not acquire their correspondent location until the internal architecture reorganizes. It is during 14-21 postnatal days that the lymphoid follicles arrange, and F4/80$^+$ macrophages are confined to the red pulp, and the three other well differentiated macrophage subsets occupy their correspondent locations, and carry out very specific functions[66,69].

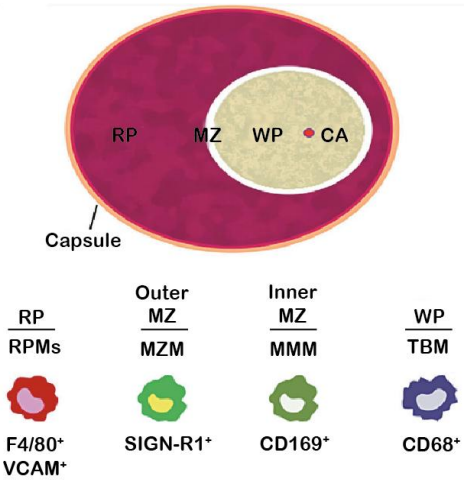

Figure 2. Adapted from Kurotaki et al. 2015. Adult murine splenic compartmentalization of TRM populations and their specific surface markers.

Red pulp macrophages reside exclusively in the red pulp, and have been phenotypically described by flow cytometry as CD11b^{lo} F4/80^{hi}VCAM-1$^+$ [69](Fig. 2). Their main function is the clearance of aged or damaged circulating red blood cells (RBC) that infiltrate through the sinusoids by a process known as erythrophagocytosis. These macrophages are in charge of the metabolization of hemoglobin (Hb), and actively participate in iron recycling[66]. As a consequence, they express a plethora of iron-related genes in order to ensure the correct regulation of the process. Immunological functions have also been attributed to RPMs in the defence against parasite infections (see 1.4.4.), as well as assistance on T cell differentiation[70]. As mentioned, F4/80 expressing cells are the first ones to appear in the spleen anlagen[66]. RPMs are described to arise during embryonic development, and are maintained during adult life with low contribution from adult HSC-derived monocytes at the steady state[27,52]. It is not clear whether they arise from yolk sac primitive macrophages[52] or

if they come from fetal liver monocytes[58]. However, RPM transcriptional master regulator has been identified as the PU.1-related factor, SPI-C[64].

Tingible body macrophages (TBM) are located in the white pulp, within the germinal centers, and can be identified by the surface marker CD68[69] (Fig. 2). Their main function is the phagocytosis of the apoptotic or auto-reactive B cells that generate in the germinal centers during the processes of proliferation and hyper-mutation of the adaptive immune response to avoid hyper-reactivity[66]. Hence, the genetic expression profile of these macrophages leans towards apoptotic cell recognition and phagocytosis[71].

In the interphase between the two pulps we can find two different populations of macrophages. As the blood is shed in the marginal zone before it reaches the red pulp, both marginal zone macrophage subsets specialize in the clearance and recognition of different agents and blood borne Ags present in the circulation[66]. Macrophages relocate to the marginal zone in the first weeks after birth, and their correct development requires LXRα (*Nr1h3*) transcriptional activity[63].

In the inner layer of the marginal zone, are the **metallophilic macrophages (MMM)**. MMMs present high expression of CD169 surface marker, also known as Siglec-1 (Fig. 2), and their main function is the recognition and withdrawal of viruses, and the activation of $CD8^+$ T cells through the presentation of viral Ags, thus triggering the adaptive response[72]. In the outer layer of the marginal zone, in contact with the red pulp, are the **marginal zone macrophages (MZM)** (Fig. 2), who phagocytose different Ags from the bloodstream, and communicate with specialized marginal zone B cells (MZ-B)[66]. This close interaction is crucial in the triggering of the adaptive response. MZ-B cells internalize these Ags and migrate to the white pulp, to the follicles, where they present them to DCs, and activate the germinal center[66]. MZM express different interaction molecules that serve as communication with MZ-B cells, such as SIGN-R1 and MARCO[73], that ensure the correct positioning of these B cells in the marginal zone. Additionally, MZM also promote central tolerance by the engulfment of blood-borne apoptotic cells, in order to inhibit a possible immune reaction to self-antigens secreted by disrupted cells in the circulation[74].

1.4. Red pulp macrophages in iron metabolism

Iron is an essential metabolite for many processes. It participates in the electron transport chain as part of the cytochromes and acts as a co-enzyme factor in different metabolic pathways, but most importantly, the highest demand of iron comes from erythropoiesis and the synthesis of Hb[75]. The majority of this demand is met thanks to endogenous iron recycling process, as dietary iron intake is not sufficient to cover it. In mice, iron requirements are proportionally a lot higher than in humans, and account for almost all the daily iron input (around 15-20 µg/day), as they lose a similar iron amount to cover their erythropoiesis needs[75].

Iron metabolism is a very well controlled global mechanism, and so there are many molecule regulators that ensure a correct equilibrium between processing, recycling and storage upon different conditions. Macrophages are the main cells in charge of iron handling throughout the organism. Depending on the tissue, different TRM populations carry out different

steps of the process: bone marrow macrophages (BMMs) support erythropoiesis; KCs process iron in the liver and together with hepatocytes, constitute the main iron store in the body[76]; RPMs behave as efficient iron-recycling factories that integrate many different signals to provide the whole organism with its specific iron requirements[76]. Still, the regulation is highly complex, and the specific role of each macrophage population is yet to be completely characterized.

1.4.1. Elimination of unwanted red blood cells

During their 40 day-lifespan in mice (120 days in humans), erythrocytes are in contact with RPMs in several occasions. The red pulp of the spleen is a highly efficient blood filter, and thus RBCs in circulation are under continuous scrutiny by RPMs[76,77]. After their useful life, RBC become senescent, and need to be removed from the circulation. This is often determined by changes in their membrane composition, loss of flexibility, and expression of proteins that alert RPMs to engulf them by a process called erythrophagocytosis[67]. There are different mechanisms described for macrophage recognition of aged or damaged RBC and their clearance. Oxidation and cluster formation of surface proteins such as BAND-3 proteins[78,79], or the exposure of PtdSer in the outer-membrane of erythrocytes resembling an apoptotic-like event called eryptosis[80–82], are two of the most common signals for erythrophagocytosis. Oxidative stress induced by different pathologies (β-thalassmia, chronic kidney disease, malaria)[82–84] can over-induce these signals, increasing RBC clearance.

The most studied macrophage-erythrocyte recognition mechanism is mediated by **CD47** receptor in the surface of RBCs. Interaction with its counter-receptor, **CD172α** (SIRP1-α) in the macrophage membrane acts as a 'don't eat me' signal and impedes erythrophagocytosis[85,86]. WT mice have been observed to rapidly phagocytose CD47-null transfused erythrocytes[85]. Pathological conditions, such as oxidative stress, can cause conformational changes in CD47 receptor, which reverses clearance inhibition, thus enabling erythrophagocytosis[87].

1.4.2. Iron recycling

Dietary iron is absorbed by the enterocytes in the duodenum through a specific transporter in their luminal face, known as **DMT-1** (Divalent metal transporter 1, encoded by *Nramp-2* gene) and liberated to circulation through its specific exporter, **FPN-1** (ferroportin-1, encoded by *Slc40a1* gene), in their basal face[88]. As ferric iron (Fe^{2+}) cannot travel by itself, it binds to the soluble protein transferrin (Tf), which carries it to the different tissues, mainly to the bone marrow to be used in erythropoiesis. However, this absorption is highly inefficient, so the main source of iron in the organism comes from macrophage recycling of aged erythrocytes[88] (Fig. 3).

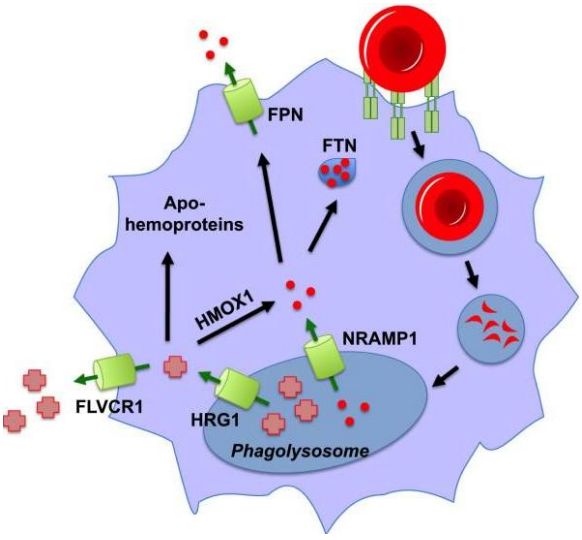

Figure 3. Adapted from Korolnek and Hamza, 2015. Possible pathways for heme and iron processing and recycling inside the RPM.

RPMs recognize and engulf aged or damaged erythrocytes, and inside the phagolysosome all cell components are processed, including Hb. The protein portion of Hb will be reused in the synthesis of other proteins, while heme will be enzymatically degraded. Heme exits the phagolysosome

through the heme exporter **HRG-1** (Heme response gene 1, encoded by *Slc48a1* gene)[89] and enters the cytosol. Finally, it can either be exported out of the macrophage through the **FLVCR1a** heme exporter (Feline leukemia virus subgroup C receptor-1, encoded by *Slc49a1* gene), a pathway that has been suggested during macrophage contribution to erythroid cells maturation[90,91], or it can be further catalyzed[88] (Fig. 3).

The cytoplasmatic heme catalytic enzyme heme oxigenase-1 (**HO-1**, *Hmox1*) degrades heme into biliverdin, CO, and Fe^{2+}, which can rather be stored inside the macrophage thanks to iron storage protein ferritin (**FTN**), or be exported through FPN-1 into the plasma (Fig. 3), where it will be transported by Tf to where it might be needed[88]. It has also been proposed that HO-1 can reside inside the phagolysosome and therefore degrade heme before it is exported into the cytosol. In that scenario, free Fe^{2+} would be released through a different endosome exporter, **NRAMP-1** (Natural resistance-associated macrophage protein-1, encoded by *Slc11a1* gene), to be stored within FTN or exported by FPN-1[88] (Fig. 3).

Erythrophagocytosis is not the only way in which iron is internalized by macrophages[92]. Erythrocytes rupture outside the macrophage liberates all their cytoplasmatic material into the extracellular matrix. Hb is stable for a short period of time, and then it rapidly degrades, liberating its contained iron. Free iron in serum is highly toxic because of its huge oxidizing capacity, that leads to the formation of oxygen radicals, and scavenging of nitric oxide (NO). In order for the macrophages to internalize all the different forms of free iron, it expresses a variety of specific receptors[92]. **CD163** is the Hb scavenger receptor, first described by Kristiansen et al. (2001)[93]. It is selectively expressed by the macrophage lineage. In humans, CD163 internalizes free Hb when it is bounded to haptoglobin (Hp), a serum protein mainly secreted by the liver, but in mice this interaction occurs without Hp, and free Hb is degraded in the phagolysosome[92]. **CD91/LRP** (Low density lipoprotein (LDL) receptor protein-1) is the macrophage receptor for free heme, when it binds to hemopexin (Hpx), another plasma protein in charge of the heme withdrawal. CD91 works in the same way CD163 does, internalizing the heme-Hpx combo[92,94].

The proper expression of all these enzymes, and scavenging and exporter proteins is crucial for an adequate iron handling, and the maintenance of homeostasis. Deregulations on just one of them can cause severe consequences, from anemia or iron overload, to tissue injury. For instance, FPN-1 constitutive deletion causes embryonic lethality in mice[95]. This iron exporter is most expressed in RPMs, enterocytes and hepatocytes. Studies in mice lacking *Fpn1* expression only in the macrophage lineage, using Cre-recombinase technique ($Fpn1^{LysM/LysM}$)[96], showed that, at the steady state, mice suffered from mild anemia, and iron retention within splenic, hepatic and bone marrow macrophages, as well as disturbed iron handling in bone marrow derived macrophages (BMDM) *in vitro*.

Similarly, HO-1 deficiency also causes serious impairments in iron homeostasis[97]. There are two isoforms of heme oxygenase enzyme: HO-2, constitutively expressed in most tissues, and HO-1, whose expression is induced by the presence of heme in the macrophage. Lack of both HO isoforms together is embryonically lethal, and $Hmox1^{-/-}$ mice, although viable, suffer from severe anemia[97]. In addition, the accumulation of unprocessed heme inside the macrophages, caused the ferroptosis (death form iron toxicity) of the RPM, KC and BMM populations, and thus all iron excess had been relocated to the kidneys to be processed by HO-2, were $Hmox1^{-/-}$ mice displayed great accumulations. In addition, Hpx

mRNA levels were significantly increased in *Hmox1*$^{-/-}$ mice, probably in an attempt to scavenge all the free heme and avoid its toxicity[97].

Parallel to FPN-1, NRAMP-1 is the phagolysosome Fe^{2+} exporter, exclusively expressed in phagocytic cells[98]. While *Nramp2* (DMT-1) is ubiquitously expressed and its mutations cause severe microcytic anemia in mice, *Nramp1*$^{-/-}$ mice did not present serious defects in iron homeostasis, but displayed a mild anemia. The symptoms aggravated after induced hemolytic anemia by phenylhydrazine (PHZ) treatment, with iron retention inside the phagolysosomes, and impaired erythropoiesis[99].

1.4.3. Regulation of iron metabolism

Iron metabolism is under tight regulation, and interference in that intricate regulation has been extensively related with different metabolic disorders. The main regulator of this complex mechanism is the **increase or decrease of iron** in the system, in any of its forms (Hb, heme, free Fe^{+2}), which triggers different signals and metabolic pathways[77,100].

Indeed, the expression of HO-1, FPN-1 and SPI-C is induced by **heme** accumulation. At the steady state, their transcription is constitutively inhibited by the transcriptional repressor BACH1 (BTB and CNC homology 1). Haldar et al. (2014) established heme as the main mediator for BACH1 degradation[101], and thus the inductor of *Spic*, *Hmox1* and *Slc40a1* expression both *in vivo* and *in vitro*. In this study, they used a Spic$^{igfp/igfp}$ reporter mouse model to track SPI-C expression in different macrophage populations, and found similar levels both in RPM and BMM, two macrophage populations deeply implicated in iron handling[101]. In the same way, increased free heme, or increased erythrophagocytosis in cultured macrophages promotes *Nramp1* expression, but not *Nramp2* (DMT-1)[98]. Parallel, HRG1 expression is also higher when the macrophage is exposed to hemin, or erythropagocytosis augments in BMDM, and its deletion impairs heme transport from the phagolysosome to the cytosol[89].

Hormonal regulation of iron metabolism is mediated by **hepcidin**[75]. As it has been mentioned before, hepatocytes are the major iron storage in the organism, although RPMs and KCs have also the capacity of storing iron in specific situations, such as infection (see **1.4.4.**). Hepatocytes are able to sense the iron serum concentrations in the organism, perhaps thanks to their privileged location in contact with the portal venous system, and regulate iron homeostasis accordingly. They are the predominant producers of hepcidin[75].

Hepcidin modulates iron availability in plasma by provoking the internalization and consequent degradation of FPN-1 in macrophages, thus impeding iron release and promoting its storage[75,102]. As a hormone, it travels through circulation from the liver affecting enterocytes in the duodenum, which would then stop dietary iron absorption, RPMs in the spleen, and KCs and hepatocytes in the liver. Hepcidin production is at the same time regulated by iron[75]. When Tf-bound iron levels are high in plasma, due for example to excessive iron absorption in the intestine, or high erythrophagocytosis rate, hepatocytes detect this excess and secrete hepcidin. Conversely, low iron levels in plasma, an increased demand in erythropoiesis or hypoxia, rapidly block hepcidin secretion, thus promoting an increase in iron recycling and liberation[75]. This feedback ensures a correct iron balance in the organism. There are many intermediate molecules that act as iron sensors and modulate hepcidin production, but the specific mechanisms of this modulation are still unknown.

In the context of post-transcriptional regulation, the **IRE/IRP** axis controls the expression of many different iron-related genes, acting as iron sensors[103]. IRP-1/2 (iron regulatory proteins 1/2) recognize IREs (iron-responsive elements) in the mRNA strands of transcribed iron proteins and bind to them. As orthologous proteins, their functions often overlap. In mice, they areknown as Aconitases, encoded by *Aco1*, and *Ireb2* respectively[103]. Upon IRP-IRE binding, the translation of a specific mRNA can rather be blocked, or stabilized, depending on the protein and the iron homeostatic conditions[104]. This way, IRE/IRP regulation conforms a highly adaptive response to the changes in the cellular iron status. Some of the iron proteins regulated by this mechanism are DMT-1 in the intestine; FPN-1; the iron storage protein FTN; the Tf receptor (TfR); ALAS (5-aminolevulinate synthase, the first enzyme of heme synthesis); and HIF2α (hypoxia-inducible transcription factor)[103,104]. Genetic ablation of both IRP1 and IRP2 results in embryonic lethality in mice.

1.4.4. Iron and inflammation

Iron homeostasis is closely linked to inflammation and immunity. It has been well documented that elevated iron serum levels tend to worsen inflammation and infection situations, while iron deficiency relatively ameliorates the symptoms of many of these pathologies (tuberculosis, malaria)[75]. Iron constitutes an important nutrient for every metabolism, and that includes microbes and pathogens. Macrophages, specifically RPMs and KCs, are able to regulate iron availability thanks to its storage in ferropoteins in their cytoplasm, thus limiting microbial proliferation and survival[105]. High iron loading is frequently associated with inflammatory pathologies, such as atherosclerosis[106], chronic liver disease[107] and neurodegeneration[108]. Therefore, inflammation constitutes a great trigger for iron retention, normally mediated by the hepcidin secretion induced by pro-inflammatory cytokines signaling (like IL-6 and IL-1β)[109], which lead to iron compartmentalization in macrophages, although the process depends on the kind of pathology[110]. The production of pro-inflammatory cytokines also promotes the production of a number of extracellular iron-scavenging proteins, such as lactoferrin, FTN, Hp and Hpx, which sequestrate iron from the plasma[77]. Conversely, hypoxia conditions after inflammation inhibit hepcidin secretion and restores iron trafficking. If the inflammation or infection conditions persist, the most common consequence is the development of the anemia of inflammation (AI), where a prolonged iron arrest causes the development of hypoferremia, erythropoiesis delay, and ultimately, anemia[77,109,110].

1.5. Bone marrow and spleen resident macrophages in erythropoiesis

The bone marrow hosts the scenario for most of the erythrocyte proliferation and maturation process in adults. From the HSC to the reticulocyte, different stages of differentiation develop in a very controlled microenvironment, in a highly specialized niche known as the erythroblastic island (EBI)[111] (Fig. 4). It consists on a central or nurse macrophage ($CD11b^{lo}F4/80^{hi}CD163^{+}CD169^{+}ER\text{-}HR3^{+}$) surrounded by erythrocyte progenitors at different maturation stages: colony-forming unit, erythroid (CFU-e), pro-erythroblast, basophilic erythroblast (Ery A), poly erythroblast (Ery B), and ortho erythroblast (Ery C)[111] (Fig. 4). The last cell division occurs at this last stage. It is asymmetrical, and produces a pyrenocyte (composed by the nuclei and several other organelles) and a reticulocyte (the rest of the cell). The pyrenocyte is engulfed by the central macrophage on a process called enucleation[111,112] (Fig. 4). After 48 hours, the reticulocyte enters the

bloodstream, where it will continue to maturate for another 24 hours[111]. Their membrane suffers drastic composition modifications, which will confer high elasticity, and become biconcave. Their lifespam in humans, is approximately 120 days, while in mice they live around 40 days[112].

The EBI can be found in every tissue that supports erythropoiesis *in vivo*, from the the fetal liver, to the adult bone marrow, and the spleen in case of emergency extramedullary hematopoiesis (EMH)[113]. However, at the earliest stages of embryonic development the first erythroblasts are thought to arise from the yolk sac blood islands independently from EBIs, and mature in the primitive circulation, but to still need to attach to a macrophage in order to enucleate[114,115]. In adult mammals, EBIs are distributed throughout the bone marrow with lo specific location. It has been suggested that EBIs are motile, and move within the marrow as their attached erythroblasts differentiate thanks to the central macrophage and its ability to interact and modify the extracellular matrix. A study that compared EBIs based on their proximity to the marrow sinusoids showed that those islands in close proximity to the sinusoids presented more differentiated erythroblasts than those localized far from them, which presented more immature erythroid cells[116].

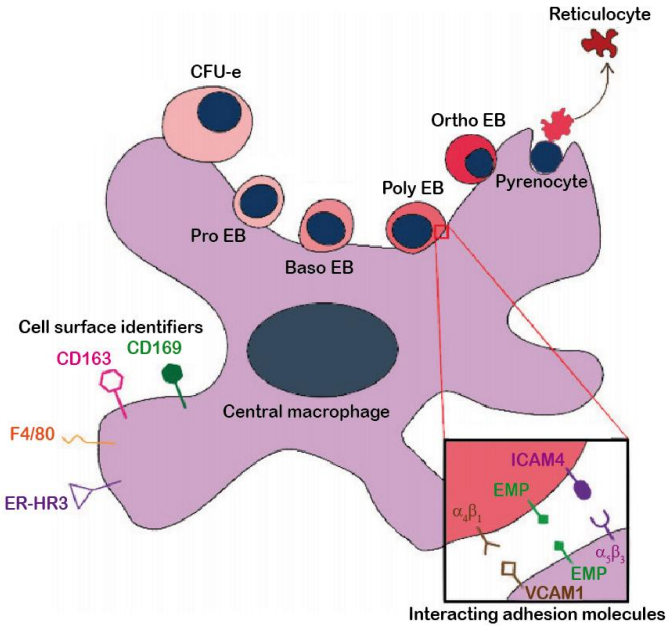

Figure 4. Adapted from Hom et al, 2015. Erythroblastic island representation. The central macrophage promotes the differentiation of the erythroid progenitors, maintaining cell-cell interactions through several adhesion molecules.

1.5.1. Functions of the central ' nursing' macrophage

The specific contribution of the central macrophage to adult erythropoiesis is not entirely clear. Studies *in vitro* have shown that free erythroblasts are able to divide, mature and enucleate by themselves, but experience far fewer divisions compared to those attached to a central macrophage and the process is, in comparison, highly inefficient[117,118], while the co-culture of erythroid progenitors with macrophages enhances their proliferation and differentiation[119]. One central macrophage handles around 30 developing erythroid cells in humans, but roughly 10 in rodents, attached through a high number of cell-cell interactions mediated by a myriad of adhesion molecules[88,120,121]. Macrophages have been probed to use these interactions to retain the erythrocyte progenitors in the bone marrow niche in order to ensure and **promote their sequential divisions and differentiation**, as well as the **transmission of nutrients and molecular signals**[76]. In fact, mouse models that lack integrins, the main interaction molecules, fail to potentiate erythropoiesis under stress conditions[122]. However, these interactions are not static. They undergo numerous changes during the differentiation of erythroblasts, and they need to allow the detachment of erythroid cells in order for them to enter circulation when they are mature[113].

Studies supporting the interaction between macrophage and RBC described the importance of **Emp** (erythroblast macrophage protein, also known as MAEA), the first adhesion molecule identified for the EBI[123]. Emp is expressed both by the central macrophage and the erythroblast, and they interact with each other, being this a prerequisite for efficient erythropoiesis. Emp-null mice die perinatally and fetuses show severe alterations in the hematopoietic department[117], and inability to form EBIs in the fetal liver[124]. Integrins are great interaction molecules in every context: **$\alpha_4\beta_1$ integrin** in erythroblasts binds to **VCAM-1** (vascular cell adhesion molecule 1) in macrophages. Interruption of this interaction using blocking antibodies causes the disruption of the island, and mutants in these molecules exhibit lethal embryonic anemia, caused by embryonic definitive hematopoietic failure[125,126]. Parallel, **ICAM-4** (intercellular adhesion molecule 4) in erythroblasts, binds to **α_V integrins** in central macrophages. Upon blockade of this interaction, there is a drastic reduction of EBIs. Furthermore, ICAM-4-null mice display a marked decrease of EBIs both *in vivo* and *in vitro*[127]. The Hb scavenger receptor **CD163** is highly expressed by BMMs[128], but the counter receptor is yet to be identified. Nonetheless, this interaction is important in the early stages of development, promoting expansion rather than differentiation *in vitro*, and is quickly lost past the pro-erythroblast stage[129]. **CD169** (sialoadhesin), also expressed by BMMs, participates in these interactions too. Its counter receptor is also unknown[130]. $CD169^+$ macrophages ensure the retention of HSCs in the bone marrow mesenchymal niche[131], and have a pivotal role in later stages of erythropoiesis, enabling rapid proliferation by establishing loose interactions with erythroid precursors. Conversely, tight interactions between erythroblasts and $CD169^-$ macrophages interrupt proliferation and promote erythrophagocytosis[132].

Another proposed function for the central macrophage is the **delivery of iron** to the developing erythroblast, but is not clear under what circumstances this inter-cellular transfer takes place[88]. The main iron source for the developing erythroblasts in the EBI is Tf, which binds to the TfR (also known as CD71) in the membrane of the erythroblast[133], and is internalized and directed to the mitochondrion to synthesize heme, and later, Hb[100]. However, central macrophages might also supply iron for the process in the absence of Tf, by the transfer of their FTN storage through an unknown mechanism[134]. FTN molecules have been discovered in the inter-cellular space between macrophages and erythroblasts[133–135]. Additionally, heme might also be transferred from the macrophage to the erythroblast through the macrophage heme exporter FLVCR1a[91,136,137] and internalized by the heme transporter HRG1 in the erythroblast[138]. These two pathways are clearly not predominant in normal conditions, but they are believed to assist during stress erythropoiesis.

Finally, the one well described and established function of the central macrophage is the phagocytosis of the expelled nuclei (**enucleation)** at the end of the differentiation of the reticulocyte. Studies performed in embryos, showed that Emp receptor interacts with different cytoskeleton proteins in both ends, mediating the process[124,139]. At the embryonic stage, erythroblasts have been described to enucleate in the fetal liver, while in adults it takes place in the bone marrow EBIs[115]. Fetal liver erythroblasts display apoptosis signals on the surface of their expelled pyrenocytes, in order to promote engulfment by fetal liver macrophages, such as the exposure of PtdSer[140]. Other studies reported that Emp-null embryos presented a significantly higher number of nucleated erythroid cells in circulation, and predominantly immature pro-erythroblasts in the fetal liver compared to their WT counterparts[124].

1.5.2. Erythropoiesis regulation

Erythropoiesis is a meticulously controlled process. Transcriptional regulation is key in the differentiation from HSC to erythroblast. The transcription factor **GATA-1** is necessary for erythroblasts survival, and its absence causes apoptosis[141]. Consequently, GATA-1-deficiency is embryonically lethal. **Soluble factors**, secreted by both macrophages and erythroblasts are also of great importance in correct progression of erythropoiesis, in order to properly respond to different signals in the organism and maintain homeostasis (IL-6, TNFα, TGFβ, IFNγ, TRAIL)[76].

But the main factor in the regulation of erythropoiesis is **erythropoietin (EPO)**[142]. This hormone, mostly secreted by the kidney in adults and by the fetal liver during embryonic development, responds to changes in tissue oxygenation. It travels through circulation and binds to EPO receptor (EPOR), which is expressed by erythroid precursors from CFU-e to the basophilic erythroblast, and by the central macrophage[142]. EPO signalling directly promotes erythroid survival, proliferation and differentiation, thus increasing the RBC count and promoting oxygen transport. Consequently, the main stimulus for the production of EPO is hypoxia[142]. In macrophages, EPO signalling contributes to the resolution of inflammation induced by hypoxia stress. In fact, EPOR levels increase in the membrane of macrophages, as does EPO serum levels[143]. Driven deletion of EPOR in peritoneal macrophages impairs their phagocytic ability towards apoptotic clearance[144]. Many studies have shown that EPO stimulation promotes an anti-inflammatory phenotype and phagocytosis in microglia during inflammation[145], and KCs proliferation in the liver. Finally, an *in vitro* study showed that EPO administration to a human EPOR over-expressing mouse model, significantly increased F4/80^{+}MHC-II^{+} macrophages in the spleen[146].

1.6. Red pulp macrophages in extramedullary hematopoiesis

A lot of studies have shown that, under steady state conditions, the absence of BMMs does not cause serious complications in mice[131]. When bone marrow erythropoiesis is compromised, due to bone marrow abnormalities, hypoxic stress, chronic inflammation, infection or massive bleeding[147,148], the process is displaced to other organs, being denominated extramedullary hematopoiesis (EMH). When this happens, central macrophages of the EBIs become an essential asset to the development of new RBCs. The main organ in charge of EMH is the spleen, more specifically, RPMs[113,131,146,149].

In homeostasis, RPMs have very specific roles in the maturation of RBC. Mature RBC infiltrate the spleen several times in order be checked for correct membrane integrity and flexibility[88]. During these checks, RPMs have the ability to remove cytoplasmatic inclusions from them (excessive iron deposits, proteins and oxidative damage accumulations) while maintaining their integrity and returning them to circulation, by a process called 'pitting'[150], although the molecular mechanism for this phenomenon is still unknown. But during EMH, RPMs also play the role of nursing macrophages in extra medullar EBIs to assist erythroblasts in their maturation. In order to study the mechanism of EMH, different approaches have been addressed. G-CSF (Granulocyte colony stimulating factor) stimulation in mice leads to the depletion of BMMs[151], causing an erythropietic defect and promoting EMH in the spleen[149,152]. Chow et al. (2013) showed that WT mice with a complete deletion of monocytes and tissue macrophages caused by clodronate liposomes infusion,

could not overcome the anemia after PHZ treatment. Conversely, BMMs directed ablation in a CD169$^{DTR/+}$ mouse model combined with a PHZ treatment only caused delayed hematocrit recovery[131].

2. LIVER X RECEPTORS

2.1. Nuclear receptor superfamily

The superfamily of nuclear receptors (NRs) contains up to 48 different transcription factors in humans, and 49 in mice, being one of the largest groups of receptors in vertebrates[153]. They participate in every transcriptional program that takes place in the cell in homeostatic conditions, regulating a plethora of physiological functions, including metabolic processes, development and cell differentiation[153]. These transcription factors are typically ligand-dependent, and have a very conserved and highly organized protein structure, consisting of 6 domains (Fig. 5): a N-terminal region, which contains a ligand-independent activation domain (AF-1, Activation Function 1, A/B), a DNA binding domain (DBD, C), a ligand binding domain (LBD, E), and a C-terminal region containing another activation domain (AF-2, Activation Function 2, F), in this case ligand-dependent, that enables the interaction between the nuclear receptor and the different co-activators and repressors that modulate their activity. Between the DBD and the LBD there is an intermediate region, of variable length, that acts as a hinge (D) when the protein folds[154]. There are three subfamilies, regarding the nature of their specific ligands[155] (Fig. 5). **Steroid receptors**, bind to steroid hormones and translocate from the cytoplasm to the nucleus as homodimers; **orphan receptors**, whose ligands had not been identified by the time of their discovery. They can either act as homodimers, or as monomers; **adopted orphan receptors**, originally classified as orphan receptors, until the discovery of their specific thanks to genomic experimental methods. These receptors are constitutively nuclear, and need to heterodimerize with the retinoic acid receptor (RXR) in order to bind to the DNA and function. Their activation can occur in three ways: through the binding with the specific ligand of the partner of RXR (RXR acts as a silent companion); through the synergic binding of the specific ligands of both receptors; through the conditional modulation of the RXR ligand, which functions as an activator only if the other ligand is present. This group includes many different possible partners for RXR, such as the Liver X Receptors (LXR), and the Farnesoid X Receptors (FXR)[155].

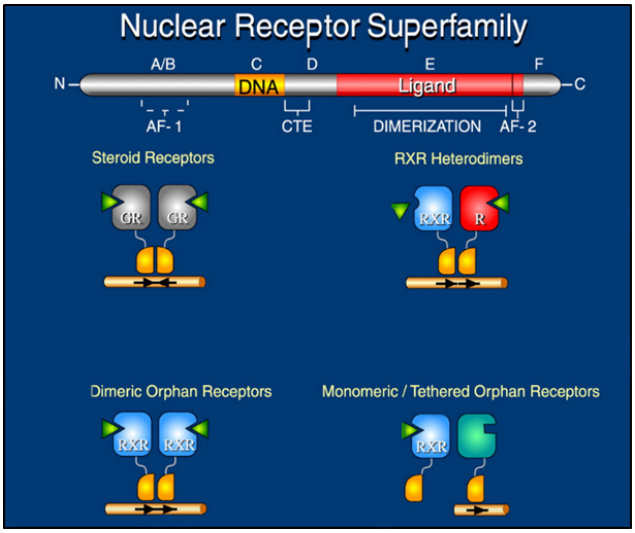

Figure 5. Adapted from Olefski, 2001. Classification of the different nuclear receptors depending on their ligands.

Nuclear receptors bind to specific DNA sequences known as Hormone Response Elements (HRE), localized in the regulatory regions of their target genes. For the non-steroid members of this family, they consist on two direct repetitions

(DR) of a hexamer with an indeterminate number of random nucleotides in the middle, with prototype repetition (NGKKYA), where, 'K' is guanine or thymine and 'Y' is cytosine or thymine. The particular sequence and the number of nucleotides in the middle is what determines the binding of one or other receptor[156]. For example, the pair RXR/PPAR will preferably bind to DR with only one nucleotide in the middle (DR1), while RXR/LXR will bind to sequences with four nucleotides in the middle (DR4)[155]. The regulation executed by these nuclear receptors can follow three different mechanisms:

Transactivation: the recognition of the specific ligand promotes structural changes in the conformation of the nuclear receptor, which will displace the co-repressor complex, facilitating the activity of the co-activator complexes, and the transcription[154].

Repression: in the absence of their ligand, the heterodimers are bound to the HRE of their target genes, and recruit co-repressor complexes that impede the transcription. These complexes are often conformed by several co-regulator molecules, such as SMRT (Silencing Mediator of Retinoid acid and Thyroid-hormone Receptors) and NCoR (Nuclear-receptor Co-Repressor)[154].

Trans-repression: the heterodimers are able to inhibit the transcriptional activity of another transcription factors without binding to the DNA, through a protein-protein interaction[157]. This mechanism has been described for LXR[158] and PPARγ[159], and entails the recognition of each nuclear receptor's ligand and a post-translational SUMOylation-mediated modification of their LBD. This process allows LXR and PPARγ to inhibit the expression of pro-inflammatory genes through the stabilization of co-repressor complexes such as NCoR, and SMRT, which are located in the binding site of the promotor region of said genes[158,159].

2.2. Liver X Receptors

Liver X Receptors (LXR) α and β, are two nuclear receptors encoded by the genes *Nr1h3* and *Nr1h2* respectively, located in two different chromosomes (11 and 19 in human, 2 and 7 in mice)[155,160,161]. LXRs function as lipid and cholesterol sensors in the cells, and their typical ligands are intermediate metabolites from the cholesterol metabolism, such as oxysterols (oxidized forms of cholesterol)[162]. LXRs heterodimerize with the RXR receptor. Very potent synthetic agonists for LXR activity have been developed (T0901317 and GW3965) as well as an antagonist (GSK1440233A)[163].

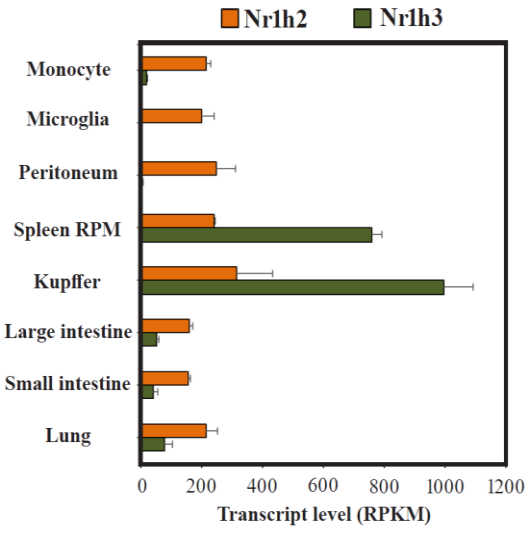

Figure 6. Data extracted and analyzed from public repository by Lavin et al. (2014). LXRα and LXRβ expression pattern in different TRM populations.

Genetically, LXRα and LXRβ share up to 75% of sequence homology in their DBD and LBD domains, both in human and

rodents, with a high degree of overlap in their target genes[164]. This means that, in most contexts, one receptor is able to compensate the other in case of necessity. However, their expression distribution throughout the organism is quite different. While LXRβ is ubiquitously expressed in every tissue, LXRα can only be detected in tissues with high metabolic activity, such as liver, kidney, intestine, adipose tissue, adrenal glands and some tissue macrophages[165]. Likewise, different TRMs present different levels of LXRα expression[16], being KCs and RPMs the populations with the highest expression (Fig. 6).

2.3. LXRs in lipid metabolism

Cholesterol is one of the essential components of cellular membranes, and is the precursor of bile acids, vitamins and steroid hormones. LXRs participate in its regulation at three levels, synthesis, absorption and catabolism[166,167]. *Cyp7a1* (Cytochrome =450, family 7, subfamily A, polypeptide 1), a limiting enzyme for bile acids synthesis, is a direct target of LXRα, and *LXRα*$^{-/-}$ mice fed with a high cholesterol diet, showed inability to metabolize cholesterol into bile acids. These mice accumulated cholesterol esters and ultimately, developed hepatic failure[168]. LXR-deficient mice and *in vitro* studies have described the effects of these nuclear receptors in the reverse cholesterol transport (RCT), the process by which the excess of peripheral tissue cholesterol and fatty acids stored inside macrophages and enterocytes is carried back to the liver by HDL (high density lipoproteins) for their elimination in form of bile acids and other catabolites[169]. Many different cholesterol metabolism related enzymes and proteins are direct targets of LXR regulation, like cholesterol transporter proteins, such as the ATP binding cassette family, ABCA1[165], ABCG1[170], ABCG5 and ABCG8[171], in charge of the correct cholesterol flow from the inside to the outside of the storage cells; extracellular cholesterol acceptor proteins, like APOE and APOC (apolipoproteins E and C)[172,173], which are part of the HDL molecules that deliver cholesterol to the liver for their elimination; and lipoprotein remodeling enzymes, like PLTP (phospholipid transfer protein) or LPL (lipoprotein lipase)[167,174]. Recent studies described the regulation by LXR of the transcription of the enzyme IDOL (inducible degrader of the LDL receptor) in peripheral tissues and macrophages[175]. IDOL is an E3 ubiquitin ligase, and degrades de LDL receptor (LDLR) by ubiquitination, stopping the uptake of LDL cholesterol, that way regulating the storage[176].

LXR also directly regulates the expression of genes that encode proteins with important functions in fatty acid synthesis, such as SREBP-1c (sterol regulatory element binding protein)[177], FAS (fatty acid synthase)[178] and ACC (acetyl CoA carboxylase)[168]. Activation of LXR activity using synthetic ligands induces the hepatic lipogenic pathway and thus elevates the plasma triglyceride levels in mice[174].

3. LXR IN MACROPHAGES

3.1. LXR in atherosclerosis

During atherosclerosis, excess of lipid material accumulates in the lumen of medium and large arteries forming the atherosclerotic plaque. As a consequence, arteries narrow causing various severe circulatory affections. Macrophages are implicated in all stages of the development of the plaques, as they are the ones that store the lipid material (cholesterol and fatty acids, primarily oxidized LDL molecules), turning into foam cells. Several studies have stated that LXR activation in these macrophages antagonizes atherogenesis, via the up-regulation of genes related to cholesterol metabolism and efflux (RCT), from cholesterol transporters (ABC family) to cholesterol acceptors (*apoe* and *apoc)*, and lipoprotein remodeling enzymes (PLTP and LPL), ensuring a correct regulation of the cholesterol metabolic pathways and lipid synthesis, and preventing the disease[179,180].

The transcriptional activity of LXRs prevents the formation of the atherosclerotic plaque during the progression of atherosclerosis in mouse models with propensity to develop the disease[181], and is able to revert it even after it has been formed. Chronic treatment with LXR synthetic agonists is able to induce the remodeling and regression of pre-existing plaques[182]. Interestingly, studies have shown that only the global absence of LXRα, and not LXRβ, associates with massive cholesterol accumulation and the acceleration of the disease in different atherosclerosis mouse models (*Apoe*$^{-/-}$ and *Ldlr*$^{-/-}$)[183–185].

3.2. LXR in immunity and inflammation

Both LXRs (α and β) are able to modulate the immune response through the repression of inflammatory genes, primarily in macrophages. Upon stimulation with LPS, TNFα, or IL-1β, they inhibit the transcription of other pro-inflammatory transcription factors, such as NF-κB, STAT and AP-1[186], and other pro-inflammatory genes, like IL-6, iNOS, COX-2 *in vitro*[169,187].

In vivo, LPS intraperitoneal injection triggered an exacerbated systemic response in *LXRαβ*$^{-/-}$ mice[186], whereas LXR synthetic agonist administration in mouse models with chronic atherogenic inflammation and hypercholesterolemia (A*poe*$^{-/-}$, *Ldlr*$^{-/-}$) drastically reduced the expression of pro-inflammatory genes[186,188]. The same outcome has been observed in mice with skin inflammation[189], and Alzheimer disease[190]. LXR activity has also an important role in the defence against microorganisms. LXR-deficient mice are susceptible to infection by *Listeria monocytogenes*[191]. *LXRα*$^{-/-}$ mice were also prone to infection with *Mycobacterium tuberculosis*[192]. Pathogen infections have been demonstrated to interfere with the correct LXR regulation of cholesterol metabolism in macrophages, establishing a link between these two facets of LXR activity. In another study, *in vitro* infection of macrophages with *Escherichia Coli* or influenza A virus caused an impairment in cholesterol efflux by the inhibition of different cholesterol carriers, such as ABCA1, ABCG1 or APOE lipoprotein[193].

3.3. LXR in apoptosis

The clearance of apoptotic material by macrophages is one of the most common mechanisms of ensuring homeostasis in the tissues, by preventing unnecessary immune reactions triggered by the accumulation of potential immunogenic Ags, which could culminate in tissue necrosis and autoimmunity[194]. This process highly affects the transcriptional program of macrophages, promoting differential genetic signatures between phagocytic and non-phagocytic cells within the same tissue[195].

In phagocytic macrophages, the engulfment of dying cells entails a considerable increase of the intracellular lipids, so they present a very active lipid metabolism that allows them to digest the ingested cellular components. This activates LXR transcriptional program, more specifically LXRα, which as was mentioned before, is most expressed in TRM. Studies by A-Gonzalez et al. (2009) demonstrated that the clearance of apoptotic thymocytes is severely impaired in the absence of LXR signaling *in vitro*, and LXR-null mice presented a large amount of accumulated unengulfed apoptotic cells in the thymus, spleen, lungs and testis, resulting in the loss of tissue homeostasis[196]. Phagocytosis of apoptotic cells was significantly enhanced when *in vitro* macrophages were stimulated with an LXR agonist[196]. Additionally, *in vitro* expression assays and transcriptional profiling, identified apoptotic mediator Mer receptor as an LXR direct target gene[197]. LXR-deficient mice often present age-dependent chronic inflammation and maintained systemic auto-immune reactions, derived from the presence of auto-antibodies and immune cells infiltrations in several tissues, which can ultimately drive to the development of a number of auto-immune diseases. However, chronic administration of synthetic LXR agonists ameliorates the progression of auto-immunity in a lupus-like disease mouse model[196].

3.4. LXRα in splenic macrophages

As was mentioned before, among the different TRM populations, splenic RPMs and hepatic KCs are the ones that present the highest levels of LXRα expression[16] (Fig. 6) compared to others, such as microglia or resident peritoneal macrophages[36]. A-Gonzalez et al. (2013) reported the implication of the expression of LXR in hematopoietic cells in the development of the macrophages of the MZ of the spleen (MZM)[63]. Immunofluorescence analysis showed that both *LXRαβ*$^{-/-}$ and *LXRα*$^{-/-}$ mice completely lacked the MZ region of the spleen, and thus presented an abnormal response to blood-borne Ags. Upon WT and *LXRβ*$^{-/-}$ bone marrow transplantation, the MZ was reconstituted in these two mouse models, revealing the genuine implication of LXRα in the development of the MZM compartment in the spleen[63].

This data enlightens the important role of LXRα, above LXRβ, in the correct hematopoietic development of the different macrophage subpopulations of the spleen, and raises the question of whether LXRα expression also affects the development of the RPM compartment, along with its functionality, both immunologically and metabolically.

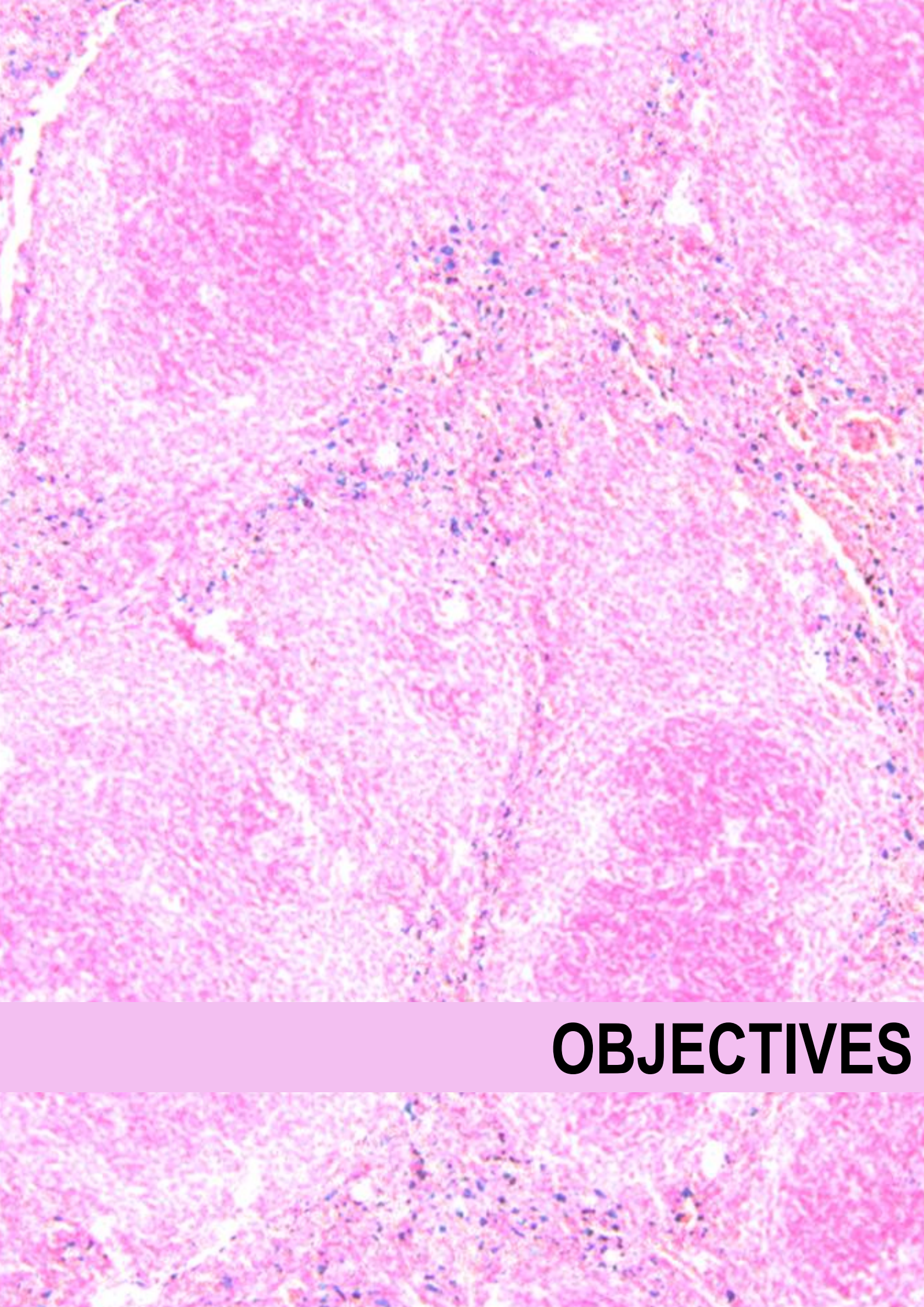

OBJECTIVES

Objectives

1. Generation of new mouse models suitable for the analysis of LXRα expression and function in different types of tissue resident macrophage populations.

2. Study of the role of LXRα nuclear receptor in the differentiation and functioning of tissue resident macrophages and their relation with iron homeostasis

3. Comparison between the transcriptional profiles of red pulp macrophage population in WT mice and LXR-deficient mice. Identification of new LXR target genes, and description of the possible metabolic pathways regulated by these nuclear receptors in this macrophage population.

4. Analysis of the possible physiopathological consequences in vivo due to defects in splenic and bone marrow macrophages in LXR-deficient mice.

5. Defining a complete transcriptional signature of iron-handling macrophages in mice and its dependence of LXRα signaling.

6. Design of a molecular model that describes the role of LXRs in the correct development and functioning of red pulp macrophages.

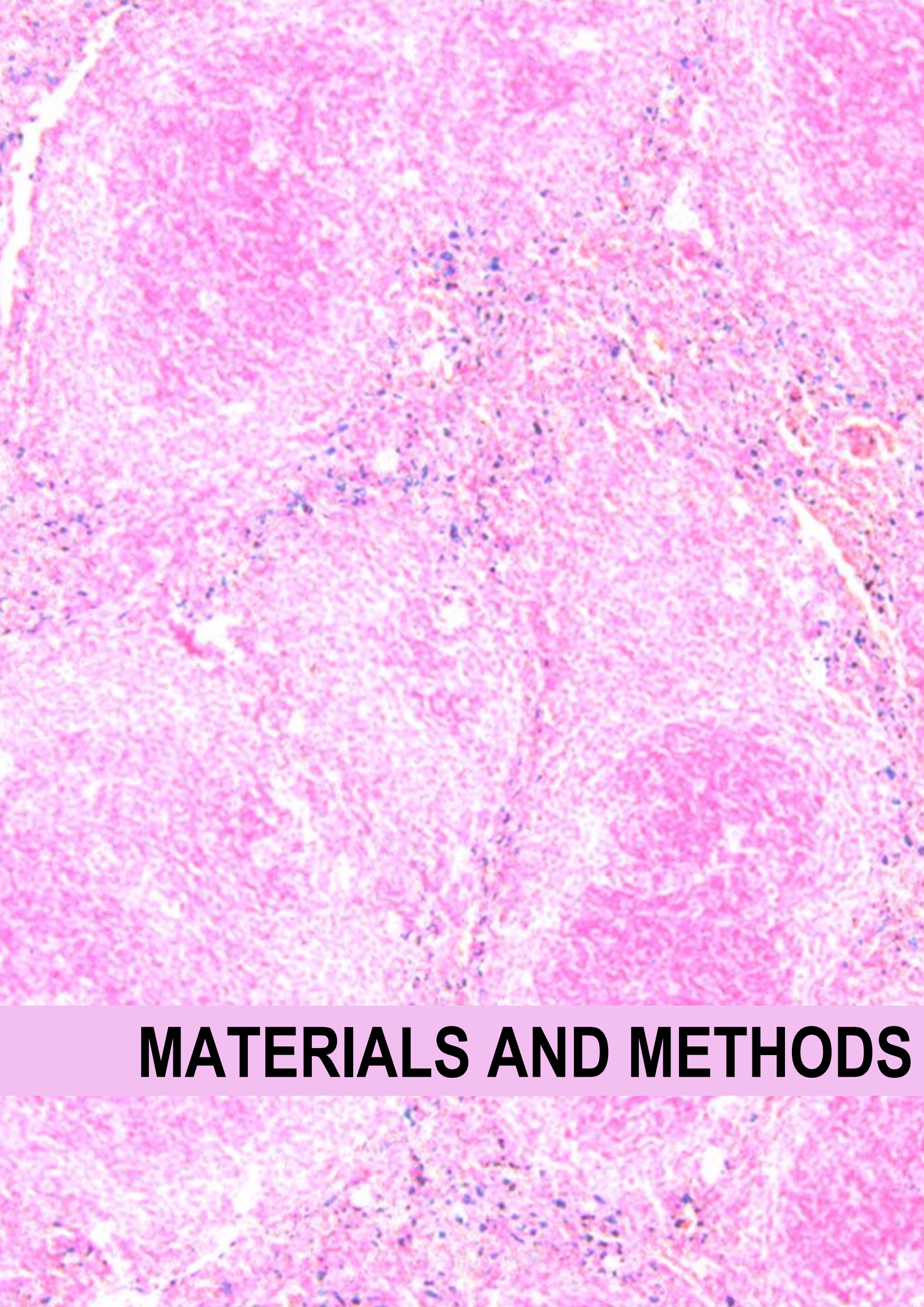

MATERIALS AND METHODS

Materials and methods

Animals

LXRα deficient and LXR double deficient (*Nr1h3*$^{-/-}$;*Nr1h2*$^{-/-}$) mice on pure C57BL/6 background were originally provided by David Mangelsdorf and have been described in our previous publications (UTSW)[63,195,196]. Mice with conditional ablation of LXRα in macrophages were generated by crossing LXRα$^{fl/fl}$ mice (previously reported in A-Gonzalez *et al*. 2013)[63] with transgenic mice expressing Cre-recombinase under the *Fcgr1* (encoding CD64) promoter[198]. These mice were harbored at the VIB Research Institute, Ghent Belgium under a collaboration with Dr. Martin Guilliams (Fig. 7E). The generation of the other two new mouse models was performed as follows: Constitutive *Knockin* mouse models LXRα -DTR/DsRed (Fig. 7A, B) and LXRα-GFP mice (Fig. 7C, D) were generated by classical targeted homologous recombination performed in murine ES cells, through electroporation of DNA target constructs generated by Red/ET recombination at the EMBL spin-off "GeneBridges" at Heidelberg, Germany. Briefly, the LXRα -DTR/DsRed target vector was created with a DNA cassette encoding for the human HB-EGF (Diphteria toxin) receptor as a fusion with the DNA encoding for the Red fluorescent protein (DsRed) from *Discosoma sp*. This strategy aimed to generate the LXRα DTR and the reporter expression together as an indicator of LXRα expression, and as a means to specifically deplete LXRα-expressing cells in the same mouse model. DsRed fluorescence, however, was not observed with any of the available techniques. At present, the reason/s for the failure to detect DsRed protein expression are unknown, but similar examples in recent literature have been also experienced[199]. Failure to see reporter expression in these mice was the reason to create the second mouse model with a targeting vector harbouring the DNA encoding the enhanced GFP (EGFP) protein. In both mouse models, DNA was inserted in frame within the first coding exon of the *Nr1h3* gene. Generation of recombinant ES cells and chimeric mice was performed at the transgenic core facilities of CNB CSIC-UAM, campus Cantoblanco and Centro Nacional de Investigaciones Cardiovasculares (CNIC) with the help of Dr. Andrés Hidalgo, Giovanna Giovinazzo and Luis M. Criado (CNIC), and Belen Pintado and Verónica Dominguez from CNB-UAM. We thank all these collaborators for their tireless efforts in the generation of these mice. All mice were maintained under pathogen-free conditions in a temperature-controlled room and a 12-hour light-dark cycle in the animal facilities of IIBM-CSIC vivarium. Experiments to specifically deplete LXRα-expressing cells using the LXRα-DTR mouse model were conducted at the CNIC animal facility under the supervision and ethical procedure of our collaborator Dr. Andrés Hidalgo. All other animal studies were conducted in accordance with institutional CSIC-UAM animal research committees.

Flow Cytometry

To characterize macrophage populations by flow cytometry, single cell suspensions from spleens and bone marrow were obtained from mice and processed by different methods. Spleen processing was performed with a Spleen Dissociator Kit (Miltenyi Biotec, 130-095-926) and gentleMACS Dissociator (Miltenyi Biotec); cell suspensions of bone marrow were obtained by gentle flux of femurs with cold PBS and centrifugation. Red blood cells (RBCs) were lysated using Versalyse lysing solution (Beckman Coulter, 2 mL for spleen and 600 µL for femur samples) for 2 minutes, washed with 10 mL of FACS buffer (PBS, 2% FBS and 5mM EDTA), and centrifuged for 300 xg for 5 minutes. After resuspension, $5x10^6$ cells were incubated in 70 µL with fluorescence-labeled antibodies for 20 min at room temperature (see gating strategy in Fig.

8). After incubation cells were washed with 1 mL of FACS buffer, centrifuged for 5 minutes at 300 xg, and cell pellets were resuspended in 200 µL of FACS buffer. Samples were analyzed in FACS Canto II Flow Cytometer (Becton-Dickinson) and data was represented using FlowJo software (Treestar, Inc.).

Cell sorting

Spleen cell suspension was obtained as described above. After RBC lysis, cells were dissolved at a concentration suggested by the Miltenyi magnetic enrichment protocol; that is 90 µL /10^7 cells of FACS Buffer (PBS, 2% FBS and 5mM EDTA) for F4/80$^+$ enrichment protocol:

- Cell purification for genome-wide transcriptional analysis: after resuspension, cells were incubated with 10 µL/10^7 cells of FcR Blocking Reagent mouse (Miltenyi Biotec, 130-092-575) for 15 minutes at 2-8°C. Next, cells were incubated with F4/80-Biotin antibody (Biorad MCA497G) at a concentration of 5 µg/mL for 20 minutes at 2-8ºC. Cell suspensions were then washed with FACS Buffer (1 mL per 10^7 cells) and centrifuged at 300 xg for 5 minutes. Pellets were resuspended in 90 µL /10^7 cells and incubated with 20 µL/10^7 cells of Anti-Biotin Microbeads (Miltenyi Biotec, 130-090-485) for 15-20 minutes at 2-8°C. Cells were washed again with 1 mL/10^7 cells of FACS Buffer and centrifuged at 300 xg for 5 minutes to eliminate the excess of Anti-Biotin Microbeads. Pellets were resuspended up to 10^8 cells in 500 µL of FACS Buffer, and applied onto MS Columns (Miltenyi Biotec 130-042-201) placed in OctoMACS™ Separator Miltenyi Biotec (130-042-109) device for magnetic separation of F4/80$^+$ cells. After collection of the positive fraction, cells were incubated with fluorescent antibodies for 20 min and sorted in a FACS-Vantage SE (Becton-Dickinson) (see sorting strategy in Fig. 9). Purified cells were directly sorted into RNA lysis buffer and RNA was purified with an RNeasy® Plus micro-kit (Qiagen, 74034) according to the instructions of the manufacturer.
- Cell purification for targeted qPCR: To analyze RPM gene expression, FACS-sorted cells were directly incubated with Cells Direct One-Step mRNA qRT-PCR Kit (Invitrogen, 46-7200) following Kit instructions. Single cell suspensions of splenocytes were obtained as indicated above in Flow Cytometry protocol. 5x10^6 cells (diluted in 70 µL) were incubated with fluorescent antibodies (see sorting strategy, Fig. 9) for 20 minutes at room temperature. Biological replicates of 500 cells were collected after sorting in 0,2 mL Eppendorf tubes containing 10 µL of 2X Reaction Mix buffer, and flash freezed in dry ice prior to RNA analysis.

Transcriptional profiling and Biological pathway analysis

Transcriptional profiling of RNA expression was studied using Affymetrix Clariom S microarrays (Applied Biosystems catalog #902930). Data from raw expression values was obtained as Log2 signals and normalized to reference genes. Data was processed by the Genomic Unit of the Complutense University of Madrid (https:ucm.es/gyp/genomica-3). Heatmap representations were performed according to logarithmic-transformed values (Log2) of fold change expression (Z-score= ± 2) and arranged in decreasing order of magnitude. Gene Ontology Biological Process Analysis (GO BP terms) was performed on transcripts classified in the three heatmap categories, under program default settings. Only significant terms (p-value>10-2) are shown.

Materials and methods

Real-time qPCR analysis

For total tissue expression, mRNA was isolated from spleens using TRI Reagent Solution (Invitrogen cat#AM9738) and reverse transcribed to cDNA using iScript cDNA Synthesis kit (Bio-Rad 170-8891) on 2720 Thermal Cycler (Applied Biosystems).

For sorted cells, mRNA extraction kit Cells Direct One-Step qRT-PCR Kit (Invitrogen, cat#46-7200) was used following Kit instructions. Samples were flash-freezed immediately on dry ice. For pre-amplification and reverse transcription to cDNA same Thermal Cycler was used. Real-time quantitative PCR analysis was performed with Mx3005P Thermal Cycler apparatus (Stratagene) and Power SYBR Green PCR Master Mix (Applied Biosystems cat#4309155). PCR primers are listed on Table 2. The amplification of cDNA was carried out with an initial denaturation of 95°C for 10 minutes, followed by 40 cycles of 95°C for 30 seconds, 55°C for 1 minute and then 72°C for 1 minute. The relative mRNA expression of target genes was normalized to 36B4 mRNA expression.

Immunofluorescence analysis

Spleens were harvested and fixed with 4% paraformaldehyde for 24 h at 4°C and were further incubated 24 h in PBS supplemented with 30% sucrose. Tissues were embedded in optimal cutting temperature (OCT) preservation liquid and cryopreserved in dry-ice. Spleens were sectioned (4-8 µm) and stained with fluorescent conjugated antibodies (see Table 3) for 1 hour, and washed three times with cold PBS. Stained sections were fixed over night with ProLong Diamond Antifade Mountant (cat#P36961) and observed under confocal microscope (espectral Zeiss LSM710). For visual analysis of the images, ImageJ (1.51 J8) software was used.

Citospin and tissue iron staining

For single-cell staining, $2x10^5$ RPM were FACS-sorted (see sorting strategy, Fig. 9) into RPMI medium (10% FBS), placed on a citospin slide-chamber and citocentrifuged in a Cyto-Chamber (Hettich Zentrifugen) at 600 xg for 2 minutes. Cells were then fixed with PFA and prepared for further staining. For tissue staining, paraffin embedded spleen sections (4-8 µm) were collected, deparaffined in xylene and washed with PBS. In both cases, Prussian Blue staining (Iron Stain ab156674, ABCAM) was used to visualize iron deposits. Slides were observed under Axiophot Zeiss microscope and pictures were analyzed using ImageJ (1.51 J8) software.

Iron (Fe^{2+}) and Hemoglobin quantification

Spleen and bone marrow tissue extracts were obtained by mechanical homogenization, and Iron assay kit (ABCAM ab83366) was used to quantify Fe^{2+} content according to manufacturer instructions. For hemoglobin analysis, blood samples (10 µL) were extracted from the mouse facial vein, diluted into 1 mL of water and centrifuged at 14.000 rpm for 5 minutes. Supernatant was collected, and 100 µL were mixed with another 100 µL of water and measured absorbance in a spectrophotometer at 540 O.D. For spleen hemoglobin analysis, tissue was collected and weighted. Hemoglobin measurement was performed by mechanical homogenization of spleen (40 mg of tissue approximately) in 500 µL of water and centrifuged at 14.000 rpm for 5 minutes. Supernatant was collected, and 200 µL were used for absorbance analysis in

a spectrophotometer at 540 O.D. Bone marrow was extracted by gentle collection of tibia content and diluted into 200 µL of water. After bone marrow extraction from the bone, samples were centrifuged at 14.000 rpm for 5 minutes. Supernatants were collected and measured absorbance in a spectrophotometer at 540 O.D.

Statistical analysis

Data was expressed as mean ± SEM. Statistical analysis was performed using Student's t test for significant differences. Values of $P<0.05$ (*) or $P<0.01$ (**), were considered to be significant, and values of $P<0.001$ (***) were considered to be very significant.

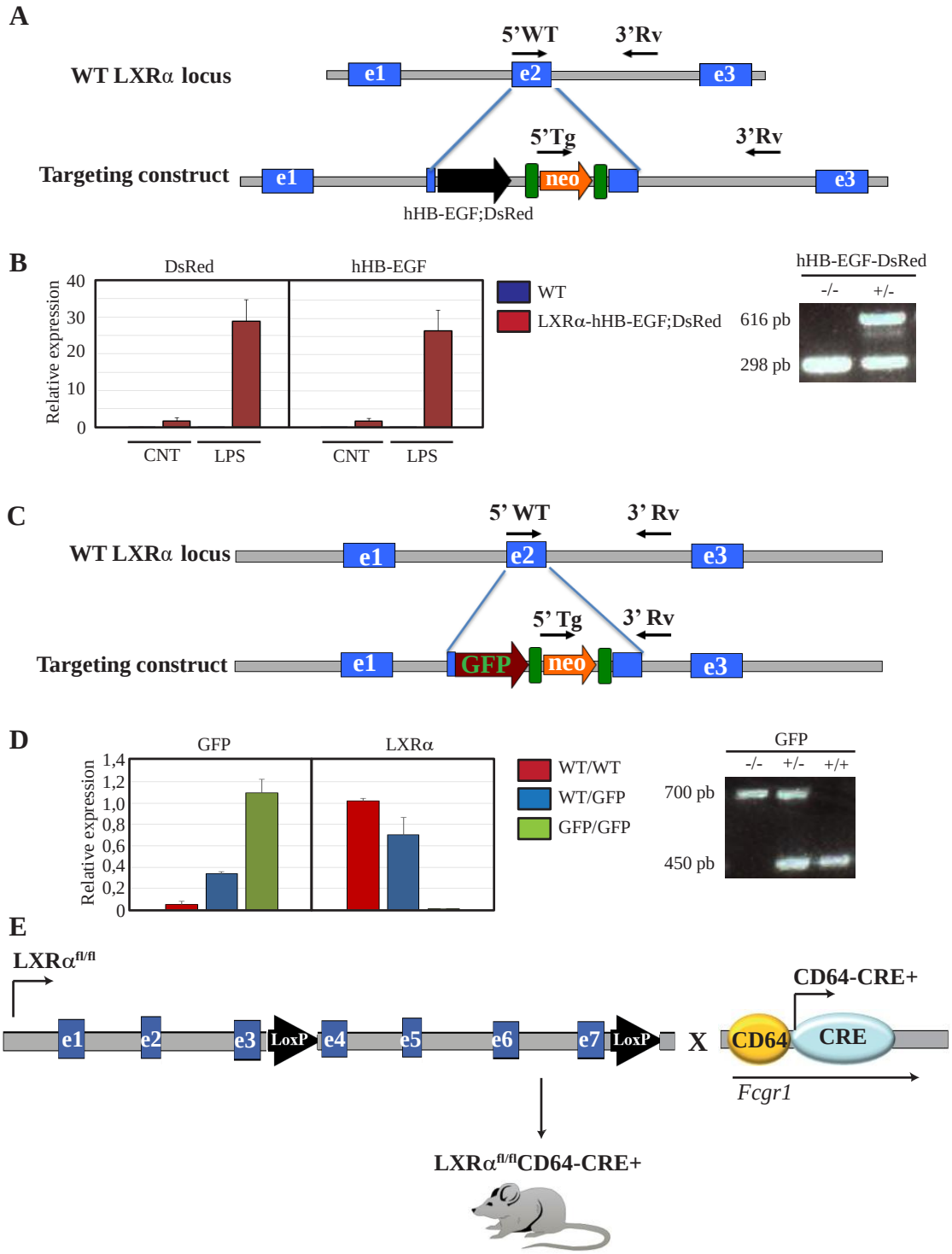

Figure 7. A) Genetic strategy for the creation of LXRα-DTR-DsRed mutant mice. **B)** Quantitative expression of DsRed and hHB-EGF of both WT and LXRα-DsRed-hH-EGF mice in basal conditions (Ctrl) and 48 hours after LPS intraperitoneal injection (1 mg/kg, 200 µl) (left); PCR genotyping of WT and LXRα-DsRed-hHB-EGF$^{+/-}$ mice (right). **C)** Genetic strategy for the creation of LXRα-GFP reporter mutant mice. **D)** RNA expression analysis by qRT-PCR of EGFP (enhanced GFP) and LXRα in total spleen samples from WT/WT, WT/GFP and GFP/GFP mice (left); PCR expression of E-GFP on WT/WT, WT/GFP and GFP/GFP mice (right). **E)** LXRα$^{fl/fl}$CD64-CRE^{+} mice genetic construct.

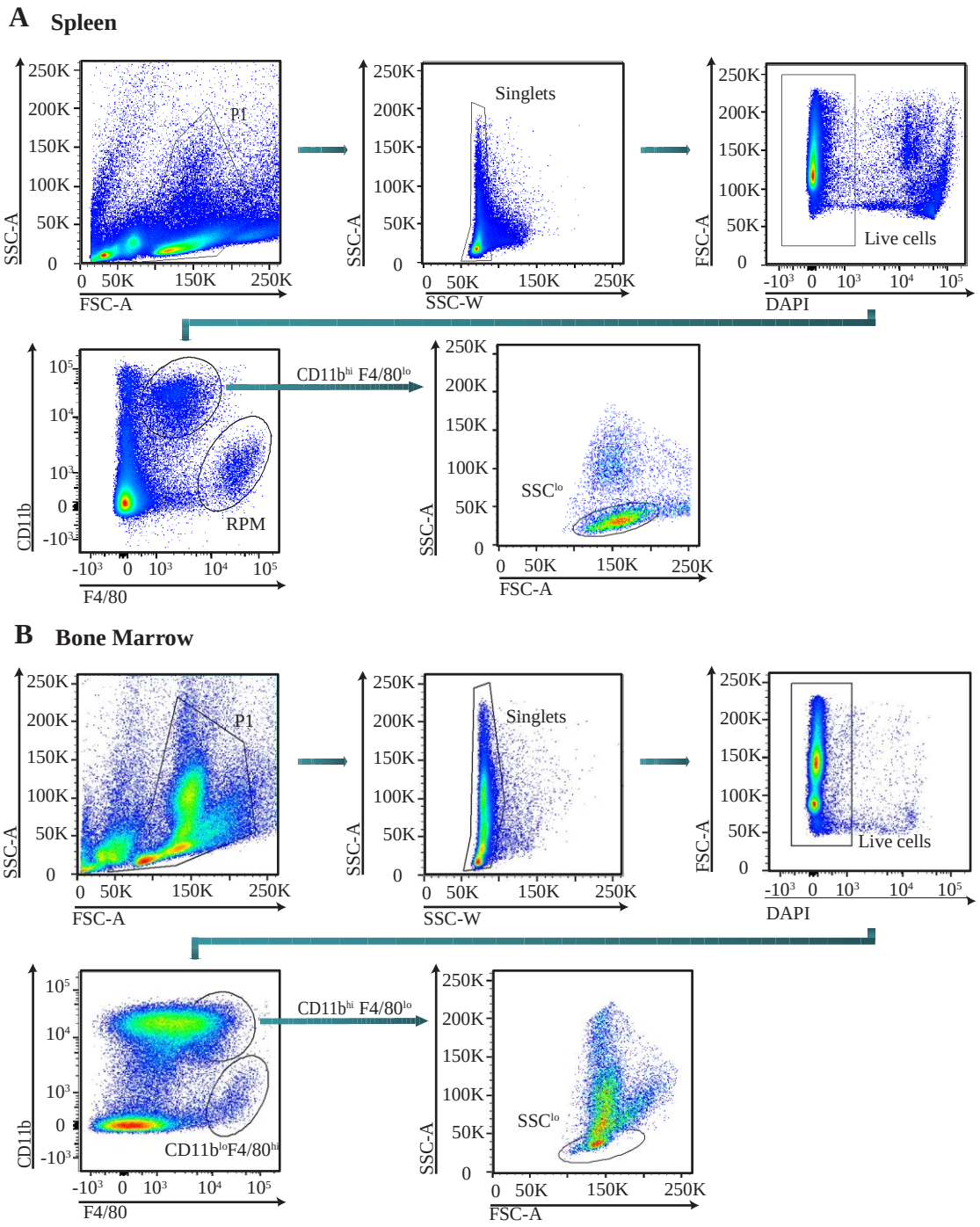

Figure 8. Flow Cytometry gating strategy for the identification of resident macrophages in the spleen **(A)** and bone marrow **(B).**

A **Sorting strategy**

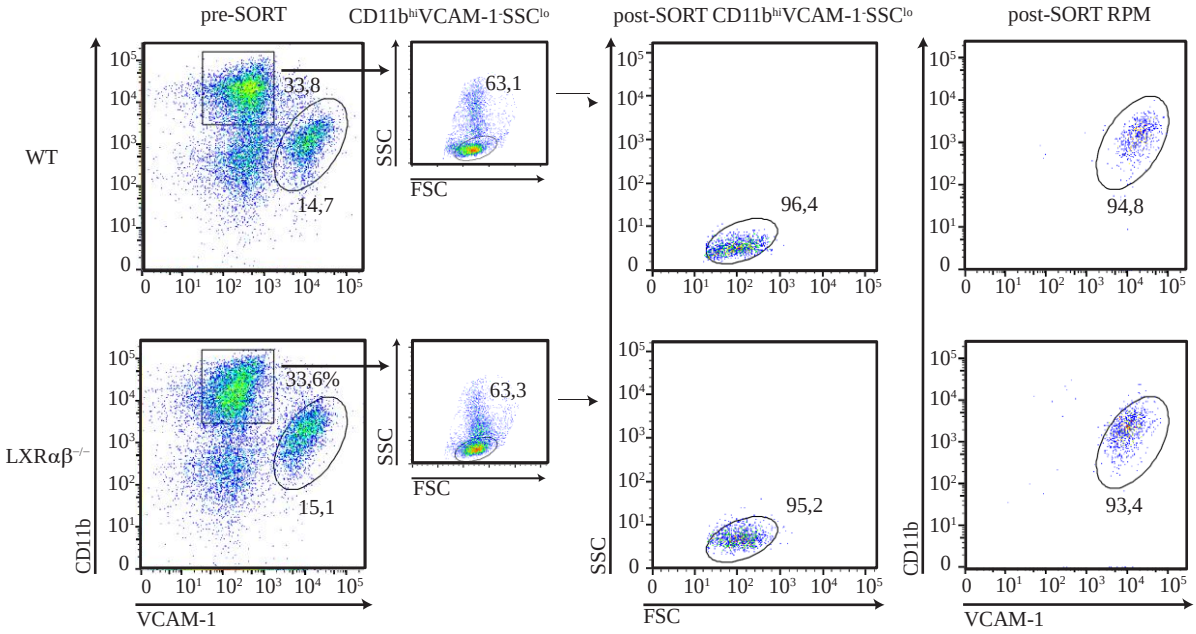

Figure 9. A) Cell Sorting strategy for CD11b^{hi}F4/80^{lo}SSC^{lo} monocyte and CD11b^{lo}F4/80^{hi} RPM purification. Pre-sort (left panels): percentages correspond to magnetic enrichment of F4/80^{+} splenocytes and subsequent analysis using expression of CD11b and VCAM-1 markers. Post-sort: Corroboration of cell purity after cell sorting (Plots on the right).

Table 1.

Genotyping	
	5' ⟶ 3'
DTR-DsRed	
Nr1h3 fwd	AAGAGATGTCCTTGTGGCT GGAG
Nr1h3 rev	GAGCGGACAGAACT CTCAAAGC
hH-EGF fwd	GTTGGGCATGACTAATTCCCAC
DsRed rev	GATTGACT TGAACT CCACCAGG
GFP	
GFP: Nr1h3fwd	CAGT CGATCCT GTGAGGACA
GFP: Nr1h3rev KI	TCTTGTAGT TGCCGT CGT CC
GFP: Nr1h3rev W T	GGT AGCTAACGGACAGCTCAT
LXRαβ$^{-/-}$	
Nr1h3 fwd	TTGTGCCCAGTCATAGCCGAAT
Nr1h3 rev	TCAGTGGAGGGAAGGAAATG
Nr1h3 rev	TTCCTGCCCTGGACACTTAC
Nr1h2 fwd	AGGTGAGATGACAGGAGATC
Nr1h2 rev	CCTTTTCTCCCGACACCG
Nr1h2 rev	GCATCCATCTGGCAGGT TC

Table 1. Genotyping primer 5´→ 3´ sequences for LXRα-hHB-EGF;DsRed, LXRα –GFP and LXRα$^{-/-}$ and LXRαβ$^{-/-}$ mouse models.

Table 2.

rt-qPCR	
	5'⟶ 3'
Vcam1 fwd	TGCGAGTCACCATTGTTCTCAT
Vcam1 rev	CATGGTCAGAACGGACTTGGA
36b4 fwd	GGCCCTGCACTCTCGCTTTC
36b4 rev	TGCCAGGACGCGCTTGT
Spic fwd	TCCGCAACCCAAGACTCTTCAA
Spic rev	GGGTTCTCTGTGGGTGACATTCCAT
Hmox1 fwd	CACAGATGGCGTCACTTCGTC
Hmox1 rev	GTGAGGACCCACTGGAGGAG
Nr1h3 fwd	CCTTCCTCAAGGACTTCAGTTACA
Nr1h3 rev	CATGGCTCTGGAGAACTCAAAGAT
Timd4 fwd	AAAGGGTCCGCCTTCACTAC
Timd4 rev	TGCTTCTTTGAGAGTGATTGGA
Cd5l fwd	TTTGTTGGATCGTGTTTTTCAGA
Cd5l rev	CTTCACAGCGGTGGGCA
Mertk fwd	ACACGGGGAATGACTCCCTA
Mertk rev	TGTCATACAGTTCATCCAAGCAGT
Abca1 fwd	GCAGATCAAGCATCCCAACT
Abca1 rev	CCAGAGAATGTTTCATTGTCCA
Slc40a1 fwd	GGGTGGATAAGAATGCCAGACT
Slc40a1 rev	ATGACGGACACATTCTGAACCA
Cd163 fwd	TCTCAGTGCCTCTGCTGTCA
Cd163 rev	CGCCAGTCTCAGTTCCTTCT
Sirpα fwd	CTGAAGGTGACTCAGCCTGAGAAA
Sirpα rev	ACTGATACGGATGGAAAAGTCCAT
Marco fwd	GGCACCAAGGGAGACAAA
Marco rev	TCCCTTCATGCCCATGTC
EGFP fwd	CGACGGCAACTACAAGAC
EGFP rev	TAGTTGTACTCCAGCTTGTGC
DsRed fwd	GAAGGGCGAGATCCACAAG
DsRed rev	TGACTTGAACTCCACCAGGTAGT
Slc11a1 fwd	GCAGGCCCAGTTATGGCTC
Slc11a1 rev	CAGGCTGAATGTACCCTGGTC

Table 2. Quantitative PCR analysis primer 5´→ 3´ sequences.

Table 3.

Flow Cytometry Antibodies					
Receptor	Fluorophore	Clone	Distributor	Cat.	Title
CD11b	PeCy7	M1/70	Biolegend	101216	0,5 µL/10^7 cells
CD11c	PerCP-Cy5.5	HL3	BD Pharmingen	560584	1 µL/10^7 cells
MERTK	PE	2B10C42	Biolegend	151505	1 µL/10^7 cells
F4/80	APC	BM8	Biolegend	123116	1 µL/10^7 cells
CD115	APC	AFS98	Biolegend	135509	1 µL/10^7 cells
VCAM-1	PE	429 (MVCAM.A)	Biolegend	105713	1 µL/10^7 cells
TIM4	PE	RMT4-54	Biolegend	130005	1 µL/10^7 cells
CD172α (SIRP1α)	PerCP-eFluor 710	P84	Invitrogen	46-1721-80	1 µL/10^7 cells
CD163	PE	TNKUPJ	Invitrogen	12-1631-82	1 µL/10^7 cells
CD163	PerCP-eFluor 710	TNKUPJ	Invitrogen	46-1631-80	1 µL/10^7 cells
CD64	PE	X54-5/7.1	Biolegend	139303	1 µL/10^7 cells

Table 3. Antibody specification for flow cytometry analysis. Fluorophores, clones and titles used for every marker are indicated.

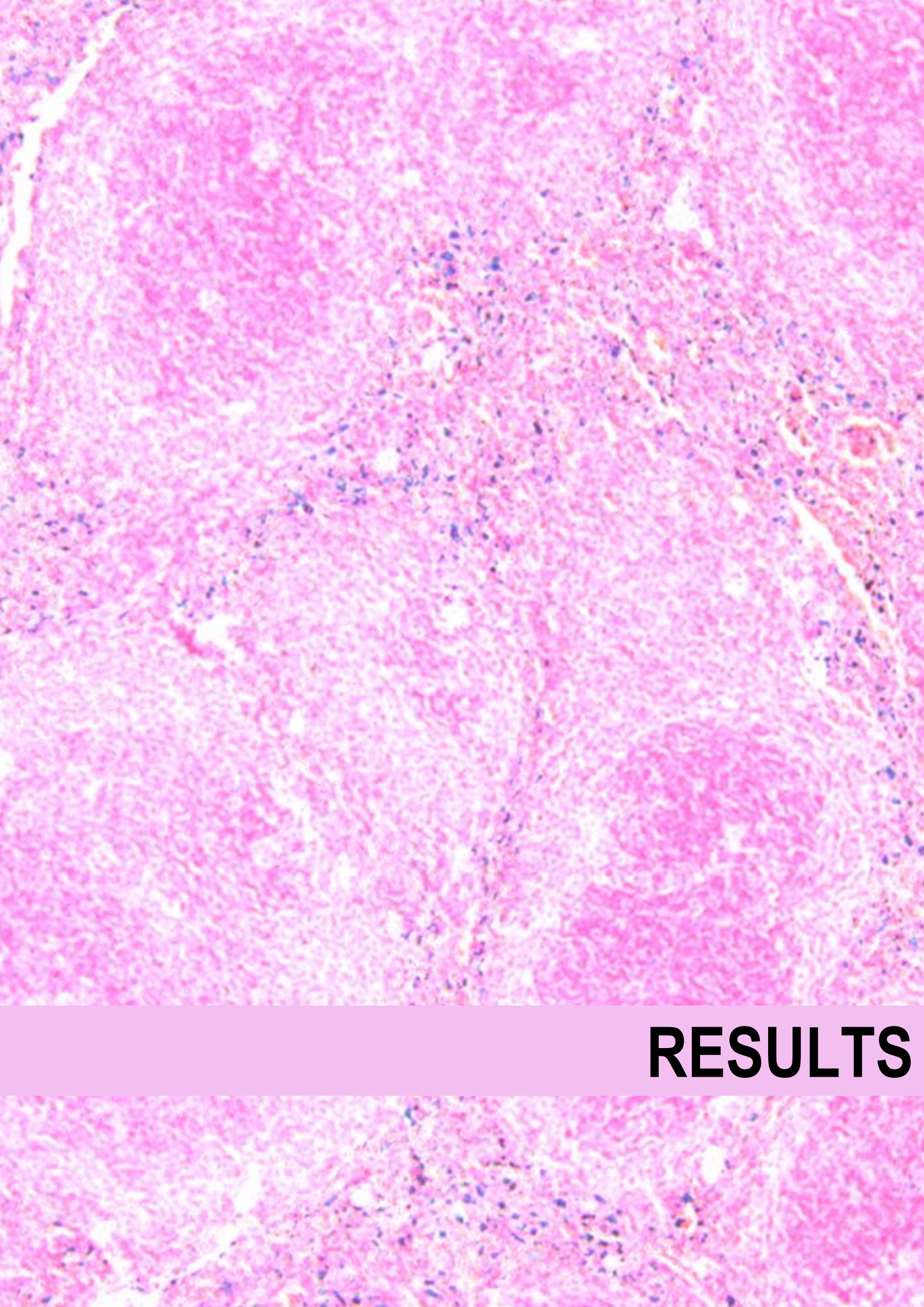

RESULTS

Results

1. LXRα is highly expressed in macrophages from the marginal zone and red pulp splenic compartments

In order to explore the in vivo regulation of RPMs through manipulation of the LXRα pathway, we created a *knockin* mouse model in which we introduced a cDNA encoding human DTR into the first coding exon of LXRα (LXRα-DTR). By targeting the DTR sequence into the LXRα coding exon, we disrupted the structure of the LXRα locus and the endogenous mechanisms that regulate LXRα expression, control the expression of DTR at physiological levels (see Fig. 7A, Materials and methods). DTR was expressed as a fusion protein with DsRed using a T2A peptide linker. Thus, our initial goal was to generate a mouse model with a dual purpose. First, the DTR expression would allow us to specifically deplete cells that normally express LXRα in tissues upon DT stimulation *in vivo*. Second, the DsRed protein would ideally allow us to visualize cells that normally express LXRα by observing DsRed fluorescence. However, even though the presence of DsRed transcript was verified by quantitative real-time PCR in the spleen (Fig 7B, Materials and methods), red fluorescence could not be detected by flow cytometry or immunofluorescence (data not shown). This experimental problem did not preclude us from continuing exploring the utility of the DTR expression in this mouse model. Since LXRα is highly expressed in liver hepatocytes, direct injection of DT into LXRα-DTR mice causes severe liver damage and acute death[200]. Therefore, to explore the effectiveness of DTR stimulation to deplete LXRα-expressing cells, avoiding the toxicity of DTR expression in hepatocytes, we used a protocol of bone marrow transplantation (Fig. 10A).

WT mice who received bone marrow from LXRα-DTR mice (LXRα-DTR→C57BL6) survived an acute DT injection after 10 weeks post-transplant (Fig. 10A). To test which bone marrow-derived cells are targeted within the splenic myeloid compartment by DTR stimulation, we analyzed the frequency of myeloid cells in the spleen. We tested whether LXRα expressing myeloid cells could be depleted by DT administration. $CD11b^{lo}F4/80^{hi}$ (RPM) compartment almost completely disappeared at 24h post DT injection (Fig. 10B). Also, $CD11b^{hi}F4/80^{lo}$ monocyte population was severely impaired, indicating that a portion of this population expresses LXRα too, to a lesser extent (Fig. 10B). These results were confirmed by immunofluorescence using CD169 and F4/80 conjugated antibodies as markers for marginal zone and red pulp myeloid cells respectively (Fig. 10C). DT injection effectively suppressed the immunofluorescence signal of both antibodies, indicating that cells expressing these markers were depleted. Thus, these functional studies using our LXRα-DTR mouse model illustrate how LXRα is highly represented in macrophages from the MZ and red pulp in the spleen and a portion of resident monocytes in the splenic red pulp compartment.

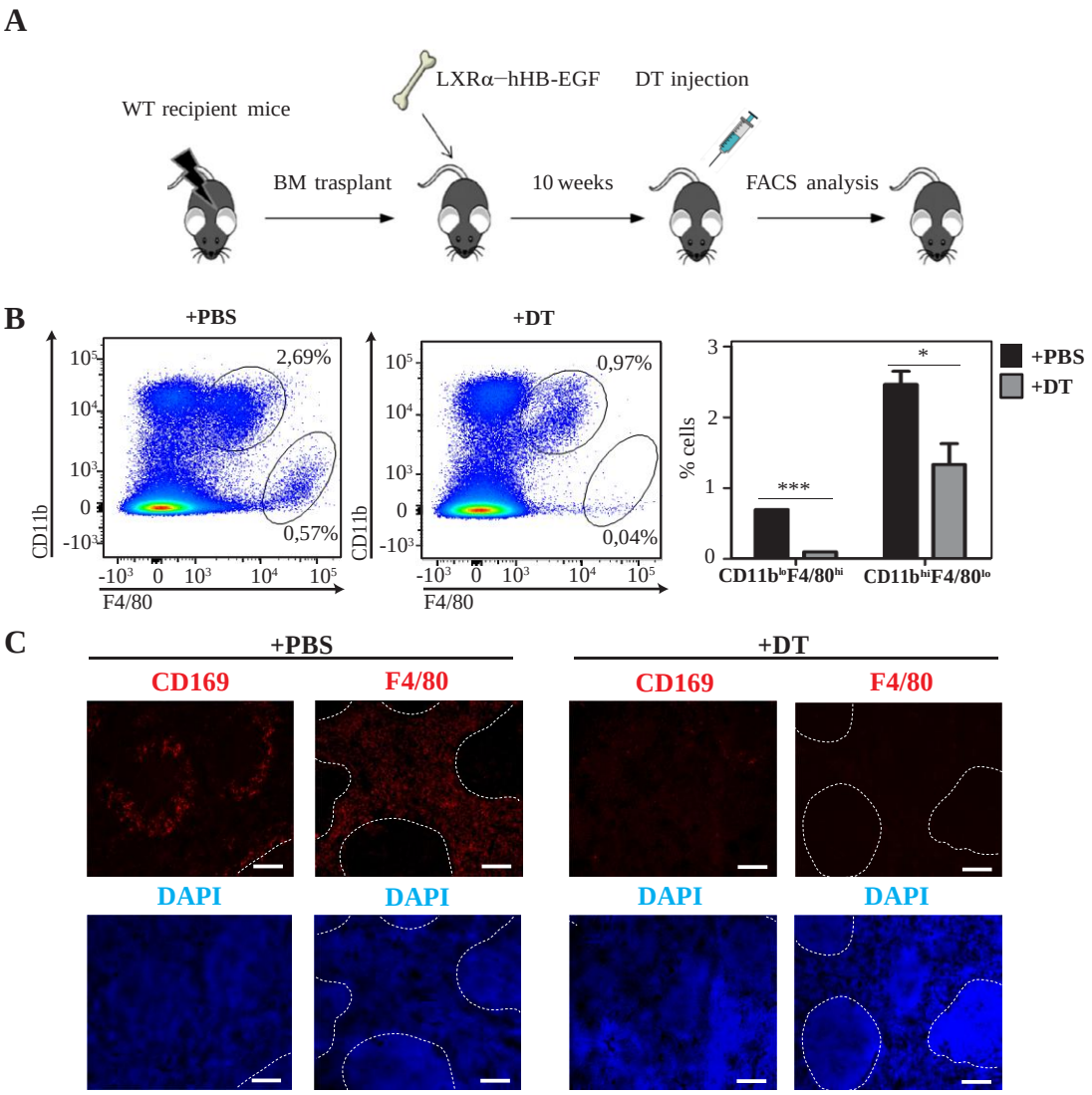

Figure 10. A) Bone marrow transplant diagram. WT recipient mice were irradiated and transplanted with LXRα-hHB-EGF bone marrow. After 10 weeks, they were injected intraperitoneally with DT (10 ηg/mouse) or PBS, and euthanized 24 hours later to analyze by flow cytometry. **B)** Flow cytometry analysis of $CD11b^{lo}F4/80^{hi}$ RPMs and $CD11b^{hi}F4/80^{lo}$ monocyte population in spleens of injected WT mice. Representative plots from 3 independent experiments with n=3, and quantifications. **C)** Immunofluorescence analysis of representative spleen sections from WT mice transplanted with LXRα-DTR bone marrow and stained with F4/80 and CD169 antibodies. Images show DT-dependent ablation of both $F4/80^{+}$ RPM and $CD169^{+}$ macrophages in DT injected mice. Scale bars = 100 μm. Data was expressed as mean ± SEM. Statistical analysis was performed using Student's t test for significant differences. Values of $P < 0.05$ (*) or $P < 0.01$ (**), were considered to be significant, and values of $P < 0.001$ (***) were considered to be very significant.

2. LXRs control the frequency of CD11b^{lo}F4/80^{hi} splenic resident macrophages

Prior studies from our group suggested that the presence of F4/80^{+} cells in the splenic red pulp was similar between WT and LXR-null mice[63]. These results were based on an immunohistochemistry (IHC) screen on multiple tissues (including the spleen) using F4/80 antibody as the sole probe for the analysis. Since F4/80 antigen is present in RPMs and monocytes within the splenic red pulp compartment, such IHC screen did not properly discriminate between these two cell types. With the advances of multicolor flow cytometry, however, we were able to make this discrimination. RPMs have been extensively characterized by the expression of surface markers as CD11b^{lo}F4/80^{hi}VCAM-1^{hi}. We also used CD11c to design a gating strategy to phenotipically define this population, as well as resident monocytes, in the spleens of LXRαβ$^{-/-}$ mice compared to WT controls.

Surprisingly, in addition to present defects in the marginal zone macrophage (F4/80^{lo}CD169^{+}) population as previously reported[63], the RPM compartment was also affected in LXRαβ$^{-/-}$ mice. These mice presented a marked reduction in CD11b^{lo}F4/80^{hi}VCAM-1^{hi} cells compared to their WT counterparts (Fig. 11A, C). In contrast, the frequency of CD11b^{hi}F4/80^{lo}SSC^{lo} monocyte population (see gating strategy in Fig. 8A and B, Materials and methods) appeared to be clearly increased in LXRαβ$^{-/-}$ mice (Fig. 11A, C). We next analyzed the levels of expression of each one of these surface markers on the RPM population, using fluorescence mean intensity (FMI) comparison. The small fraction of CD11b^{lo}F4/80^{hi} macrophages that remains in LXRαβ$^{-/-}$ spleens presented lower levels of F4/80 and VCAM-1, whereas CD11b and CD11c levels appeared to be higher in these mice compared to their WT controls (Fig. 11B).

These results indicate that, not only the percentage of RPMs is reduced in LXRαβ$^{-/-}$ mice, but they also have a different phenotype compared to WT RPM, displaying reduce expression of F4/80 or VCAM-1 antigens. In contrast, LXR-deficient mice exhibit a higher representation of splenic monocytes.

As has been explained in the introduction of this work, BMMs display phenotypical and functional similarities to RPMs, and have been suggested to share a common origin with them[101]. Indeed, RPMs and BMMs share a common panel of expression markers, and they both require the transcription factor SPI-C for their development. The levels of macrophage-associated markers analyzed for RPMs above were also tested in BMMs, including F4/80 and CD11b, and the results showed that the percentage and number of CD11b^{lo}F4/80^{hi} BMMs was markedly reduced in LXR-deficient mice compared to WT controls (Fig. 12A, B). Similar to the red pulp of the spleen, LXRαβ$^{-/-}$ mice also presented an increase in CD11b^{hi}F4/80^{lo}SSC^{lo} monocyte population (Fig. 12A. B). These results indicate that the two related populations of resident macrophages in the spleen and the bone marrow require an intact LXR activity for their correct distribution in the steady state.

Next, we wonder whether the CD11b^{hi}F4/80^{lo}SSC^{lo} monocytes accumulation that we appreciated in the spleens and bone marrow of LXR-deficient mice could constitute and attempt of the bone marrow HSC-derived progenitors to fill the impaired RPM niche in these mice. Further flow cytometry analysis of the blood using the monocyte markers CD11b and CD115, showed a clear increase of the BM-derived circulating monocytes in LXR-deficient mice compared to WT controls (Fig. 12C).

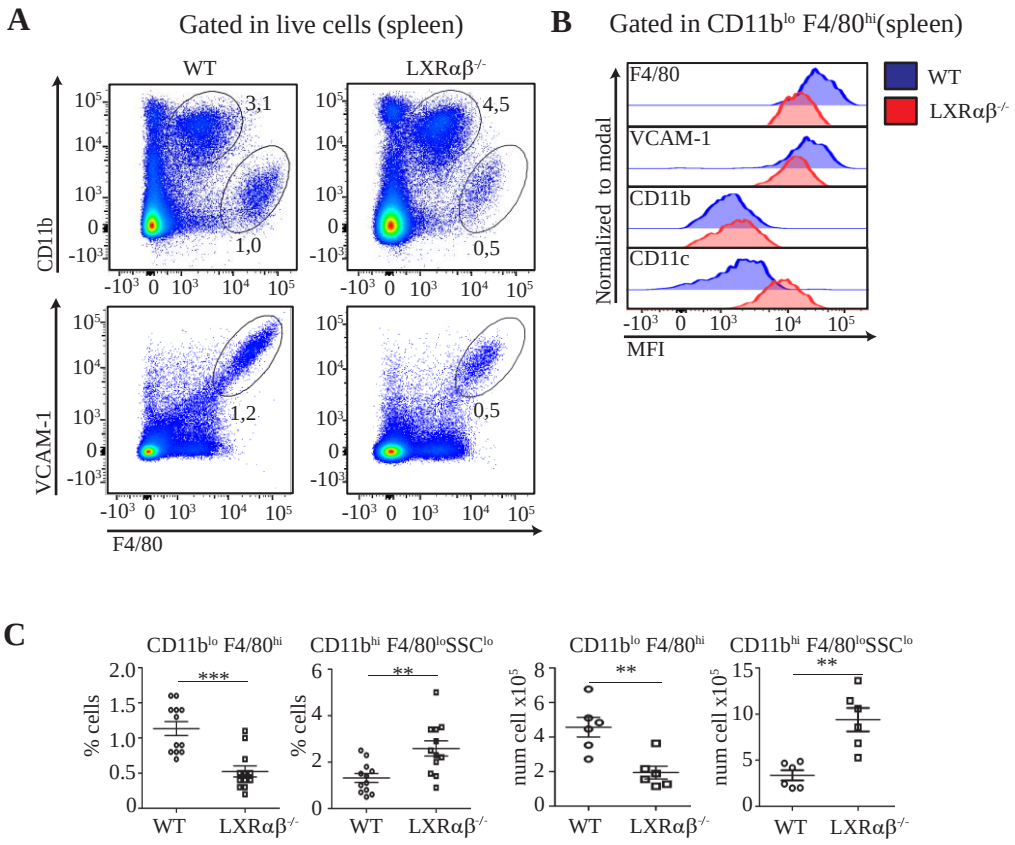

Figure 11. A) Flow cytometry analysis from WT and LXRαβ$^{-/-}$ spleens. Red pulp macrophages were identified as CD11b^{lo}F4/80^{hi}VCAM-1^{hi}. Myeloid population containing monocytes was distinguished as CD11b^{hi}F4/80^{lo}. Representative plots of three different experiments, with n=3 mice or more. **B)** Mean Fluorescence Intensity (MFI) signal of F4/80, CD11b, VCAM-1 and CD11c was analyzed in CD11b^{lo}F4/80^{hi} cells both in WT and LXRαβ$^{-/-}$ RPM population using flow cytometry. Representative of n=3 experiments. **C)** Quantification of CD11b^{lo}F4/80^{hi} and CD11b^{hi}F4/80^{lo} populations in spleen samples of WT and LXRαβ$^{-/-}$ mice. CD11b^{hi}F4/80^{lo} population was further gated to distinguish monocytes as SSC^{lo} within the CD11^{hi}F4/80^{lo} gate (see gating strategy in Fig. 8A and B, Materials and methods). N=12. Data was expressed as mean ± SEM. Statistical analysis was performed using Student's t test for significant differences. Values of $P < 0.05$ (*) or $P < 0.01$ (**), were considered to be significant, and values of $P < 0.001$ (***) were considered to be very significant.

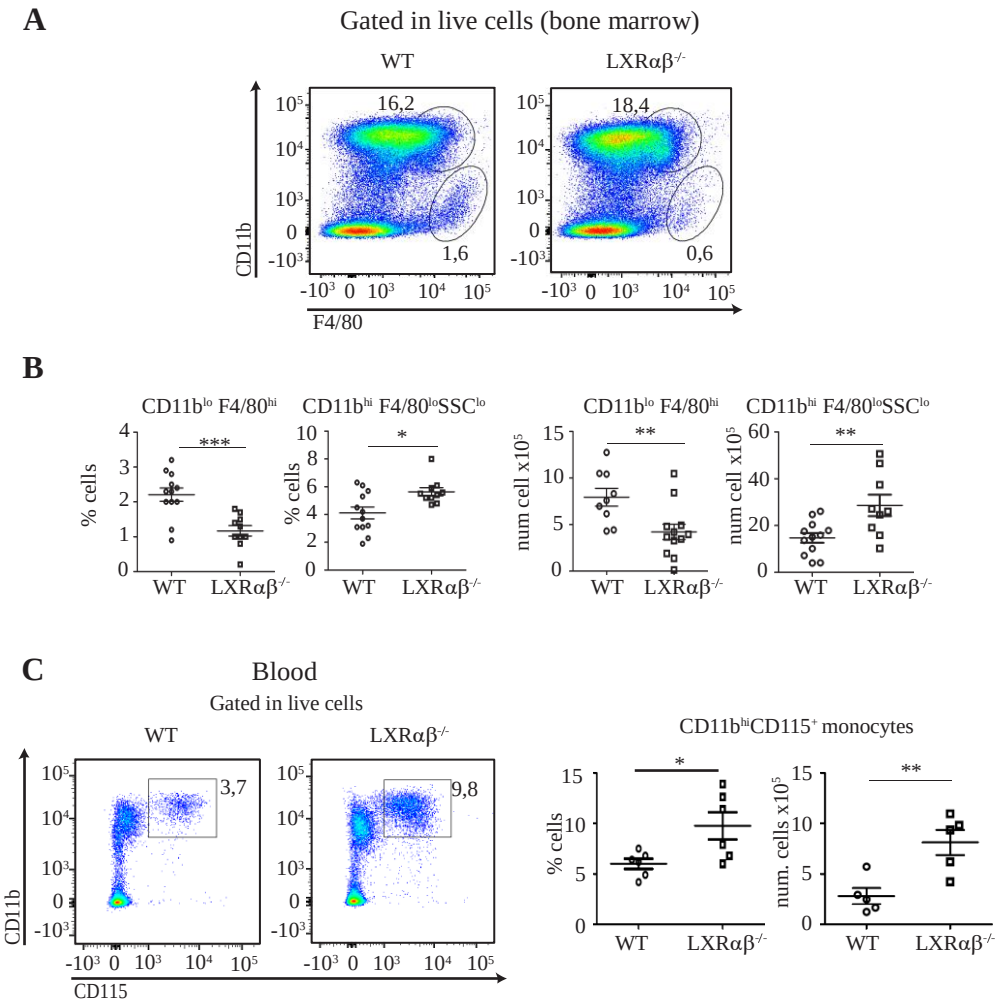

Figure 12. A) Flow cytometry analysis of resident bone marrow macrophage (BMM) and bone marrow monocyte populations in WT and LXRαβ$^{-/-}$ mice. Representative plots from three different experiments, n=3 mice or more. **B)** Quantifications of BMMs and monocyte populations. N=12. (see gating strategy Fig. 8A and B, Materials and methods). **C)** Flow cytometry analysis (left) and quantifications (right) from blood CD11b^{hi}CD115^{hi} monocytes in WT and LXRαβ$^{-/-}$ mice. Representative plot from two different experiments, n=3. Total N=6. Data was expressed as mean ± SEM. Statistical analysis was performed using Student's t test for significant differences. Values of P < 0.05 (*) or P < 0.01 (**), were considered to be significant, and values of P < 0.001 (***) were considered to be very significant.

It is possible that the reduction in CD11b^{lo}F4/80^{hi} RPMs and BMMs observed in LXR-deficient mice could be the result of defects in the stromal microenvironment of each affected tissue, or it could be due to an intrinsic cellular defect. As has been previously described, RPMs are known to be derived from primitive embryonic precursors, and they need minimal contribution from BM-derived cells for their replacement or proliferation[27,52] under homeostasis. However, Hashimoto et al. (2013) described that RPM and monocytes in the spleen are effectively replaced over time by BM transplant approaches after genotoxic insults, such as ionizing radiation[27]. To explore if replacement of bone marrow-derived cells in LXR-deficient mice could rescue the defects in macrophage differentiation, we performed BM transplantation experiments.

Results

LXRαβ$^{-/-}$ BM was injected into irradiated WT mice (LXRαβ$^{-/-}$→WT), and the reciprocal combination was also performed with WT BM and LXRαβ$^{-/-}$ mice as recipients (WT→LXRαβ$^{-/-}$). Monocyte and macrophage populations were analyzed 10 weeks post-transplant. Transplanted WT bone marrow into LXRαβ$^{-/-}$ mice was able to reconstitute the RPM compartment to WT levels (0,8%), whereas the reverse phenotype was observed in LXRαβ$^{-/-}$→WT mice, where RPM frequency was reduced to LXRαβ$^{-/-}$ mice levels (0,4%) (Fig. 13A). However, while the CD11b^{hi}F4/80^{lo}SSC^{lo} monocyte population was comparable in percentage to LXRαβ$^{-/-}$ mice (2%) in LXRαβ$^{-/-}$→WT mice, LXRαβ$^{-/-}$ mice who received WT bone marrow experimented an excessive increase (3%) (Fig. 13A). Regarding the bone marrow compartment, the frequency of BMM populations of transplanted mice also correlated with the original values of the donor BM in each case (2,5% for WT→LXRαβ$^{-/-}$ mice and 1% for LXRαβ$^{-/-}$→WT mice), but the CD11b^{hi}F4/80^{lo}SSC^{lo} monocyte populations once again showed a surprising increase in both cases (Fig. 13B). These results indicate that the frequency of RP and BM resident macrophage populations, is controlled by the LXR pathway in cells derived from the bone marrow. Also, data concerning the conformation of the monocyte compartment in these tissues was not conclusively supported by these bone marrow transplant experiments. Nevertheless, we could appreciate a tendency towards monocyte overproduction after irradiation-mediated depletion.

Therefore, to better understand the contribution of LXR to the development of splenic and BM macrophage and monocyte populations, we generated BM chimeras with congenically marked donor cells. We used WT mice as recipients, and a combination of LXRαβ$^{-/-}$ and WT-DsRed bone marrow in a 1:1 proportion as donor cells (Fig. 14A). At 4 weeks post-transplant, we confirmed that the ratio of DsRed^{+} vs DsRed^{-} (WT/LXRαβ$^{-/-}$) cells in peripheral blood was similar, indicating correct grafting of both donor genotypes (Fig. 14B). After 10 weeks, mice were euthanized and analyzed by flow cytometry. Remarkably, the percentage of CD11b^{lo}F4/80^{hi} RPM and BMM that were also DsRed^{+} was roughly 2/3 higher than the one for DsRed^{-} negative cells in both the spleen and the bone marrow, indicating a profound defect of LXR-deficient donor cells to differentiate into RPM or BMM (Fig. 14C). The reciprocal scenario was observed for CD11b^{hi}F4/80^{lo}SSC^{lo} spleen and bone marrow monocytes. The proportion of monocytes that were DsRed^{-} resulted in 70 to 75 percent in spleen and bone marrow respectively, compared to DsRed^{+} cells (Fig. 14C). These results indicate that LXR-deficient BM-derived hematopoietic cells present an intrinsic defect to develop into RPM and BMM within their target tissues, while being predisposed to a CD11b^{hi}F4/80^{lo}SSC^{lo} monocyte accumulation in spleen and BM, and that his accumulation exacerbates in BM transplanted mice.

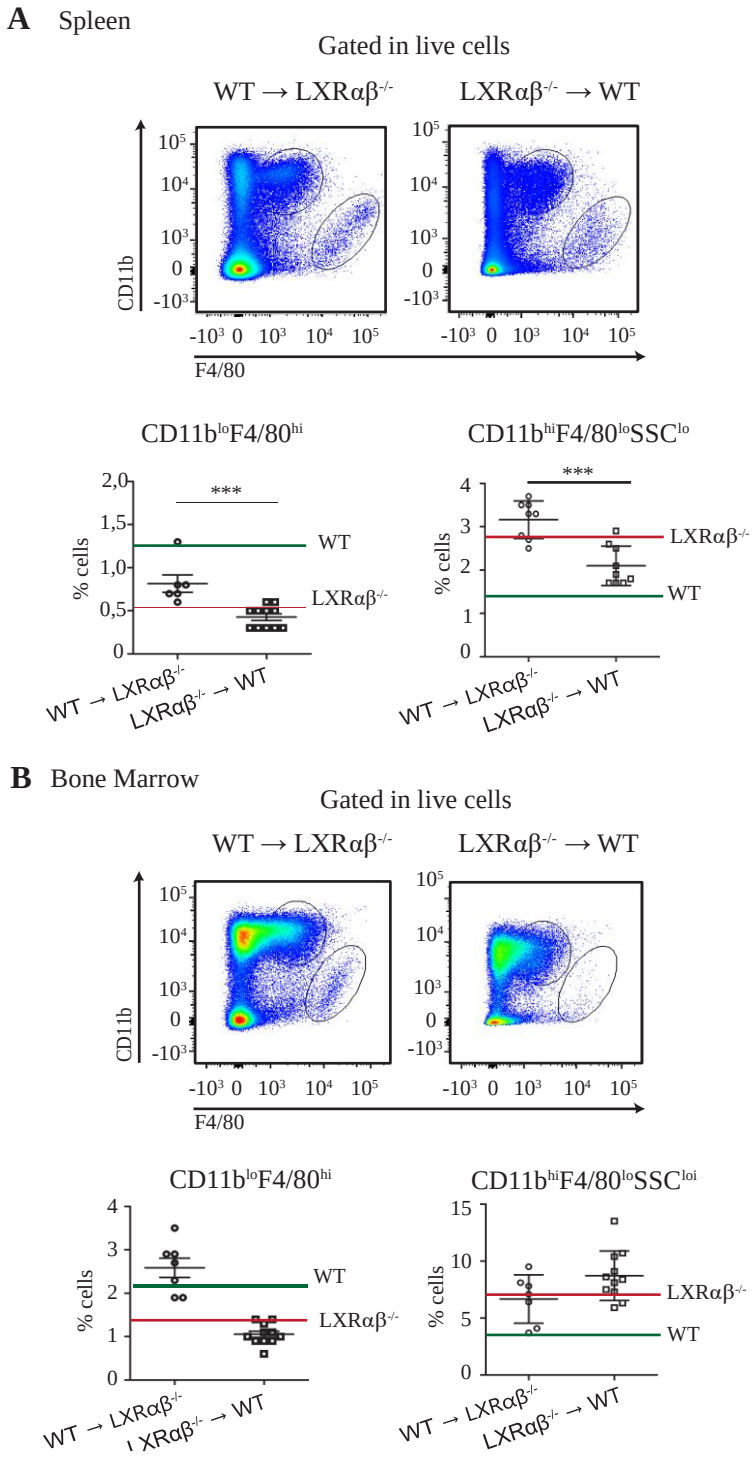

Figure 13. Flow cytometry analysis and quantifications from bone marrow transplanted mice. Splenic **(A)** and bone marrow **(B)** resident macrophage and monocyte population replenishment 10 weeks after irradiation and correspondent bone marrow transplantation. Representative plots from one experiment of n=6 or more. Green lines represent normal WT frequencies for each population, and red lines represent LXRαβ$^{-/-}$ levels. Data was expressed as mean ± SEM. Statistical analysis was performed using Student's t test for significant differences. Values of $P < 0.05$ (*) or $P < 0.01$ (**), were considered to be significant, and values of $P < 0.001$ (***) were considered to be very significant.

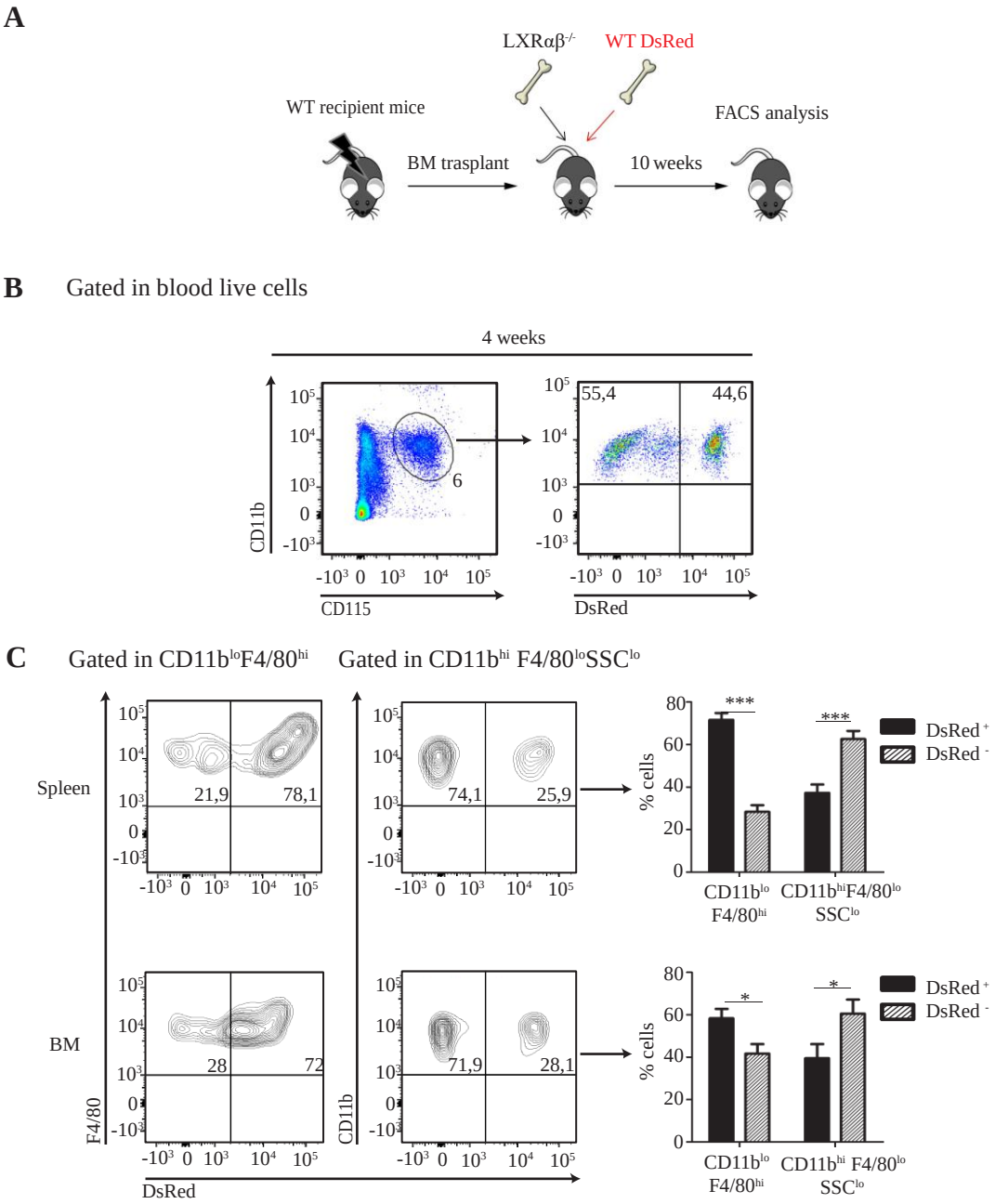

Figure 14. A) Transplant experimental design to generate bone marrow chimeras. WT-DsRed and LXRαβ$^{-/-}$ bone marrow were mixed (1:1) to obtain a chimeric donor cell pool, and recipient WT mice were euthanized 10 weeks after transplant. **B)** Representative flow cytometry blood comprobation of the correct grafting of the chimeric bone marrow in recipient mice 4 weeks after the transplantation. Blood samples were collected from the submandibular vein. **C)** Representative density plots (left) and quantifications (right) from two independent experiments (n=4 or more mice per group), showing DsRed positive or negative cell proportions, gated in macrophage and monocyte populations in spleen (top panels) and bone marrow (lower panels) of recipient mice. Data was expressed as mean ± SEM. Statistical analysis was performed using Student's t test for significant differences. Values of $P < 0.05$ (*) or $P < 0.01$ (**), were considered to be significant, and values of $P < 0.001$ (***) were considered to be very significant.

3. LXRαβ$^{-/-}$ mice present iron accumulation in the spleen and deregulation of iron related gene expression

As mentioned before, one of the main functions of resident RPM, and also BMM and liver Kupffer macrophages, is the uptake of senescent or damaged erythrocytes to degrade heme and recycle their iron content[76,77]. We therefore analyzed whether the defects observed in RPM and BMM compartment in LXR-null mice could correlate with an impairment of the correct iron handling/recycling metabolism in the spleens and BM of LXRαβ$^{-/-}$ mice. To test this premise, spleen sections were stained with an established histological dye that detects iron accumulation within tissues. Prussian-Blue staining of spleen sections revealed an intense iron accumulation that was mostly confined in the red pulp of the spleen in LXRαβ$^{-/-}$ mice compared to WT spleens (Fig. 15A). Quantification of iron content in spleen homogenates showed a ~2 fold accumulation in LXRαβ$^{-/-}$ mice compared to WT spleens (Fig. 15B), and this accumulation was maintained in elder mice (data not shown). In contrast, the amount of iron per tibia in LXR-deficient BM was reduced compared to WT BM (Fig. 15B). Parallel differences were observed between WT and LXRαβ$^{-/-}$ mice when hemoglobin concentration was quantified in spleens and BM (Fig. 15B).

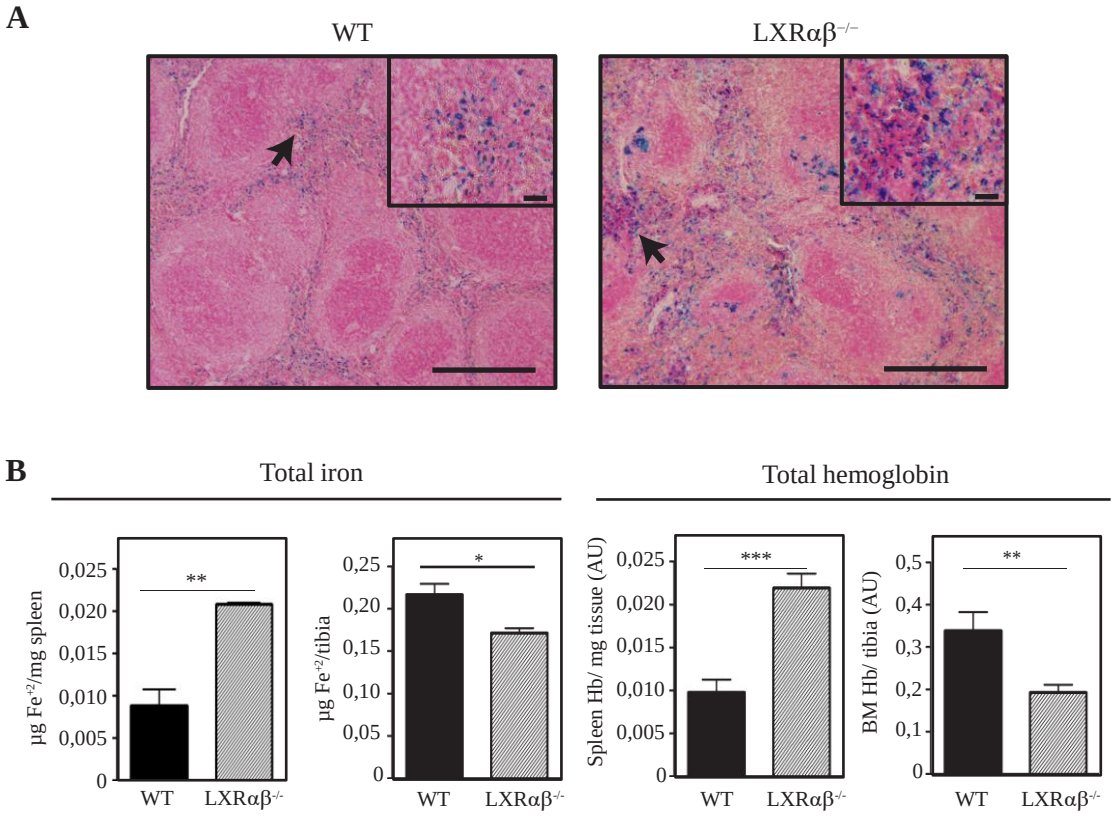

Figure 15. A) Paraffin-embedded spleen sections (4-6 µm) were stained with Prussian-Blue and counterstained with hematoxilin. Scale bar=1mm in original size, 50 µm in inset images. Images show representative micrographs from four different mice. **B)** (Left) Ferric iron quantifications (µg/mg spleen, and µg/tibia), (rigth) total tissue hemoglobin content, from spleen and BM of 12 week-old WT and LXRαβ$^{-/-}$ mice, n=3 or more. Data was expressed as mean ± SEM. Statistical analysis was performed using Student's t test for significant differences. Values of $P < 0.05$ (*) or $P < 0.01$ (**), were considered to be significant, and values of $P < 0.001$ (***) were considered to be very significant.

Results

Because the main hematopoietic organ in adult mice is the BM, most of the recycled iron travels through blood circulation from the spleen to this tissue to complete erythropoiesis[88]. That is why, together, the iron accumulation in the red pulp of the spleen and the reduction of iron content in the tibias of LXR-deficient mice, could entail an erythropoiesis defect.

To test this theory, we tried to assess whether the iron accumulation in the red pulp corresponded with an accumulation of unengulfed RBCs. Flow cytometry analysis of the splenic RBC compartment using the surfaces markers CD45 and TER119 in 8 weeks-old mice showed a clear accumulation in LXR-deficient mice compared to WT mice (Fig. 16A, B). $CD45^{-}TER119^{+}$ cells are described to be mature RBCs, while $CD45^{+}TER119^{+}$ cells would correspond to erythroid cells in development. When we analyzed the bone marrow RBC compartment of these mice, the results correlated with the iron and hemoglobin quantifications: LXR-deficient mice displayed lower frequencies of $TER119^{+}$ total cells compared to their WT counterparts (Fig. 16A, B). As the bone marrow is the prime site for erythropoiesis in adult mice[111], we then expanded the analysis attempting to identify the different maturation stages of erythroid cells and their frequencies in WT and LXR-null mice. $TER119^{+}$ cells were further gated using CD44 surface marker, and FSC-size parameter[201], and divided into six different populations, where I-IV represent nucleated erythroblasts, and V and VI represent enucleated erythrocytes. LXR-deficient mice presented erythroblast accumulation from stages I to IV, but the frequencies of V and VI were lower compared to WT mice (Fig. 16A, B). We hypothesized that this could be due to an impaired systemic iron balance. During the last stages of erythroblasts maturation, hemoglobin levels rise and the iron demand is higher[120,123]. A defective recycling in the spleens of LXR-deficient mice could affect the termination of erythropoiesis in the bone marrow, causing accumulation of immature erythroblasts. Additionally, macroscopic examination of dissected femurs revealed that $LXR\alpha\beta^{-/-}$ bones appear paler than WT controls at 40 weeks of age, which further supports the obtained data of diminished erythroid constituents in the marrow of old LXR-deficient mice (Fig. 16C).

Next, we quantified the number of peripheral blood erythrocytes, the hematocrit and the hemoglobin concentration of 8 and 40-week old WT and $LXR\alpha\beta^{-/-}$ mice. As shown in Fig. 16D, even though there are no differences between genotypes in young mice, there is a noticeable reduction in erythroid parameters in older $LXR\alpha\beta^{-/-}$ mice compared to WT controls, suggesting that iron recycling impairment caused by LXR absence aggravates with age. Together, these results indicate that LXR is important for normal iron homeostasis and the maintenance of proper erythropoiesis in mice.

To explore whether the cause/s of defective iron homeostasis in $LXR\alpha\beta^{-/-}$ mice were connected to defects in iron handling by splenic macrophages, we isolated RPM of both WT and $LXR\alpha\beta^{-/-}$ mice and stained them with Prussian Blue. Many purified $LXR\alpha\beta^{-/-}$ RPM accumulated excessive iron in their cytoplasm (Fig. 17A). The quantifications of this iron correlated with the increment observed in total iron in $LXR\alpha\beta^{-/-}$ spleens (Fig. 17A). These data indicate that $LXR\alpha\beta^{-/-}$ RPM are unable to properly control intracellular iron contents, which results in excessive iron accumulation in the splenic red pulp.

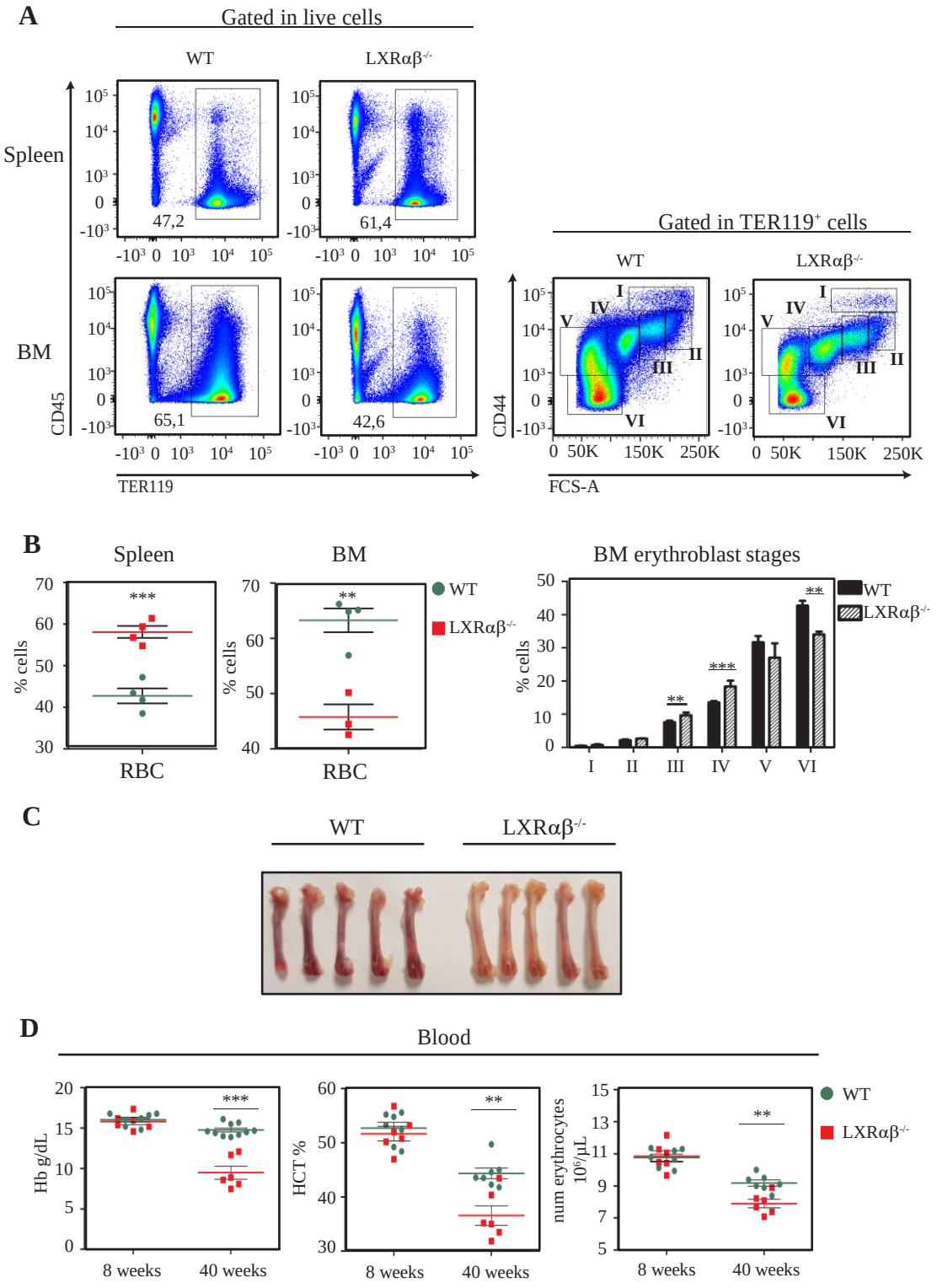

Figure 16. A) Flow cytometry analysis of TER119+ RBC accumulation in spleens and bone marrows of WT and LXRαβ-/- mice. Different erythroblast maturation stages are also analyzed in the bone marrows of these mice. Representative plot from n=3 or 4 mice. **B)** Quantifications from RBC accumulation in spleens and bone marrows (left) and from bone marrow erythroblasts stages (right) in WT and LXRαβ-/- mice. N=3 or 4. **C)** Photographic comparison of WT and LXRαβ-/- mice femurs coloration. **D)** Blood measurements of hemoglobin concentration (g/dL, left), hematocrit percentage (middle) and total number of erythrocytes (10^6/µL), from 8 and 40 weeks old WT and LXRαβ-/- mice. N= 6 or more. Data was expressed as mean ± SEM. Statistical analysis was performed using Student's t test for significant differences. Values of $P < 0.05$ (*) or $P < 0.01$ (**), were considered to be significant, and values of $P < 0.001$ (***) were considered to be very significant.

The inability of the remaining LXRαβ$^{-/-}$ RPM to properly handle intracellular iron, could be a consequence of an iron overload due to the macrophage population deficiency these mice present. But, since LXRs are transcription factors, we inferred that this defect could also be explained by a loss of regulation of key genes involved in iron metabolism in the macrophage. We analyzed the expression of several iron-related genes in the spleen, such as *Spic*, *Slc40a1* (FPN-1), and *Hmox1* (HO-1). Expression of these genes was decreased in LXRαβ$^{-/-}$ spleens compared to WT controls, suggesting that intracellular iron metabolism might be compromised (Fig. 17B). Reduced expression of these iron-metabolic genes in whole spleen RNA could be anticipated because LXRαβ$^{-/-}$ spleens contain fewer RPM expressing these genes. Interestingly, however, the expression of *Sirpa* (encoding SIRP1α), the key receptor involved in senescent RBC clearance, was higher in LXRαβ$^{-/-}$ spleens (Fig. 17B). As expected, the expression of *Marco* (MARCO) and the LXR target *Cd5l* (also known as AIM) used as controls, was absent in LXRαβ$^{-/-}$ mice (Fig. 17B).

These results indicate that loss of LXRα and LXRβ results in abnormal accumulation of iron in the splenic red pulp, which is largely due to iron overload in resident RPM. This deregulation of iron metabolism in the spleen and bone marrow in LXRαβ$^{-/-}$ mice, could originate a pathological scenario that results in reduced iron availability for erythropoiesis in the bone marrow of LXRαβ$^{-/-}$ old mice and development of anemia over time.

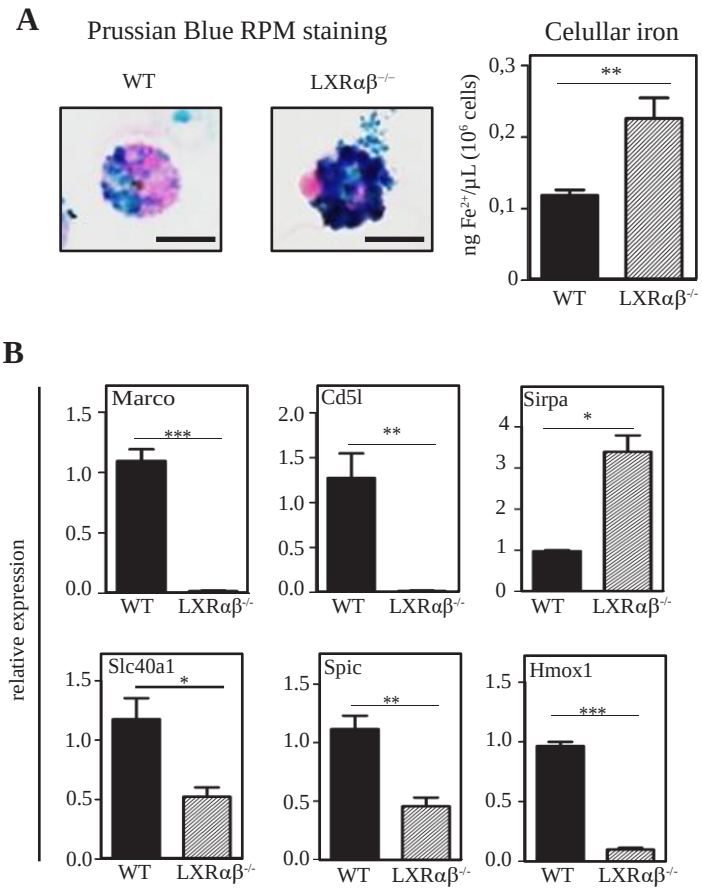

Figure 17. A) Prussian Blue iron staining of purified RPM (scale bar = 10 µm) and iron quantifications expressed in ng Fe^{2+}/µL normalized to 1x10^6 sorted cells. N=4. **B)** Total spleen gene expression from different iron-related genes, and LXR targets. Representative from two different experiments, with n=3. RNA expression was graphed as relative to 36B4 expression. Data was expressed as mean ± SEM. Statistical analysis was performed using Student's t test for significant differences. Values of P < 0.05 (*) or P < 0.01 (**), were considered to be significant, and values of P < 0.001 (***) were considered to be very significant.

4. LXRs are essential for the regulation of red pulp macrophage transcriptional phenotype.

The results presented above indicate that loss of LXRα and LXRβ causes several pathophysiological consequences in the red pulp of the spleen and the bone marrow. This led us to speculate whether severe decline in RPM was the solely cause for the iron mishandling in these mice, or if, on the other hand, LXRα and LXRβ could also have a role in the regulation of other genes implicated in iron metabolism.

In order to identify LXR-regulated genes that might play a role in iron metabolism, and to explore the reason/s for reduced quantity of resident RPM in LXRαβ$^{-/-}$ mice, we performed transcriptional profiling of FACS sorted CD11b^{lo}F4/80^{hi} RPM from WT and LXRαβ$^{-/-}$ mice (see sorting strategy in Fig. 9, Materials and Methods). In addition to RPM, we also performed microarray analysis of isolated CD11b^{hi}F4/80^{lo}SSC^{lo} monocytes from both genotypes. We reasoned that, to identify the core transcripts that clearly define LXR activity in RPM, the most interesting genes set for our study would be those genes highly represented in RPM over monocytes. We cross-referenced genes whose expression was higher in WT RPM than in WT monocytes, and at the same time presented impaired transcription in LXRαβ$^{-/-}$ RPM. A gene cluster of approximately 180 genes highly represented in WT RPM showed aberrant expression in LXR-deficient RPM. For the validation of our strategy we confirmed that, among the top regulated genes of this analysis, appeared several LXR known targets, including *Cd5l*, *Abca1*, *Apoc1* and *Cd38* (Fig. 18A).

Using gene ontology (GO) tools, we found various biological functions associated with LXR-dependent genes in RPM, including lipoprotein and cholesterol metabolism genes, as expected (Fig. 18B). Interestingly, other functions that clearly correlate with LXR activity in these cells are linked to activation of the immune response (Fig. 18B). Although these genes are likely not directly implicated in the regulation of iron metabolism, they could possibly contribute to the transcriptional signature of RPM identity. The analysis also highlighted the importance of LXRα, which appeared to be one of the top genes whose expression is predominant in RPM compared to monocytes (Fig. 18A).

Remarkably, several genes that belong to the specific core of gene expression that defines the RPM identity compared to other tissue macrophages[65] were also greatly downregulated in LXR-deficient mice, including *Cd55*, *Clec9a*, *C6*, *C2* and *Cd163* (Fig. 18A). Indeed, Principal Component Analysis (PCA) of this data revealed that LXRαβ$^{-/-}$ RPM clustered separately from WT RPM, indicating that LXR activity is important for the establishment of RPM identity by means of transcriptional regulation. However, WT and LXRαβ$^{-/-}$ CD11b^{hi}F4/80^{lo}SSC^{lo} monocytes showed more closely related transcriptional profiles (Fig. 18C). This data indicates that the influence of LXRαβ activity in splenic myeloid cells is more pronounced in mature RPM than in monocytes.

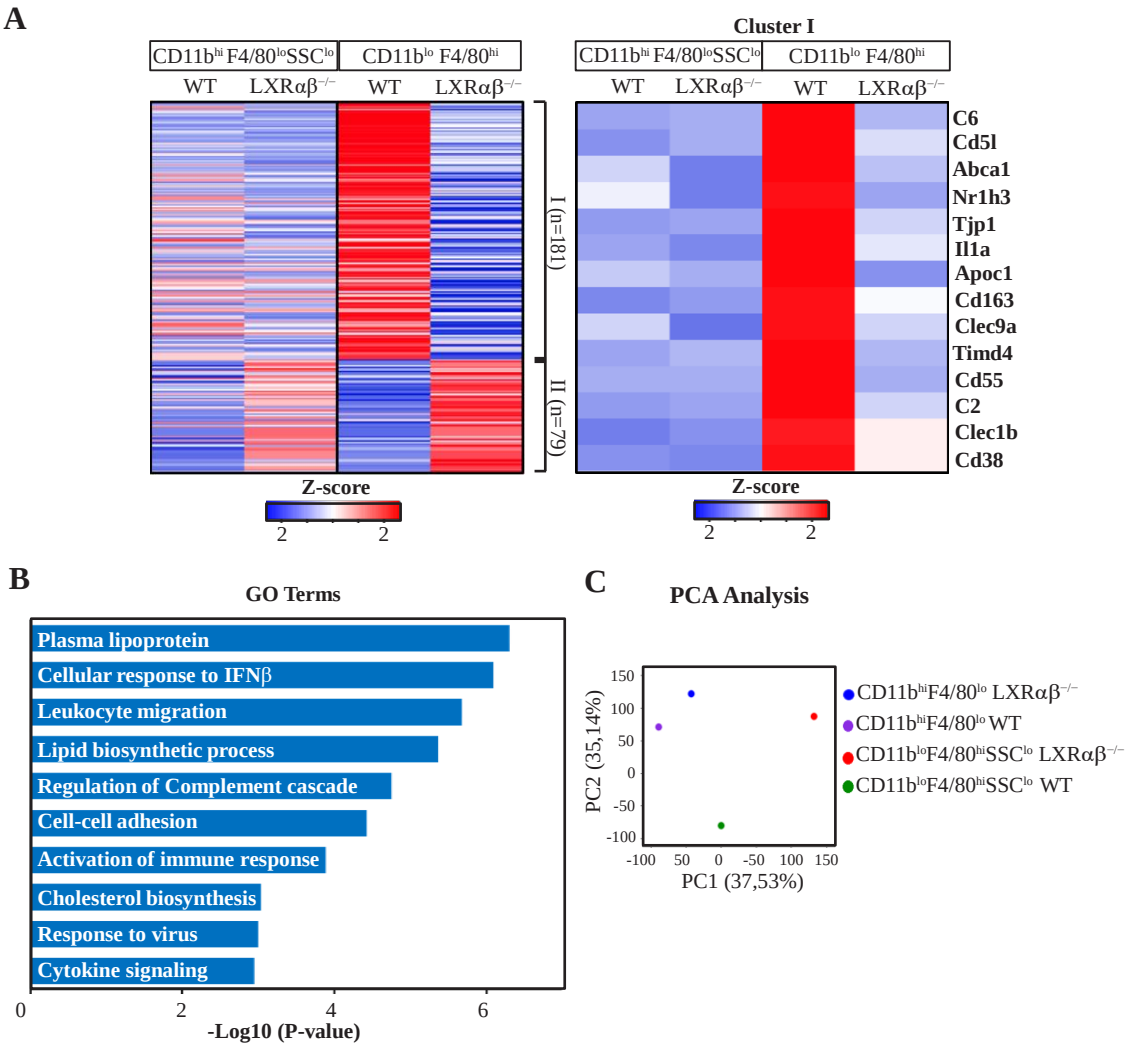

Figure 18. A) Hierarchical clustering heatmap analysis of RNA expression from WT and LXRαβ$^{-/-}$ purified CD11b^{lo}F4/80^{hi} RPM and CD11b^{hi}F4/80^{lo} monocytes. **B)** GO annotation pathways for Cluster I differentially expressed genes. **C)** Principal Component Analysis (PCA) of RPM and monocyte gene expression profile both in WT and LXRαβ$^{-/-}$ purified cells.

We continued the survey of our gene list to find other LXR-regulated genes in purified RPM that might play a role in iron homeostasis under steady-state conditions. One particular gene that concentrated our attention was *Cd163* (Fig. 18A), a member of the scavenger receptor cysteine-rich (SRCR) superfamily of proteins. CD163 mediates the uptake of hemoglobin-haptoglobin (Hb-Hp) complexes by macrophages and has also been reported to play important roles in the clearance of free hemoglobin released after RBC extracellular in order to avoid the oxidation of substrates by iron molecules[100]. Also expression of *Timd4*, a marker of tissue resident macrophages, was critically downregulated in LXRαβ$^{-/-}$ RPM (Fig. 18A). We confirmed *Cd163*, *Timd4*, *Cd5l* and *Abca1* transcriptional downregulation in sorted RPM by quantitative PCR (Fig. 19). We also found that expression of key iron metabolic genes, such as *Hmox1* (HO-1) and *Slc40a1* (FPN-1), was also impaired in LXRαβ$^{-/-}$ RPM (Fig. 19). These proteins act in concert during the process of intracellular heme metabolization, and the transition for iron recycling. However, the expression of *Spic*, which is crucial for the RPM survival, was intact in LXRαβ$^{-/-}$ RPM compared to WT (Fig. 19). These results indicate that LXR activity controls

the expression of several groups of genes in RPMs that can be categorized by their biological functions, including cholesterol metabolism, the immune response and the regulation of the complement cascade. Also, they revealed that expression of selected genes important for the metabolization of heme and iron are severely affected in LXRαβ$^{-/-}$ RPM, including *Cd163*, *Hmox1* and *Slc40a1*.

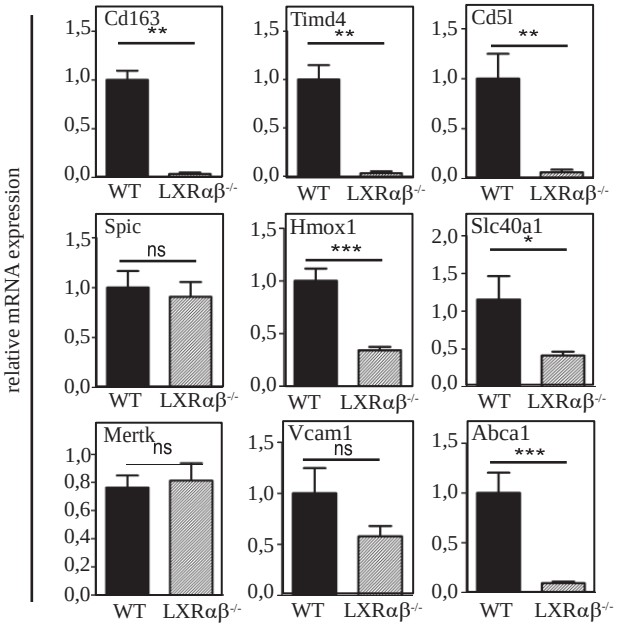

Figure 19. Real-time qPCR analysis of different iron related and LXR target genes in RNA samples from purified WT and LXRαβ$^{-/-}$ RPM. N=6. Data was expressed as mean ± SEM. Statistical analysis was performed using Student's t test for significant differences. Values of $P < 0.05$ (*) or $P < 0.01$ (**), were considered to be significant, and values of $P < 0.001$ (***) were considered to be very significant.

We corroborated by flow cytometry analysis that the expression differences observed in several transcripts in our RNA analysis were also maintained at the protein level. Strikingly, we observed that not all RPM express CD163 under homeostasis. Consistently, roughly 30-35% of total RPM were CD11b^{lo}F4/80^{hi}CD163^{+} in WT mice, and this subpopulation was completely absent in LXRαβ$^{-/-}$ mice (Fig. 20A, C). TIM4, whose expression was observed in the majority of WT RPM, also showed defective expression in LXRαβ$^{-/-}$ RPM (Fig. 20A, C). Conversely, other established tissue macrophage surface markers such as CD64, MERTK or VCAM-1, reached normal levels in the remaining RPM that reside in LXRαβ$^{-/-}$ spleens, as did erythrocyte-CD47-receptor SIRP1α (Fig. 20A). Analysis of dual expression of CD163 and TIM4 markers showed that double positive WT CD11b^{lo}F4/80^{hi} RPM represented around 25% of the total population, and that virtually all CD11b^{lo}F4/80^{hi}CD163^{+} RPM in WT mice are TIM4^{+} (Fig. 20B). Consistent with the individual analysis, we did not find any subpopulation of cells in LXRαβ$^{-/-}$ mice characterized as CD11b^{lo}F4/80^{hi}CD163^{+}TIM4^{+} (Fig. 20B). Partial/total absence of TIM4^{+} and CD163^{+} RPM respectively, in LXRαβ$^{-/-}$ mice, might indicate that their expression could be transcriptionally controlled by LXR activity or rather that the cells expressing these proteins might be lost in LXRαβ$^{-/-}$ spleens.

Flow cytometry analysis of bone marrow macrophages showed similar results as the spleen. In WT mice, CD11b^{lo}F4/80^{hi}CD163^{+} cells correspond to approximately 50% of the BMM compartment, and this subpopulation was

almost completely absent in LXRαβ$^{-/-}$BM. CD11b^{lo}F4/80^{hi}TIM4^{+} macrophages were also diminished from 80% in WT BM, to 30% in LXRαβ$^{-/-}$ BM, and the rest of macrophage surface markers tested remained at normal levels (Fig. 21A, B).

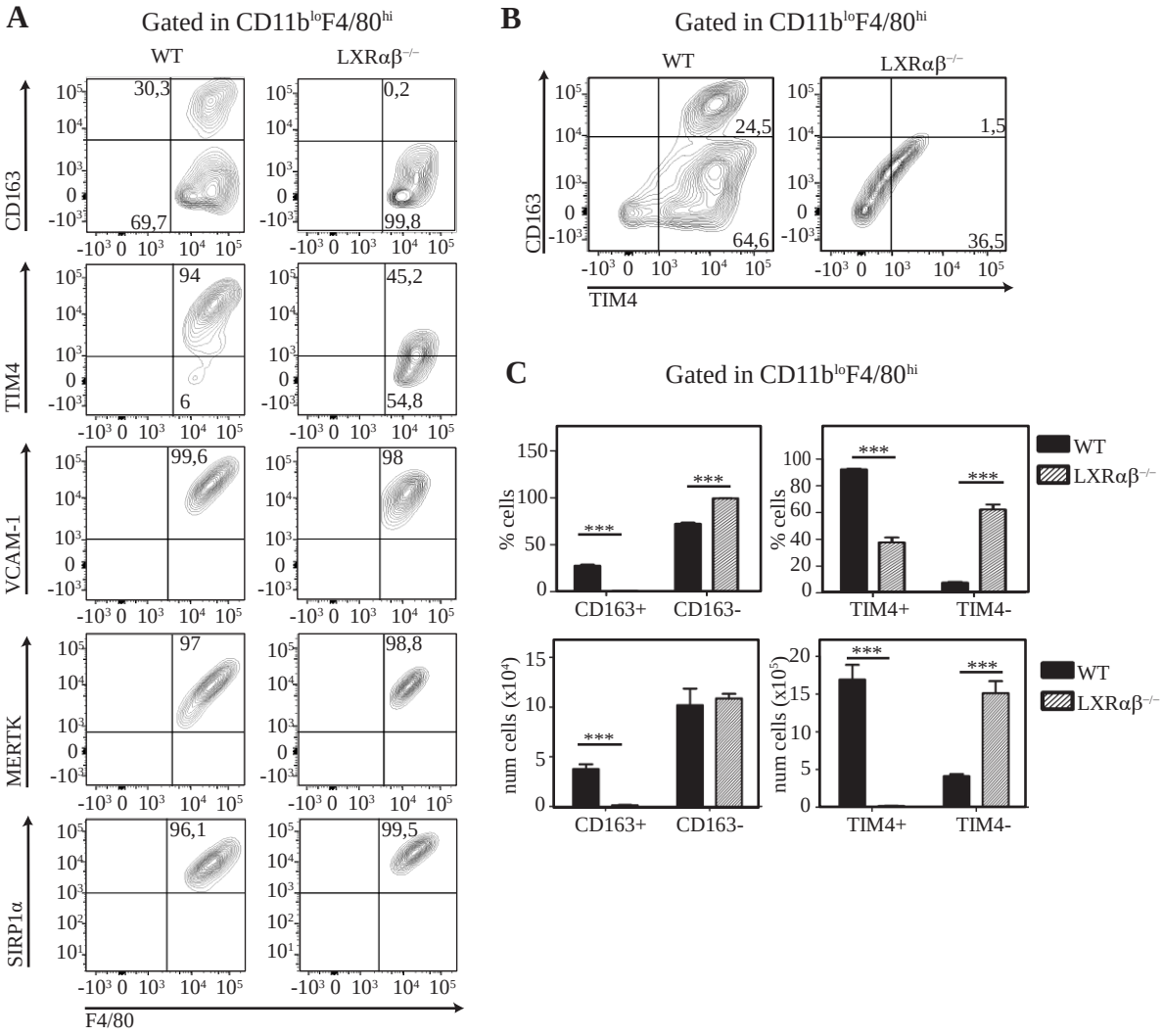

Figure 20. A) Spleen flow cytometry countour plots showing expression of surface marker receptors in CD11b^{lo}F4/80^{hi} WT and LXRαβ$^{-/-}$ RPMs. Representative from two different experiments of n=3 or more. **B)** Flow cytometry double panel of TIM4 and CD163 of WT and LXRαβ$^{-/-}$ RPM**. C)** Quantification of CD163^{+} and TIM4^{+} RPM percentages (top) and number of cells (bottom) in WT and LXRαβ$^{-/-}$ mice spleens. N=6 or more. Data was expressed as mean ± SEM. Statistical analysis was performed using Student's t test for significant differences. Values of P < 0.05 (*) or P < 0.01 (**), were considered to be significant, and values of P < 0.001 (***) were considered to be very significant.

LXR could be responsible for the regulation of the transcription of *Cd163* gene, and thus its absence results in the absence of CD163 receptor in RPM. But our previous data consistently established that LXR-null mice present a RPM deficiency (Fig. 11A-C) and the remaining macrophages are now characterized as CD11b^{lo}F4/80^{hi} CD163^{-} (Fig. 20A, B), so the possibility for LXR to be responsible for the development of a CD11b^{lo}F4/80^{hi}CD163^{+} RPM subpopulation in the spleen could exist. To answer this question, we analyzed the absolute cell numbers of CD163^{+} and CD163^{-}, and TIM4^{+} and TIM4^{-} RPM subpopulations in WT and LXRαβ$^{-/-}$ spleens. The results showed that the numbers of CD163^{+} RPM in WT spleens correlated with the RPM deficiency that LXRαβ$^{-/-}$ mice displayed (Fig. 20C). CD163^{-} RPM counts in LXRαβ$^{-/-}$ mice matched

with those in WT controls (Fig. 20C). In addition, TIM4^{+} cells were absent in LXRαβ$^{-/-}$ spleens in favor of TIM4^{-} subsets, once again suggesting that all CD163^{+} RPM highly expressed TIM4, and this expression decreased in the absence of LXR (Fig. 20C).

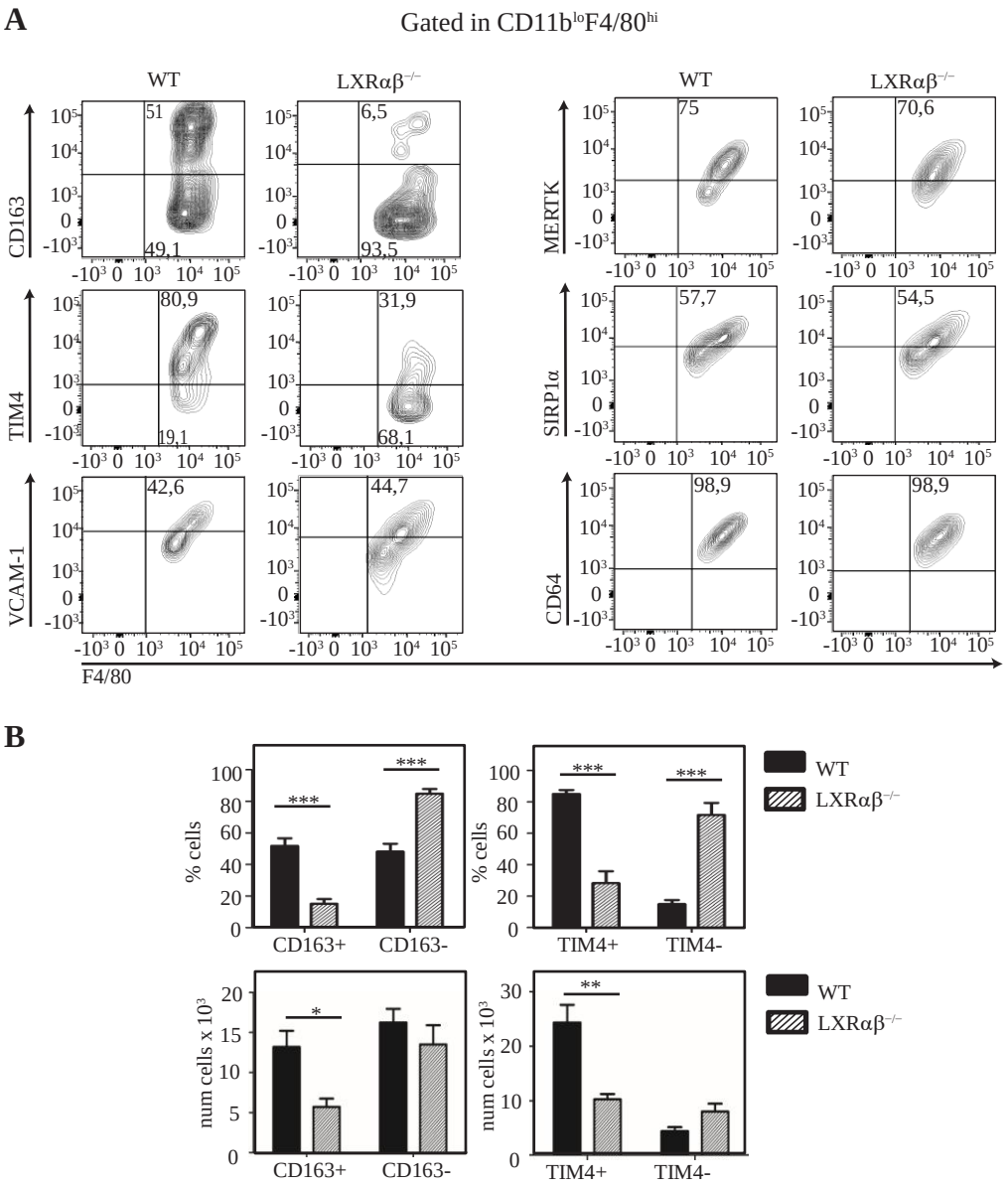

Figure 21. A) Bone marrow flow cytometry analysis of CD163, TIM4, VCAM-1, MERTK, SIRP-1α and CD64 expression in BMMs from WT and LXRαβ$^{-/-}$ mice. Contour plots gated on CD11b^{lo}F4/80^{hi} BMM. Representative from 2 independent experiments with n=5 or more. **B)** Quantification analysis of CD163^{+}/CD163^{-} and TIM4^{+}/TIM4^{-} percentage and number of BMMs in WT and LXRαβ$^{-/-}$ mice, n=5 or more. Data was expressed as mean ± SEM. Statistical analysis was performed using Student's t test for significant differences. Values of $P < 0.05$ (*) or $P < 0.01$ (**), were considered to be significant, and values of $P < 0.001$ (***) were considered to be very significant.

Collectively, our transcriptional analysis, together with flow cytometry data of the RPM compartment in WT mice revealed the existence of two different CD11b^{lo}F4/80^{hi} RPM subsets within the spleen, CD11b^{lo}F4/80^{hi}CD163^{+}TIM4^{+} and CD11b^{lo}F4/80^{hi}CD163^{-}TIM4^{+}, being the first one completely absent in the red pulp of LXRαβ$^{-/-}$ mice.

5. LXRα transcriptional program is required for the correct development of the red pulp macrophage compartment

Our results so far indicate that LXRαβ$^{-/-}$ mice exhibit an important reduction of splenic CD11b^{lo}F4/80^{hi} RPM compared to WT controls, apparently associated with the absence of a specific subset characterized as CD11b^{lo}F4/80^{hi}CD163^{+}TIM4^{+} RPM. Our previous reports[63] established that LXRα, but not LXRβ, is required for the development of MZ macrophages in the spleen. Since LXRα is one of the top transcription factors expressed in splenic RPM (Fig. 6, Introduction), we speculated that LXRα might as well predominate defining the RPM transcriptional regulation. To investigate the *in vivo* role of LXRα within the myeloid compartment of TRMs, we generated a mutant reporter mouse. Our strategy, similar to the LXRα-DTR, was to replace the first coding exon of the murine LXRα gene with a cDNA cassette of the enhanced green fluorescent protein (EGFP), that would be expressed whenever LXRα transcription was active (Fig. 7C and D, Materials and methods). For simplicity, we named this mutant reporter line LXRα-GFP. Mice carrying one or two EGFP alleles, WT/GFP or GFP/GFP, were heterozygous or homozygous for LXRα, respectively. This method permitted not only the generation of an LXRα-deficient locus but also the analysis of LXRα expression within the specific cell subsets of interest.

Whereas WT/WT mice showed no green fluorescence when analyzed by flow cytometry, WT/GFP mice presented a proportion of CD11b^{lo}GFP^{hi} cells that mirrored the physiological frequency of CD11b^{lo}F4/80^{hi} RPM population, indicating that virtually all CD11b^{lo}F4/80^{hi} RPM are in fact LXRα^{+} (Fig. 22A). Remarkably, GFP/GFP mice (LXRα$^{-/-}$) exhibited a significant reduction of CD11b^{lo}GFP^{hi} RPM, comparable to that observed in LXRαβ$^{-/-}$ mice, suggesting that LXRα activity is a dominant factor determining the presence of CD11b^{lo}F4/80^{hi} RPM (Fig. 22A). Fluorescence Intensity Analysis showed that the GFP fluorescence mean of the CD11b^{lo}F4/80^{hi} RPM population was higher in LXRα$^{GFP/GFP}$ cells when compared to LXRα$^{WT/GFP}$ RPM, indicating that cells containing two copies of EGFP exhibited higher fluorescence. LXRα$^{WT/WT}$ control littermates showed residual fluorescence, corresponding to the autofluorescence of these cells (Fig. 22A).

A modest proportion of CD11b^{hi} cells gained GFP expression in LXRα$^{WT/GFP}$ and LXRα$^{GFP/GFP}$ mice under steady-state conditions (Fig. 22A). Haldar et al. (2014) described a subset of SPI-C^{+} monocytes that expanded in the spleen of SPI-C$^{GFP/GFP}$ mice after RPM depletion caused by ferroptosis, that could possibly constitute the RPM precursor cells (denominated "pre-RPM") upon stress situations[101]. This CD11b^{hi}GFP^{lo} cell population, which expresses low levels of LXRα compared to CD11b^{lo}F4/80^{hi} RPM, could resemble that pre-RPM subset. We explored the use of commercially available Heme (Hemin) to mimic an experimental heme/iron overload *in vivo*. We then performed an intraperitoneal injection of heme to stimulate the iron recycling machinery in the spleens of WT/GFP and GFP/GFP mice, and observed a mild expansion of the CD11b^{hi}GFP^{+} population in LXRα$^{WT/GFP}$ and LXRα$^{GFP/GFP}$ mice, which was more accentuated in the last case (Fig. 22B). To reproduce the experiments by Haldar et al. (2014), we depleted the RPM compartment using PHZ treatment to cause massive RBCs hemolysis, and subsequent RPMs ferroptosis. The total absence of RPMs forced a more acute expansion of the CD11b^{hi}GFP^{+} population than heme stimulation did, far more so in the case of GFP/GFP mice compared to WT/GFP mice (Fig. 22B). This supports the possibility of the existence of a novel subset of resident myeloid cells in the spleen, that might be up-regulated under special conditions upon tissue requirements.

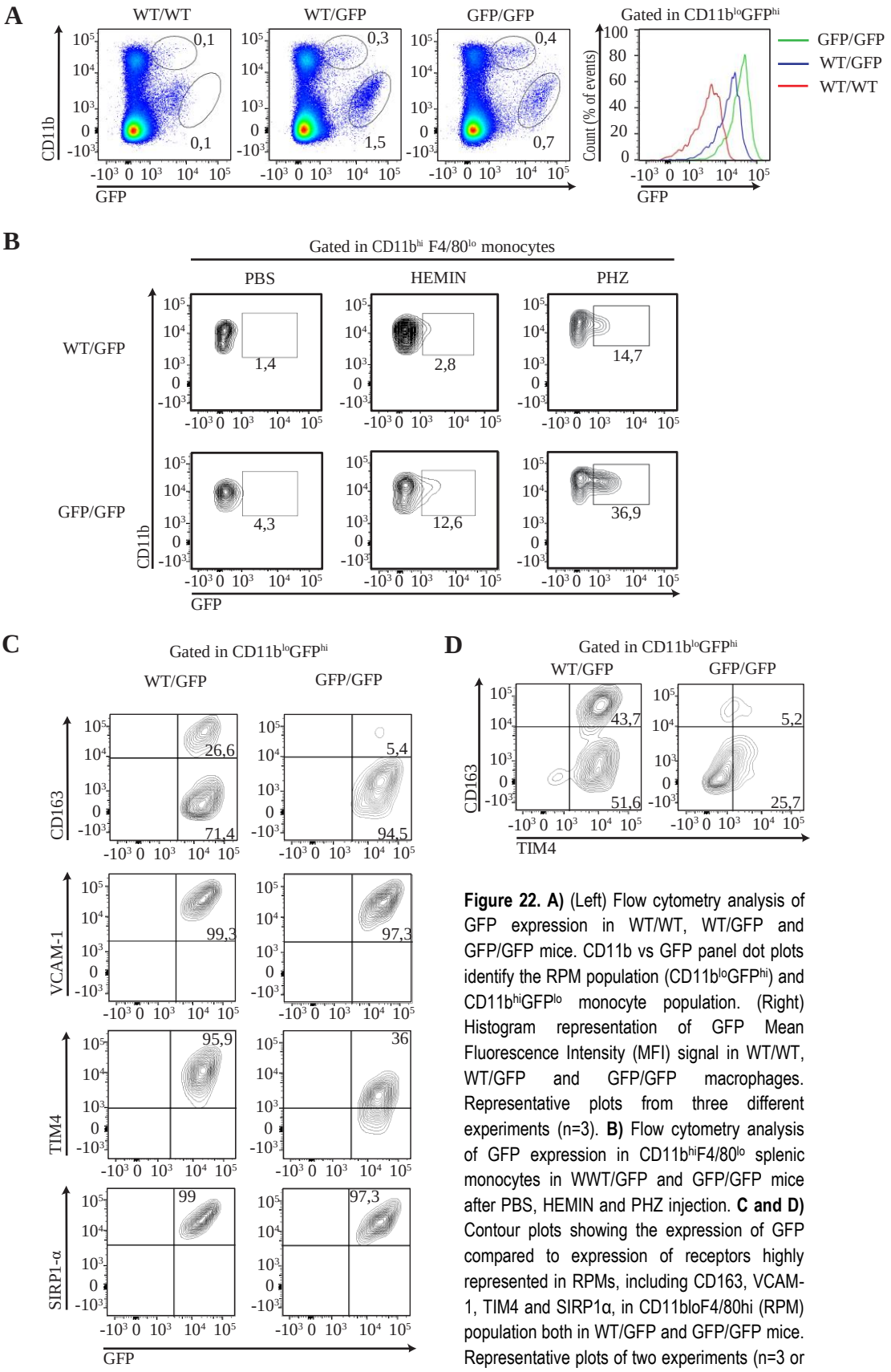

Figure 22. A) (Left) Flow cytometry analysis of GFP expression in WT/WT, WT/GFP and GFP/GFP mice. CD11b vs GFP panel dot plots identify the RPM population (CD11b^{lo}GFP^{hi}) and CD11b^{hi}GFP^{lo} monocyte population. (Right) Histogram representation of GFP Mean Fluorescence Intensity (MFI) signal in WT/WT, WT/GFP and GFP/GFP macrophages. Representative plots from three different experiments (n=3). **B)** Flow cytometry analysis of GFP expression in CD11b^{hi}F4/80^{lo} splenic monocytes in WWT/GFP and GFP/GFP mice after PBS, HEMIN and PHZ injection. **C and D)** Contour plots showing the expression of GFP compared to expression of receptors highly represented in RPMs, including CD163, VCAM-1, TIM4 and SIRP1α, in CD11bloF4/80hi (RPM) population both in WT/GFP and GFP/GFP mice. Representative plots of two experiments (n=3 or 4).

Results

CD11b^{lo}GFP^{hi}CD163^{+} and CD11b^{lo}GFP^{hi}TIM4^{+} RPM subpopulations reached approximately 30% and 95% respectively in LXRα$^{WT/GFP}$ mice, correlating well with the proportions of subsets of RPM observed in LXRα$^{WT/WT}$ control mice (Fig. 22C, D). Surprisingly, GFP^{+} cells in the spleens of LXRα$^{WT/GFP}$ mice include both the CD163^{hi} and CD163^{lo} subpopulations (Fig. 22C). LXRα$^{GFP/GFP}$ mice exhibit a dramatic reduction of CD163^{hi} (but not CD163^{lo} cells) and TIM4^{+} cells, which corresponded with the ratio observed in LXRαβ$^{-/-}$ mice in both cases (Fig. 22C, D). VCAM-1 and SIRP1α markers were expressed in most of the CD11b^{lo}GFP^{hi} RPM population, consistent with the phenotype described for LXRαβ$^{-/-}$ mice (Fig. 22C). These results procured by flow cytometry analysis revealed that, in the spleen, LXRα is expressed in F4/80^{hi}, CD163$^{hi/lo}$, and TIM4^{+} cells in LXRα$^{WT/GFP}$ mice, whereas upon LXRα deficiency in LXRα$^{GFP/GFP}$ mice, CD163^{hi} and TIM4^{+} cells disappeared.

We reached the same conclusions using a different gating approach, and analysing the GFP^{hi} cell compartment in the whole spleens of both LXRα$^{WT/GFP}$ and LXRα$^{GFP/GFP}$ mice. GFP^{hi} cells in the spleen of LXRα$^{WT/GFP}$ mice expressed high levels of F4/80, CD163 and TIM4, and low levels of CD11b, consistent of LXRα being highly represented in mature CD11b^{lo}F4/80^{hi}CD163^{+}TIM4^{+} RPM (Fig. 23). Conversely, in GFP^{hi} cells of LXRα$^{GFP/GFP}$ spleens, we noticed the absence of CD163 expression, and a considerably lower TIM4 expression (Fig. 23).

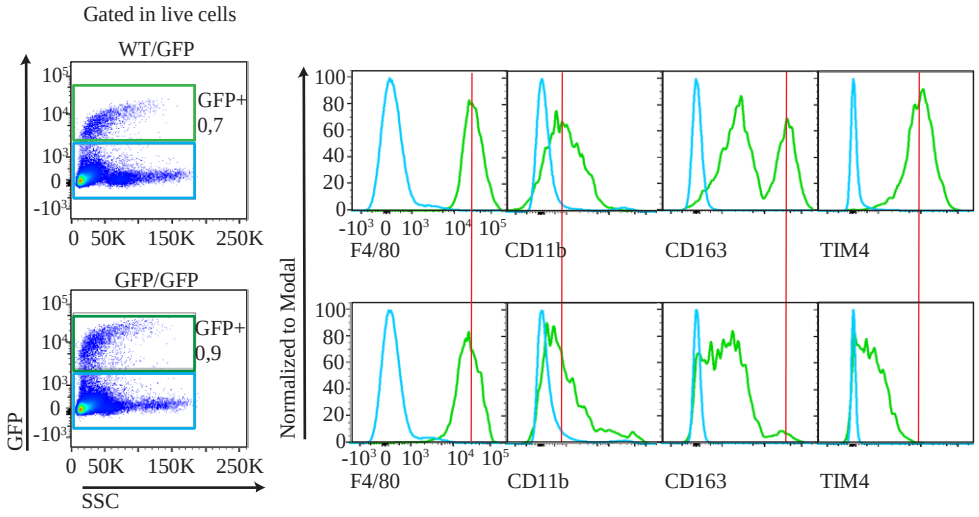

Figure 23. (Left) Macrophage surface expression from GFP^{+} (green) versus GFP^{-} (blue) total spleen cells. (Right) Mean Fluorescence Intensity (MFI) analysis expression profile of F4/80, CD11b, CD163 and TIM4 macrophage receptors in WT/GFP and GFP/GFP mice. Representative plots of two experiments (n=3 or 4).

These observations were also confirmed using our previously reported C57/Bl6 LXRα$^{-/-}$ (single deficient) mouse line. We found a consistent reduction in the frequency of CD11b^{lo}F4/80^{hi} RPM, and the subpopulations of macrophages expressing CD163 and TIM4 were absent in LXRα$^{-/-}$ mice, concluding that two different LXRα mouse mutant lines produce the same phenotype within the splenic myeloid cell compartment (Fig. 24A-E).

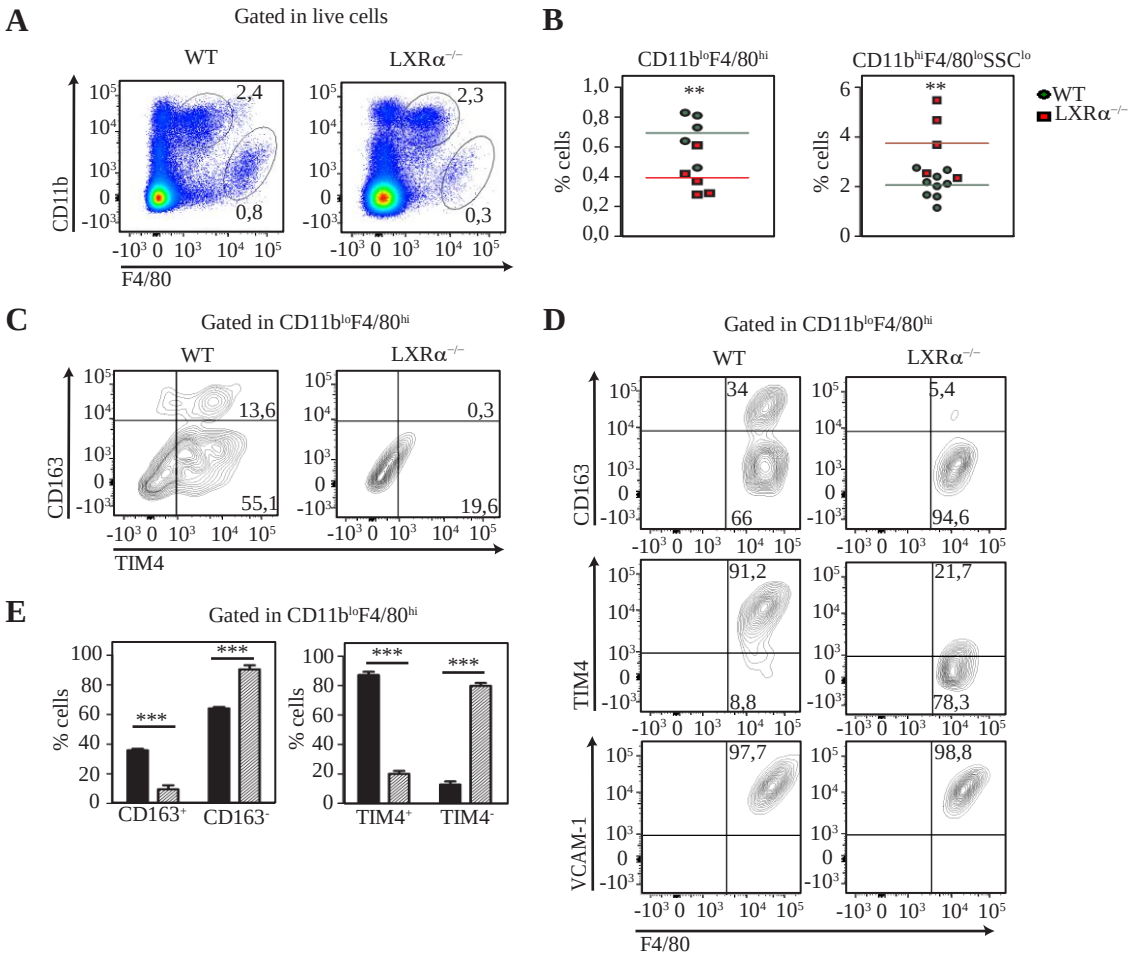

Figure 24. A) Flow cytometry analysis of CD11b^{lo}F4/80^{hi} RPM and CD11b^{hi}F4/80^{lo}SSC^{lo} monocyte populations in spleens from WT and LXRα$^{-/-}$ mice. Representative dot plots of two experiments, n=3. **B)** Quantifications from n=6 (WT) or 5 (LXRα$^{-/-}$) RPM populations. **C** and **D)** WT and LXRα$^{-/-}$ RPM expression of CD163, TIM4 and VCAM-1 macrophage receptors. Representative contour plots of two experiments, n=3. **E)** CD163^{+} and TIM4^{+} RPM quantification in spleens from WT and LXRα$^{-/-}$ mice. N=3 or more. Data was expressed as mean ± SEM. Statistical analysis was performed using Student's t test for significant differences. Values of P < 0.05 (*) or P < 0.01 (**), were considered to be significant, and values of P < 0.001 (***) were considered to be very significant.

Moreover, in order to place our new data in the context of our previous findings of LXRα and the MZ macrophages[63], we perform confocal microscopy employing fluorescence conjugated antibodies and the LXRα reporter mice to determine the localization of GFP^{+} cells in the spleen architecture. Using CD169 as a marker of inner MZ macrophages, we observed CD169^{+} (red fluorescence) cells in the appropriate MZ location in both LXRα$^{WT/WT}$ and LXRα$^{WT/GFP}$ mice (Fig. 25A). Merged fluorescence analysis identified double positive CD169/GFP cells (yellow signal) that were observed in the splenic MZ in LXRα$^{WT/GFP}$ mice. LXRα$^{GFP/GFP}$ mice presented very few CD169^{+} cells, that do not appear in the inner splenic MZ nor express GFP signal either (Fig. 25A). These results are consistent with the idea that LXRα expressed in MZ macrophages determines their development and localization[63]. In addition to the MZ, we also focused our attention to the red pulp of the spleen. Using F4/80 as a marker (red) to localize red pulp myeloid populations, we did not find any specific location of GFP^{+} cells within the red pulp, which were homogenously distributed, in either LXRα$^{WT/GFP}$ or LXRα$^{GFP/GFP}$ mice (Fig. 25B). The reduction in CD11b^{lo}F4/80^{hi} RPM observed in LXRαβ$^{-/-}$ mice was hardly noticeable in LXRα$^{GFP/GFP}$ as these mice

present increased numbers of F4/80+ red fluorescence due to accumulation of CD11b^{hi}F4/80^{lo}SSC^{lo} monocytes, as described above in this work (Fig. 25A). Thus, studies performed in this reporter mouse model allowed us to identify GFP^{hi} cells in the spleen, as the CD11b^{lo}F4/80^{hi} RPM pool, and to link the development of this population with LXRα activation.

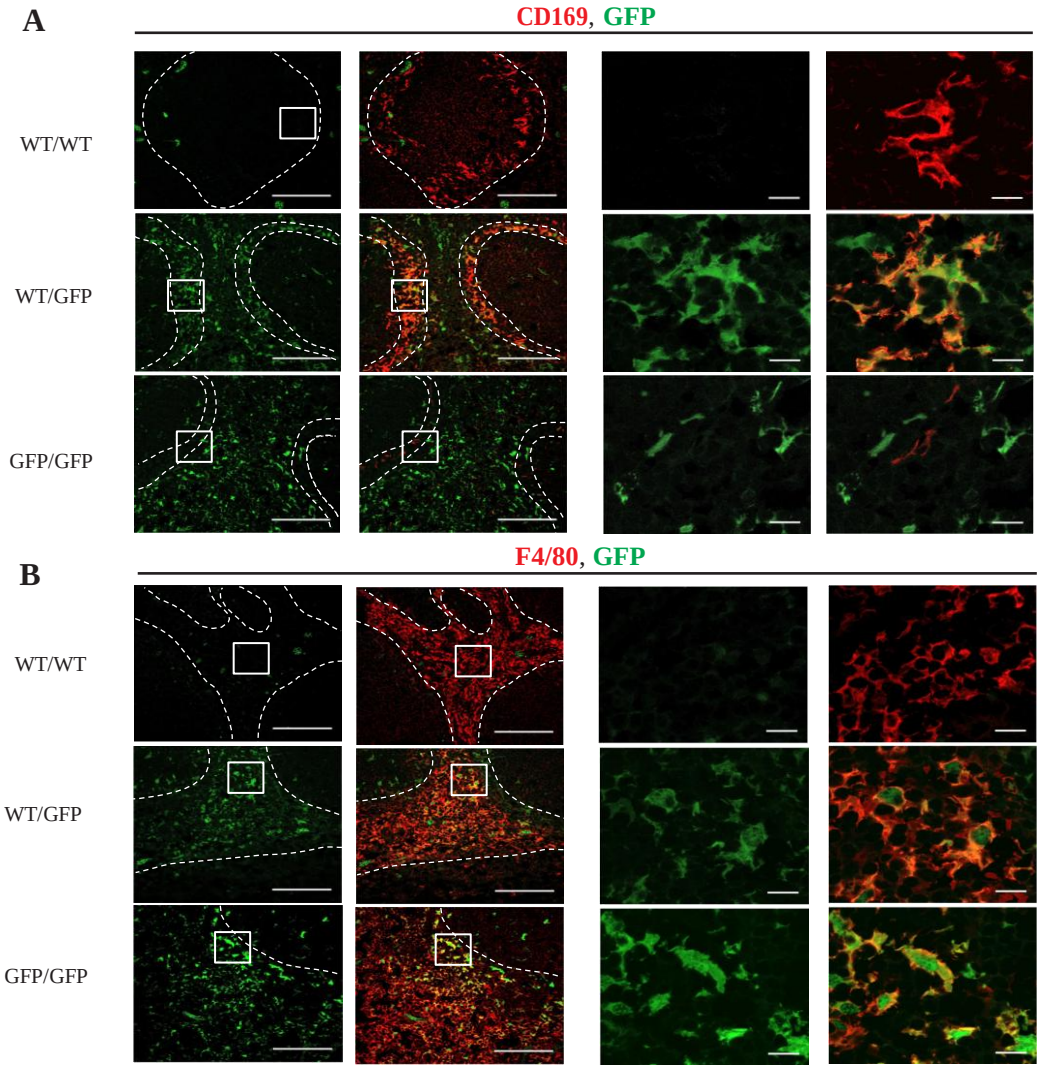

Figure 25. Spleen immunofluorescence analysis from WT/WT, WT/GFP and GFP/GFP mice using GFP **(A and B)**, CD169 **(A)** and F4/80 **(B)** as markers of LXRα, red pulp myeloid cells and marginal zone macrophages respectively. GFP/GFP mice lack CD169+ (red) macrophage population in the marginal zone. F4/80+ (red) signal in these mice corresponds with an increased F4/80^{lo} monocyte population. Merged red+green fluorescence corresponds to GFP and F4/80 expression overlaping in the cell. Scale bar = 1mm in 20X images (left) and 10 µm in 63X zoom (right).

6. Study of LXRα deficiency in macrophages *in vivo* in CD64CRE;LXRα$^{fl/fl}$ mice

As was mentioned before, previous studies have established *Spic* transcription factor as the key regulator of RPM development, thus being absolutely necessary for the correct functioning of the iron recycling machinery[64,101]. Heme accumulation in RPM promotes the targeted degradation of the SPI-C constitutive inhibitor, BACH1, that way allowing SPI-C induction and its transcriptional activity. *Spic*$^{-/-}$ mice exhibit a highly compromised CD11b^{lo}F4/80^{hi} RPM compartment[64], as well as lack of CD163^{+} and TIM4^{+} cells (Fig. 26A), indicating that it is required for the development of the entire RPM program in the spleen. To test whether SPI-C was required for LXRα expression within CD11b^{lo}F4/80^{hi} RPM and CD11b^{hi}F4/80^{lo}SSC^{lo} monocytes, we collected the remaining RPM and the monocytes present in *Spic*$^{-/-}$ mice and compared their expression of LXRα compared to WT cells. Surprisingly, levels of LXRα expression were comparable between WT and *Spic*$^{-/-}$ mice in both myeloid populations (Fig. 26B).

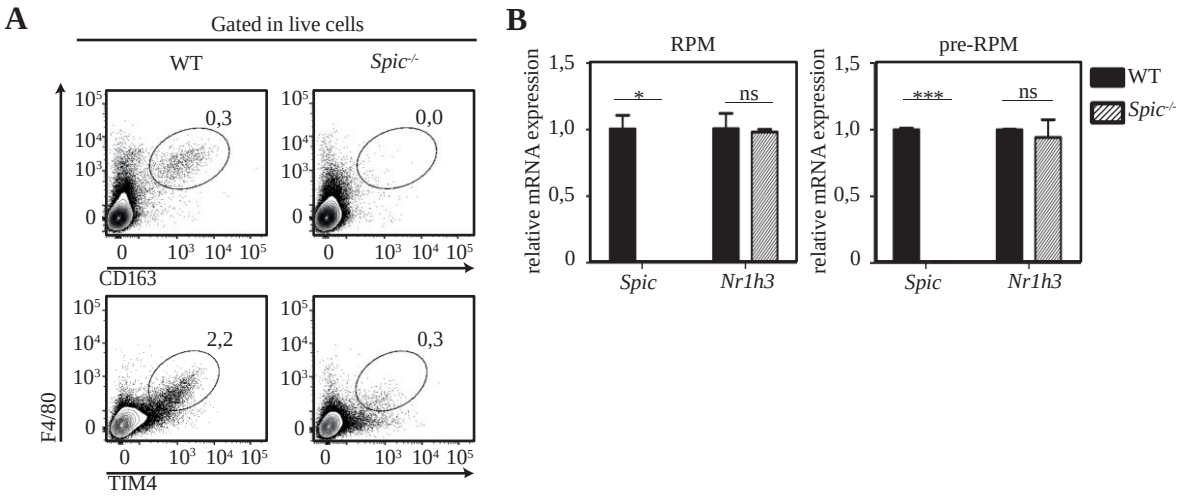

Figure 26. A) Flow Cytometry analysis of CD163 and TIM4 expression in WT and *Spic*$^{-/-}$ RPMs. Representative plots from n=2. **B)** Quantitative expression of Spic and LXRα in isolated RPM and pre-RPM, in WT and *Spic*$^{-/-}$ mice (n=2). Data was expressed as mean ± SEM. Statistical analysis was performed using Student's t test for significant differences. Values of P < 0.05 (*) or P < 0.01 (**), were considered to be significant, and values of P < 0.001 (***) were considered to be very significant.

In order to better understand the influence of LXRα activity in CD163 and TIM4 expression in RPM, we employed a recently created macrophage-restricted conditional knock out mouse model that used CRE-recombinase technology to delete LXRα expression in all the myeloid cells that express *Fcgr1* (encoding CD64), which are mostly mature macrophages[198] (Fig. 7E, Materials and methods).

As a control for these experiments, we used LXRα$^{fl/fl}$ mice that phenotypically behaved as WT mice, and compared the analysis in parallel with our WT and full LXRα$^{-/-}$ mice. While WT and LXRα$^{fl/fl}$ mice displayed a comparable 30% of

Results

CD11b^{lo}F4/80^{hi}CD163^{+} macrophage subset, both CD64CRE-LXRα$^{fl/fl}$ and LXRα$^{-/-}$ mice presented a similar reduction in CD11b^{lo}F4/80^{hi}CD163^{+} RPM (Fig. 27A-C). The same decrease was detected in CD64CRE;LXRα$^{fl/fl}$ mice for TIM4 expression employing MFI analysis (Fig. 27A-C). To our surprise, we found no differences between the total cell number of CD11b^{lo}F4/80^{hi} RPM in LXRα$^{fl/fl}$ and CD64CRE;LXRα$^{fl/fl}$ mice (Fig. 27D). Meanwhile, these cell counts showed a diminished CD11b^{lo}F4/80^{hi}CD163^{+} RPM subset, but an increased CD11b^{lo}F4/80^{hi}CD163^{-} RPM subset in CD64CRE;LXRα$^{fl/fl}$ mice compared to their LXRα$^{fl/f}$ controls (Fig. 27D). These results suggest that, even though LXRα is required for CD163 and TIM4 expression, the loss of this transcription factor has a major impact in the frequency of total RPM population only when it is absent in germline. When LXRα is depleted within a restricted *Fcgr1*-expressing cells frame, the expression of CD163 and TIM4 are the major abnormalities observed when compared to a full deletion of LXRα in other mutant mice. Immunofluorescence analysis using a CD163 monoclonal antibody confirmed the absence of CD163-expressing cells in CD64CRE;LXRα$^{fl/fl}$ and LXRα$^{-/-}$ spleens (Fig. 27E).

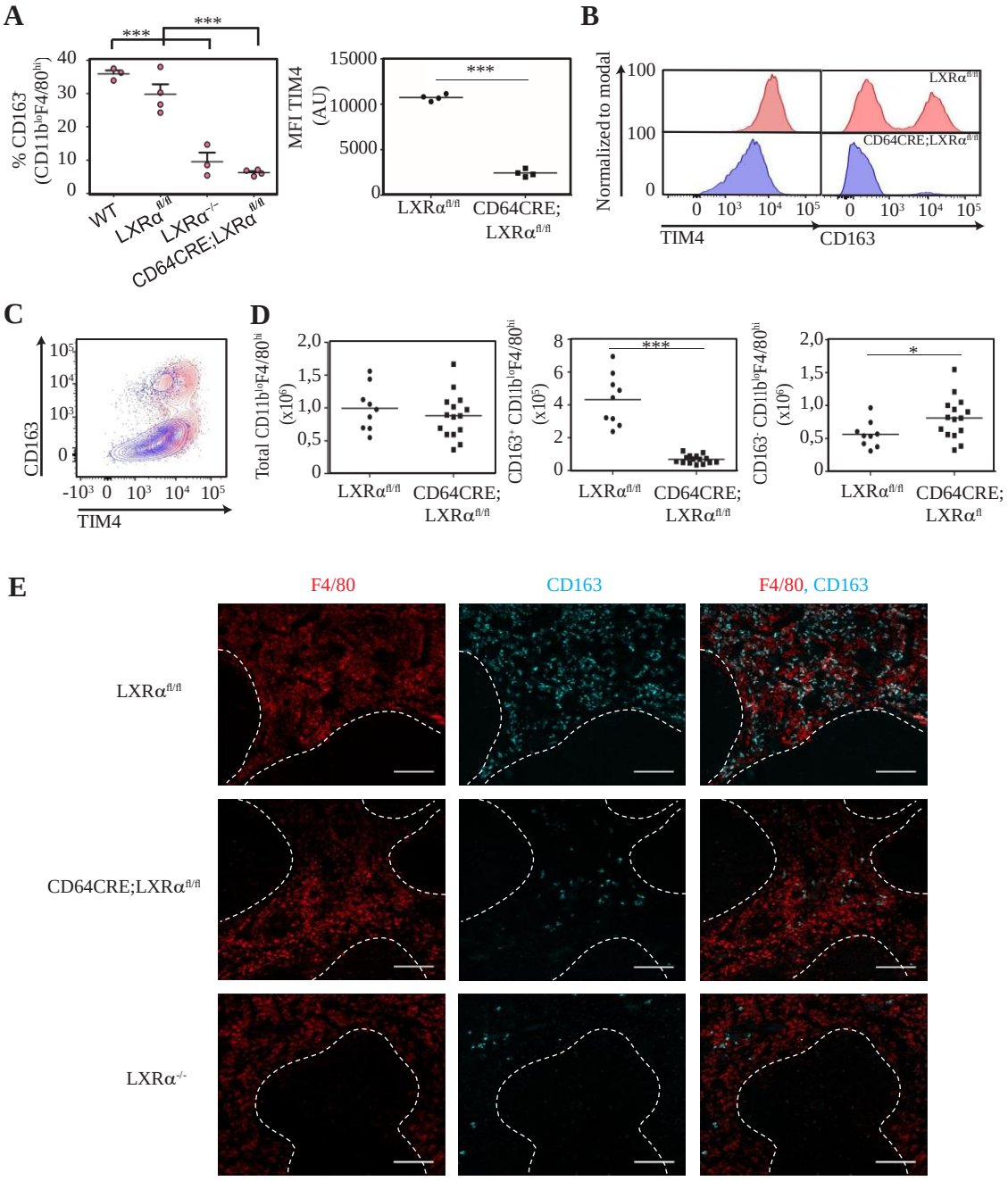

Figure 27. A) (Left) Quantification from flow cytometry analysis of the expression of CD163 in WT, LXRα$^{fl/fl}$, LXRα$^{-/-}$ and CD64CRE;LXRα$^{fl/fl}$ RPMs (n=3 or 4). (Right) Quantification of MFI analysis of TIM4 expression in LXRα$^{fl/fl}$ and CD64CRE;LXRα$^{fl/fl}$ RPMs (n=4). **B)** Histogram representation of TIM4 and CD163 fluorescence intensity in LXRα$^{fl/fl}$ (top, red) and CD64CRE;LXRα$^{fl/fl}$l (bottom, blue) RPMs. Representative of two experiments, n=3 or more. **C)** Contour plot showing CD163^{+}/TIM4^{+} cell population in spleens of LXRα$^{fl/fl}$ (red) and CD64CRE;LXRα$^{fl/fl}$ (blue) mice. Representative plots of two experiments, n=3 or more. **D)** Absolute cell number quantifications from total RPM population (left), CD163^{+} RPMs (middle) and CD163^{-} RPMs (right), in LXRα$^{fl/fl}$ (n=9) and CD64CRE;LXRα$^{fl/fl}$ (n=14) mice. Data was expressed as mean ± SEM. Statistical analysis was performed using Student's t test for significant differences. Values of P < 0.05 (*) or P < 0.01 (**), were considered to be significant, and values of P < 0.001 (***) were considered to be very significant.

7. Transcriptional regulation by LXRα determinates the identity of CD11b^{lo}F4/80^{hi}CD163^{+}TIM4^{+} macrophages in the spleen that are critical for iron handling.

Our results presented above enlightened the possibility of the existence of at least two different subpopulations within the RPM compartment in the spleen: a population identified by surface expression of CD11b^{lo}F4/80^{hi}CD163^{+}TIM4^{+}, that is dependent on high LXRα expression, and another one, CD11b^{lo}F4/80^{hi}CD163^{-}TIM4^{+}, that remains in the spleen in the absence of LXRα.

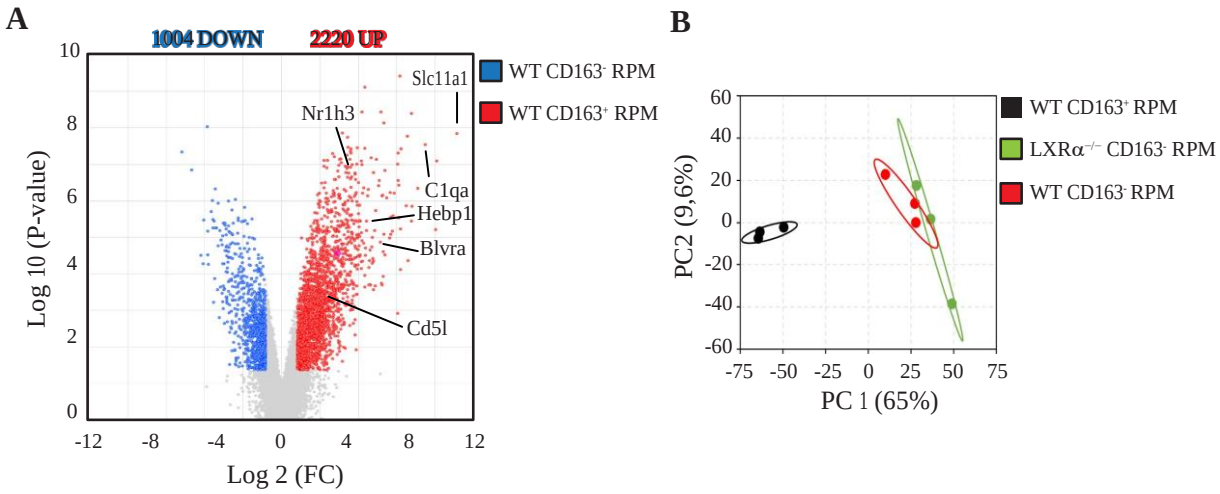

Figure 28. A) Volcano Plot gene expression profile representation of purified WT CD163^{+} vs CD163^{-} RPM. Up-regulated genes are depicted in red, and down-regulated genes in blue. **B)** Principal Component Analysis shows the clustering pattern of global gene expression differences between WT CD163^{-} (green), CD163^{+} (black) and LXRα$^{-/-}$ CD163^{-} (red) RPM.

To further characterize them, we performed transcriptional profiling analysis by cell sorting these two subpopulations from WT and LXRα$^{-/-}$ mice. Volcano plot representation from this data showed that, in WT mice at the steady state, these two subsets had very different gene expression profiles. CD11b^{lo}F4/80^{hi}CD163^{+}TIM4^{+} macrophages displayed higher expression of *Nr1h3* gene (LXRα) and several LXRα direct target genes (*Cd5l*, *Abca1* among others) than CD11b^{hi}F4/80^{lo}CD163^{-}TIM4^{+} macrophages (Fig. 28A). Comparing the whole data set through a Principal Component Analysis (PCA), we found that WT and LXRα$^{-/-}$ CD11b^{lo}F4/80^{hi}CD163^{-}TIM4^{+} macrophages clustered together, but they showed a distant pattern of expression compared to WT CD11b^{lo}F4/80^{hi}CD163^{+}TIM4^{+} subset (Fig. 28B).

Closer analysis using a heatmap representation revealed two perfectly marked clusters of genes with differential transcription between CD163 expressing and non-expressing macrophages in WT mice (Fig. 29A, B). CD163 expressing WT macrophages upregulated the transcription of 2220 genes, whose expression was very low in CD11b^{lo}F4/80^{hi}CD163^{-}TIM4^{+} WT macrophages (Fig. 29B). Gene ontology (GO) terms showed that, among the biological functions related to these clusters, were immune system process, phagocytosis and lipid and iron metabolism (Fig. 29A).

The opposite situation was observed in the case of the other cluster. Remarkably, LXRα$^{-/-}$ CD11b^{lo}F4/80^{hi}CD163^{-}TIM4^{+} macrophages perfectly mirrored the transcriptional program that exhibit their WT CD163^{-} counterparts, therefore indicating that the major transcriptional pathways expressed in CD163^{-} cells do not rely greatly on LXRα activity (Fig. 29A, B). Several iron metabolic genes had high expression values in WT CD11b^{lo}F4/80^{hi}CD163^{+}TIM4^{+} RPM, such as specific iron and hemoglobine transporters (*Slc11a1* and *Hebp1* respectively) or heme catabolic enzymes (*Blvra, Hmox1, Alas1, Ncoa1*), the iron exporter FPN-1 (*Slc40a1*) and other iron regulating proteins (*Aco1, Hfe*) (Fig. 29B). Several genes encoding for complement proteins were also highly expressed in CD11b^{lo}F4/80^{hi}CD163^{+}TIM4^{+} macrophages (*C1qa*, and *C6*) (Fig. 29B). Together, this transcriptional analysis of CD163^{+} and CD163^{-} RPM revealed that LXRα activity determines the appearance of a specific subset of red pulp resident macrophages, specialized in iron recycling and metabolization.

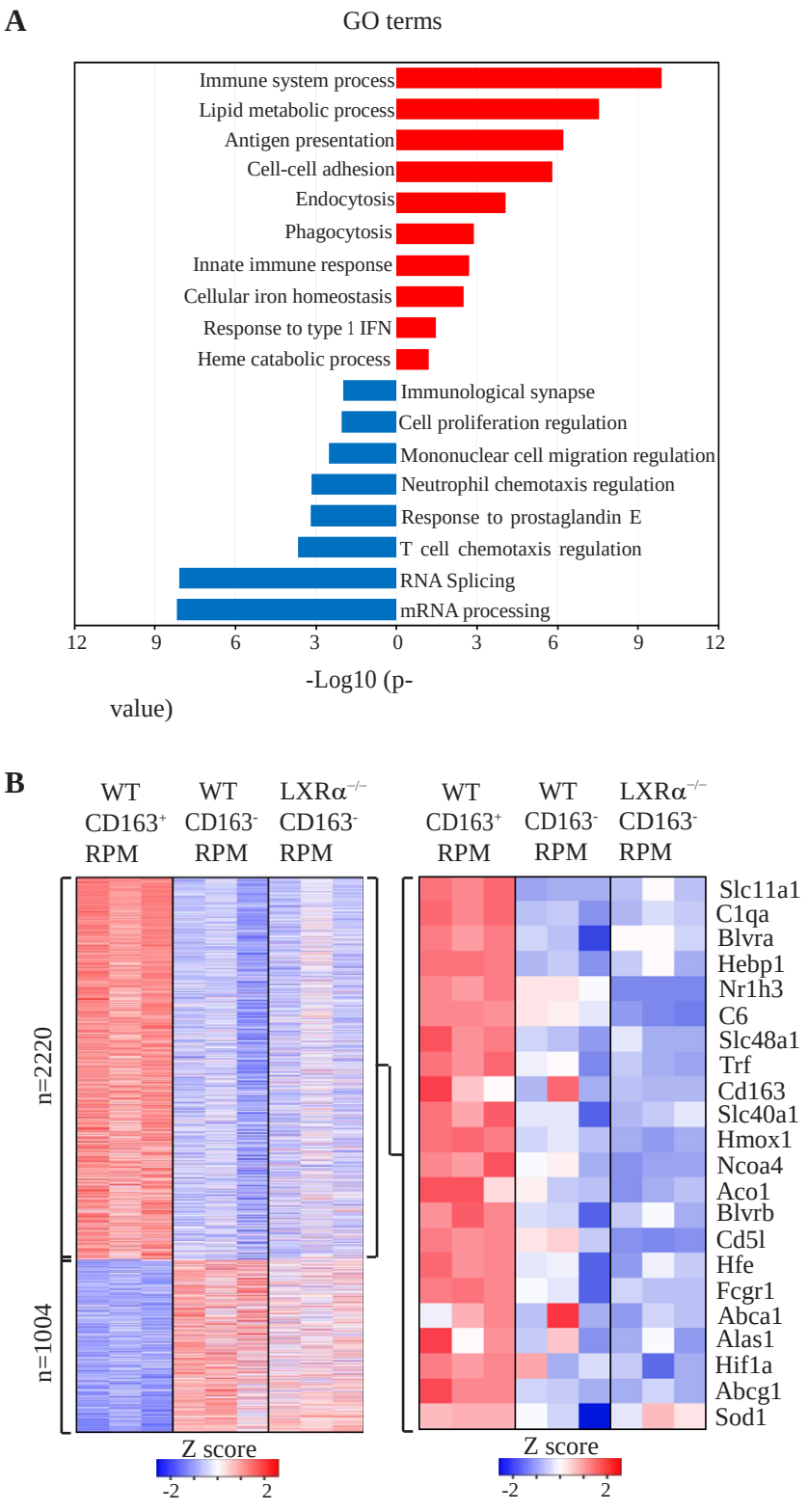

Figure 29. A) Gene ontology analysis and **(B)** Heatmap representation of top-regulated iron and haemoglobin related genes in WT CD163^{+}, WT CD163^{-} and LXRα$^{-/-}$ CD163^{-} RPM. GO Terms correspond to main functions of Cluster I genes.

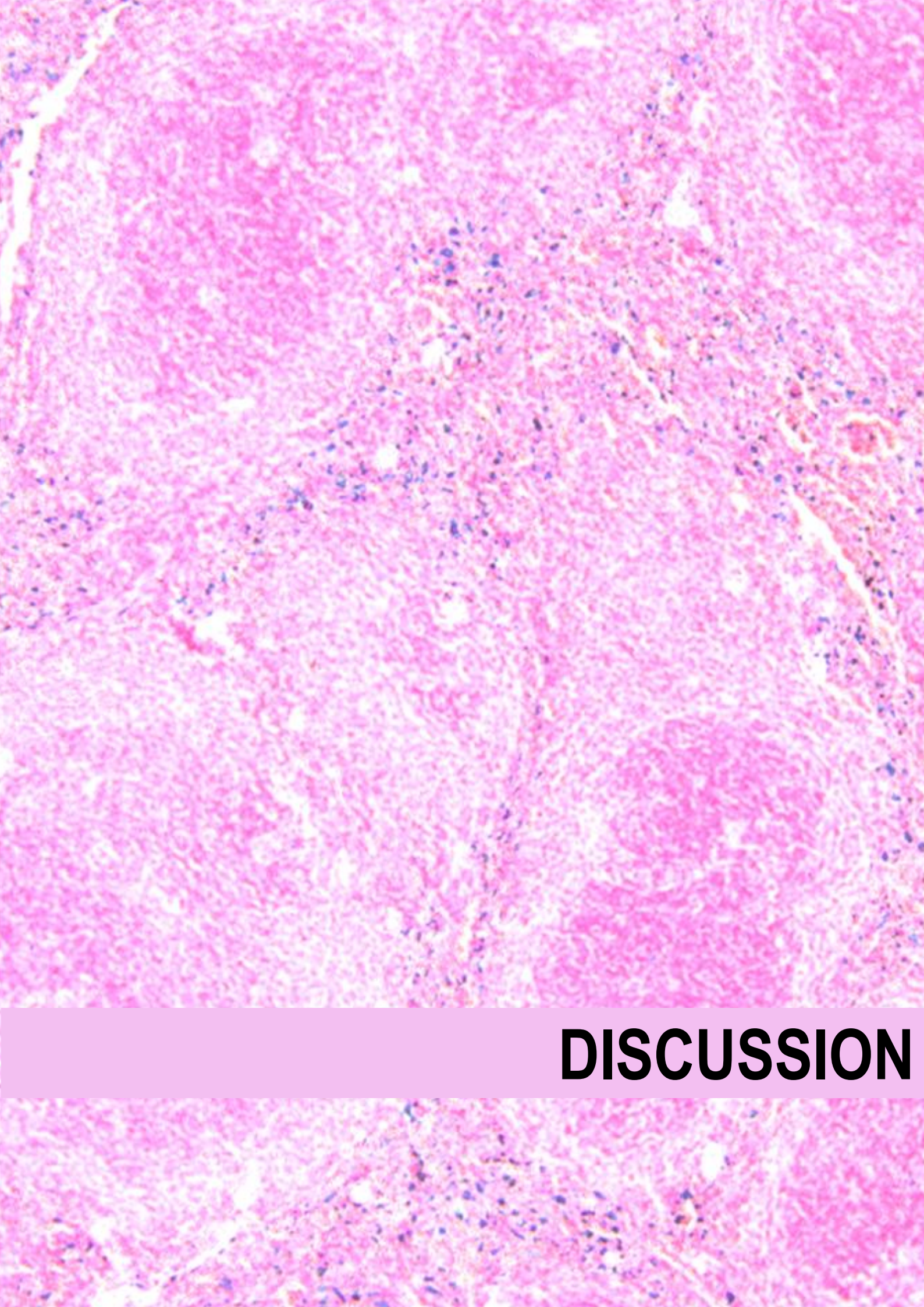

DISCUSSION

Discussion

1. LXRα and LXRβ present differential roles in macrophages

LXRα and LXRβ are nuclear receptors that play a crucial role in the transcriptional regulation of whole body cholesterol metabolism[169]. In addition, a growing body of literature has implicated LXRs in many different metabolic and homeostatic processes in the organism, beyond cholesterol pathways[202]. Previous studies from our group and others have demonstrated that LXRs also participate in diverse aspects of macrophage transcriptional machinery, including inflammation and host defense[195,196]. Although both receptors are expressed in a variety of cell types, their importance in metabolic and inflammatory processes in peripheral tissues rely greatly on their expression in macrophages[16,179,184]. Regarding the relative importance of each LXR isoform, studies *in vitro* over the last 10-15 years have reported that many of the functions of LXRα and LXRβ are virtually overlapping. However, the notable differences on their expression pattern in tissues suggested that, in different contexts, LXRα and LXRβ should have individual, non-redundant functions *in vivo*[165]. Indications that LXRα and LXRβ exhibit distinct transctriptional roles are slowly emerging, some of them have been uncovered by our group. For example, Ramon-Vázquez *et al*. (2019) used bone marrow derived immortalized LXRα or LXRβ-expressing macrophage lines to identify a whole set of genes differentially regulated by each receptor, and described that LXRα regulated a higher number of ligand-dependent genes than LXRβ[203]. Also, other *in vivo* studies support a higher implication of LXRα in specific processes. During atherogenesis, regulation of macrophage biological actions mediated by LXRα, over LXRβ has shown beneficial effects by reducing atherogenic lesion formation in mice[183,204]. In addition, the individual absence of LXRα causes severe problems in the differentiation of two macrophage populations that reside in the splenic marginal zone, MMM and MZM[63]. Therefore, given the long-standing interest of our group in LXR biology in macrophages, we decided to explore additional individual functions for LXRs in macrophages with newly created mouse models. In particular, our group generated new mouse models suitable for the analysis of LXRα expression and function in different types of tissue resident macrophage populations.

2. The identity of tissue resident macrophages is determined by a combination of origin and microenvironment

Tissue resident macrophages have critical roles in immunity, inflammation and tissue homeostasis[36]. However, their maintenance, origin and fate are not entirely clear. Initially proposed to be derived from circulating monocytes[205], we now know that adult macrophages originate from several successive waves of embryonic, neonatal and adult hematopoiesis[35]. The net contribution of embryonic precursors versus adult hematopoiesis to the complex network of tissue resident macrophages is an area of intense research. Several studies have demonstrated that different TRMs throughout the organism have different turnover rates and rely differently on HSCs progenitors to maintain themselves[51,57,58], so it would not be unprecedented to speculate with the possibility that the microenvironment plays an important role in shaping the identity of a particular macrophage population. It is likely that the balance between genetic programs determined by their

ontogeny, versus plasticity induced by local signals is crucial for this identity. Growing evidence supports the idea that the tissues, and the signals they produce, are key promoters of macrophage specification and diversity[62]. In this scenario, embryonic progenitors would seed different tissues as 'unprogrammed' cells, and then receive different cues that would shape their transcriptional activity[60]. This differentiating mechanism goes hand in hand with the idea that, when for some reason a macrophage niche empties, new adult HSCs-derived monocytes are able to fulfill that niche, and differentiate into the correspondent TRMs[60]. Recent studies by the Ido Amit and Martin Guilliams labs demonstrated this concept with elegant articles[16,206]. One of these, described this phenomenon by using engineered mouse models in which depletion of hepatic KCs (in a KC-DTR mouse model) promoted the infiltration of BM-derived Ly6C^{hi} monocytes, that seeded the empty niche in the liver within 14 days, and reconstituted the resident macrophage population. These monocyte-derived KCs were able to self-maintain independently and perfectly developed the functions of embryonic KCs. Analysis of their transcriptional profile showed that these monocyte-derived KCs were highly homologous to embryonic KCs[206]. The mechanisms that govern these renewal patterns are not completely understood and may well be controlled by several parameters, including local-specific microenvironment, inflammation and perhaps other cues yet to be defined.

3. LXRs in the context of tissue macrophage differentiation

The notion that a discrete transcription factor drives the generation of a specific TRM population from the early stages or embryonic development, by molding the progenitor transcriptional core program, has been described by other groups in other contexts. This is the case for *Id3* and KCs[62], *Runx3* and Langerhans cells[207], *Gata6* and large peritoneal macrophages[208], or *Pparg* for alveolar macrophages[65,209]. For the RPM and the BMM compartments, Murphy and colleagues identified SPI-C as their master regulator, controlling the generation of these macrophage populations[64,101]. Indeed, *Spic*$^{-/-}$ mice lack most of the CD11b^{lo}F4/80^{hi}VCAM^{hi} macrophages in the spleen and bone marrow, suggesting that these two TRM populations share a common origin, due to their strikingly similar surface markers expression and their SPI-C dependency for their appearance and maintenance[101]. The study by Lavin *et al*. (2014) deposited a compelling reservoir of datasets from mRNA transcripts expressed in purified isolated tissue macrophages[16]. This study complements and expands the colossal public repository generated by the IMMGEN consortium on tissue macrophages[65]. Data extracted and analyzed from the Lavin study highlighted the prominent expression of LXRα in liver and spleen macrophages[16] (Fig. 6, Introduction). We were interested in such prominent expression of LXRα in red pulp macrophages, since our previous study on LXRα and the cellular biology of spleen macrophages, revealed no gross differences in the frequency of F4/80^{+} cells present in the red pulp between WT and LXR-deficient mice. Such conclusion was based on an IHC screen using F4/80 antibody as the pan-macrophage marker[63]. However, red pulp resident monocytes (CD11b^{hi}F4/80^{lo}SSC^{lo}) also express detectable levels of F4/80 on their surface. Looking at that data in retrospect, it is conceivable that our original immunohistochemical analysis could have missed any existing differences in the number of "true" RPMs located in the red pulp of the spleen of WT and LXR-deficient mice. Importantly, our LXRα-hHB-EGF-DsRed mouse model allowed us to corroborate and definitively establish that LXRα is highly expressed in RPMs (CD11b^{lo}F4/80^{hi})

(Fig. 10B, C). After LXRα-DTR bone marrow transplant into WT recipient mice, DT injection specifically depleted the spleen resident RPMs and both marginal zone populations, proving that LXRα is in fact functionally expressed in these two macrophage subsets (Fig. 10C). Unexpectedly, the administration of the toxin also caused a significant decrease of the CD11b^{hi}F4/80^{lo} monocyte population in the spleens of transplanted mice. LXRα is not normally expressed (or very poorly expressed, compared to RPMs or KCs) by classic monocytes[16,210], but this partial depletion exposed the existence of a monocyte intermediate subset within the CD11b^{hi}F4/80^{lo} monocyte population that expressed LXRα. These results may imply that a subset of monocytes in the spleen could have functional implications that are dependent on LXRα, perhaps involved in the differentiation towards RPMs.

4. LXRs and the proper maintenance of the red pulp macrophage compartment in the spleen

Our studies using LXR double deficient and LXRα single deficient mice add a new layer of complexity to the transcriptional regulation of macrophage heterogeneity in tissues. Using flow cytometry analysis, we were able to establish that both LXRαβ$^{-/-}$ and LXRα$^{-/-}$ mice present defects in the proper establishment of the RPM population in the spleen, and the resident macrophage population in the bone marrow (Fig. 11A-C, 12A, B). In the absence of LXRα, not only marginal zone macrophages are affected, but also the two resident macrophage populations in the red pulp of the spleen and the bone marrow are notably compromised compared to WT controls. However, the profound defect in the total number of RPMs and BMMs observed in *Spic*$^{-/-}$ mice clearly indicates a more dominant role for SPI-C in their development. In LXR-deficient mice, we consistently observed a range between 30-50% defect in the percentage of resident RPMs and BMMs, compared to WT mice. Conversely, the CD11b^{hi}F4/80^{lo}SSC^{lo} resident monocyte populations were markedly increased in these two tissues in our LXR-deficient mice (Fig. 11A-C and 12A, B). Murphy and colleagues (2014) elegantly described, using a *Spic*$^{iGFP/iGFP}$ reporter mouse, that macrophage precursors expressing SPI-C (what they called “pre-RPMs”) within the monocyte compartment in the spleen, were able to locally replenish the resident macrophage pool under stress situations, such as PHZ-induced hemolysis. The absence of RPMs, together with the accumulation of free iron liberated from ruptured erythrocytes, promoted the expansion of a SPI-C-expressing population of monocytes for the replenishment of the empty macrophage niche[101]. Therefore, monocytes exposed to excess heme increased SPI-C expression under hemolytic stress conditions and constituted a functional precursor of resident RPMs. These studies suggested that embryonic-derived resident macrophage populations self-maintain under homeostasis, independently from HSCs progenitors, and only receive help from monocytes when they are unable to perpetuate, or under stress conditions that compromise resident macrophage viability[211].

We found a possible correlation between these results, and our observations on CD11b^{hi}F4/80^{lo}SSC^{lo} monocyte accumulation in the spleens and bone marrows of our LXR-deficient mice (Fig. 11A, C and 12 A, B). We speculate that this accumulation in LXR-deficient spleens might respond to signals aiming to replenish the partially empty RPM compartment

in these mice. After transplantation of WT or LXRαβ$^{-/-}$ bone marrows into LXR-deficient and WT mice respectively, RPM and BMM frequencies resembled the phenotype of the donor mice after 10 weeks, but the resident monocyte compartment showed elevated levels in all cases, both in spleen and bone marrow (Fig. 13A, B). Even though the results were not conclusive in this regard, we could discern a tendency of CD11b^{hi}F4/80^{lo}SSC^{lo} monocyte over-proliferation in both tissues. The transplantation of a chimeric bone marrow (WT-DsRed;LXRαβ$^{-/-}$) into WT recipients shed valuable light into this matter. Not only were we able to detect an intrinsic defect within LXRαβ$^{-/-}$ BM-derived progenitors to repopulate the RPM compartment, thus confirming the importance of the LXR transcriptional program in the development of this population, but also determined their predisposition towards a monocyte accumulation (Fig. 14A-C).

The integration of this data with the current knowledge, further supported our hypothesis that LXR absence could in fact induce a partial niche availability in the red pulp and the bone marrow macrophage compartments, and thus the CD11b^{hi}F4/80^{lo}SSC^{lo} monocyte accumulation in those tissues could constitute an attempt to repopulate that niche. The mechanisms that govern this monocyte accumulation in LXR-deficient mice are currently unknown and more studies are needed to depict the exact signals that promote the monocyte expansion. One additional parameter in this equation is the tendency towards pro-inflammation observed in LXR deficient mice. Inflammatory signals *per se* could be involved in the monocyte expansion independently of their role in RPM differentiation. Future experiments analyzing proliferation of *ex vivo* transferred monocytes could shed some light on these issues. Collectively, integrating our new conclusions with previous data regarding LXR signaling, and its activity in tissue macrophages, we concluded that LXRα is a key determinant for the correct development of the RPM and BMM compartments.

Another important aspect to discuss is the possible interdependency between LXRα and SPI-C. Given the important role of SPI-C in the development of RPM and BMM populations, we hypothesized that SPI-C activity might be the dominant factor and would operate upstream of LXRα in the transcriptional pathway that controls the development of RPMs and BMMs. To our surprise, quantitative PCR analysis showed similar levels of LXRα (*Nr1h3*) expression in WT RPMs and the few RPMs remaining in *Spic*$^{-/-}$ spleens, and this was also the case for the resident monocyte population (Fig. 26B). Our transcriptional profiling analysis, and quantitative PCR, showed that LXR-deficient RPMs and CD11b^{hi}F4/80^{lo}SSC^{lo} monocytes also presented similar levels of *Spic* expression compared to WT controls (Fig. 19). However, upon iron stress by heme administration of PHZ-induced hemolysis, CD11b^{hi}F4/80^{lo}SSC^{lo} monocytes also activate the LXRα transcriptional program (Fig. 22B), in the same way they do with SPI-C expression[101], suggesting a similar pathway for both transcription factors. These observations eliminated the possibility that either SPI-C or LXRα expression could be dependent on one another, and suggested that both transcription factors control separate (perhaps parallel signaling) pathways in the RPM development process. Similar results could be expected for the BMM population, but further analyzes are required to ascertain this fact.

Discussion

5. Loss of LXR alters the red pulp macrophage transcriptome

Our study uncovered that LXR signaling controls a part of the RPM transcriptional program. This conclusion was clearly extracted from our transcriptional profile analysis. While LXR-deficient CD11b^{hi}F4/80^{lo}SSC^{lo} splenic monocytes present a very similar genetic footprint to their WT counterparts, the transcriptional program of LXR-deficient RPMs appears to be far from that of WT RPMs (see PCA analysis, Fig. 18C). In conjunction with the previous observations, this supports the idea that LXR expression is necessary for de acquisition of a full RPM program, while being dispensable for splenic monocyte development. We clustered our gene analysis by comparing the expression of genes highly represented in RPM over monocytes. A set of 181 genes were identified to be highly up-regulated in WT RPMs compared to monocytes, which resulted in very low expression in LXR-deficient RPMs (Fig. 18A). Conversely, another set of 79 genes displayed the opposite situation, and were highly expressed by LXR-deficient RPMs but presented very low levels of expression in WT RPMs (Fig. 18A). The genes that LXR activity controls, are involved in a wide array of biological actions. Some of the top enriched cellular functions that appear regulated in our profile by LXR in RPMs were related to immune regulation and inflammatory signaling (see Gene Ontology terms, Fig. 18B). LXR activation in macrophages has been historically associated to anti-inflammatory phenotypes, including work done by our group[169]. It should be pointed out that most of those studies were conducted *in vitro* under conditions of pre-stimulation with potent synthetic agonists and bacterial LPS in thioglycollate macrophages[186,193,212]. However, our current study shows that loss of LXR in RPMs under homeostatic conditions results in lower expression of innate immune related genes, including complement factors, cytokines and cell adhesion molecules (Fig. 18A). Although our current results could be considered contradictory to previous studies that reported LXR-dependent anti-inflammatory actions, we conclude that they fit well with the susceptibility of LXR-deficient mice to blood-borne pathogen infections[191]. Loss of regulation of cytokines and complement factors in LXR deficient mice may compromise the monitoring function of splenic macrophages and may possibly affect the initiation of adaptive immunity against pathogens. Since the spleen is the primary site for blood filtration in mammals, this organ is in charge of the clearance of aged, infected or dysfunctional red blood cells from circulation to avoid harmful effects. Then, as part of this filtration task, the red pulp scans blood for pathogens[66]. If the RPM compartment is not fully functional in LXR-deficient mice and stressed or infected RBC are not properly cleared, disease situations such as anemia or malaria infection could be exacerbated in these mice. More studies along these lines are planned for the near future. Thus, this distinctive transcriptional regulation observed in LXR-deficient RPMs demonstrates that not only LXR controls a part of the RPM genetic program, but also the number and functions of macrophages present in the splenic red pulp.

6. LXR activity in red pulp macrophages and the implications for iron metabolism

The splenic red pulp traps senescent, dead or opsonized cells, mostly RBCs[66]. Thus, one of the important tasks of resident RPMs is the recycling of their iron content[76,88]. Iron is an essential element in the organism, and the correct balance in its

metabolism is crucial for the maintenance of global homeostasis. As a fundamental component of hemoglobin, it constitutes a limiting compound in the generation of new erythrocytes, and deregulations in its normal cycle could directly affect erythropoiesis, being often the cause for different kinds of pathologies[77,88,120,142] (see Introduction, sections **1.4**-**1.6**). But mostly, impairment of iron recycling constitutes an immediate cause of anemia[75,100]. Our results in LXR-deficient mice discovered significant iron depositions within the red pulp of the spleen, notably appreciated both by histological staining (Fig.15A, B) and at the cellular level (Fig.17A). In addition to the iron overload within the resident macrophages, the red pulp of LXR-deficient mice presented RBC accumulation combined with a notable decrease in the percentage of total RBCs in the bone marrow (Fig. 16A, B). This combination suggested a defective RBC clearance in the spleen, and a possible subsequent defect in erythropoiesis in the bone marrow. In addition, in circulating blood, hematocrit levels appeared normal in 8-weeks old mice, but were clearly diminished in 40-weeks old LXRαβ$^{-/-}$ mice, who displayed aged-dependent anemia, and lower concentrations of serum Hb (Fig. 16D). When we studied the bone marrow erythroid compartment in detail we found that LXR-deficient mice displayed an accumulation of the first differentiation stages of erythroblasts, but suffered a significant decrease in the percentage of erythroblasts in the late maturation stages (reticulocyte)[111,201] (Fig. 16B). During these late phases of erythroblast maturation, iron is required for the synthesis of Hb[88]. It is possible that the accumulation of iron in the spleen of LXR-deficient mice causes the reduction of iron availability in the bone marrow, needed for the completion of erythropoiesis, thus causing anemia in the long term.

LXR activity has been previously shown to participate in apoptotic cell clearance[196], so it is conceivable to suspect that accumulation of excessive RBCs in the spleen of LXR-deficient mice might be due to defects in the clearance process. Although the expression of CD172α, the key receptor for CD47-altered senescent RBCs, presented similar levels in WT and LXR deficient mice, it is possible that the overall reduced RPM population may compromise senescent RBCs engulfment. In addition, given the many similarities between apoptosis and eryptosis[213], the possibility exists for LXRα to regulate a common mechanism for the two processes. RBCs engulfment, like apoptotic clearance, raises the lipid content inside the macrophage, thus enhancing the expression and activity of LXRs[195], so it seems logical that the absence of this transcription factor could affect erythrophagocytosis. The possible clearance failure in the spleen of LXR-deficient mice, and the transcriptional dysregulation in iron handling by their RPMs may affect Hb synthesis, thus hampering erythropoiesis. It would be interesting to study the implications of this impairment in the context of infectious diseases like malaria, where the stimulation of LXR activity could promote and accelerate the digestion of infected erythrocytes, or pathologies with defective erythropoiesis, like β-thalassemia, where defective erythrocytes accumulate in the circulation and organs[84].

Our RNA study (Fig. 18A) was obtained from purified bulk RPM samples. This initial approach assumed that all RPMs belonged to just one subset of similar cells with similar functions that reside in the red pulp of the spleen. The observed defects in iron metabolism in the spleen and bone marrow prompted us to look for genes whose transcription might be defective in our mouse mutants. In this regard, one of the top regulated genes whose RNA transcription was LXR-dependent was the hemoglobin scavenger receptor, CD163. Further flow cytometry analysis allowed us to discover the existence of two very well defined RPM populations in WT mice, differentially identified by the expression of CD163 receptor. As a member of the scavenger receptor cysteine-rich (SRCR) superfamily, CD163 was found to act as a high-

affinity hemoglobin receptor[93]. In humans, where it has been extensively studied, CD163 is expressed by almost all tissue resident macrophage populations, and their monocyte intermediates. The two main functions attributed to CD163 are the hemoglobin scavenging, and its activity as an adhesion molecule in erythroblastic islands[129]. CD163 expression has been described to significantly increase in human macrophages during the acute inflammatory phase, thus suggesting a role for this receptor in the modulation and resolution of inflammation in the tissues[214]. Additionally, a soluble form of CD163 has been also described in human patients[215], with important functions in inflammation resolution, atherosclerosis[216], and control of infectious diseases[217].

In mice however, the expression pattern of CD163 in the macrophage lineage has not been completely defined, although it is known that monocytes do not present the CD163 surface marker[218,219]. In another study, this receptor has been described to sequestrate Hb without the participation of Hp[219]. Our data shows that approximately 30% of the RPM population in mice is $CD163^+$, and that this proportion increases up to 50% in the bone marrow (Figs. 20 and 21) in WT mice, describing for the first time the expression pattern for this receptor in TRM in the spleen, and its dependency on LXRs transcriptional regulation.

7. LXRs control the generation of a specific subset of $CD163^+$ resident macrophages

Our data shows that LXR-deficient mice present an almost complete absence of CD163-expressing macrophages in the red pulp of the spleen, and the bone marrow (Figs 20 and 21). We confirmed, by cell number quantification, that the frequency of CD163-expressing macrophages in WT spleens and bone marrows correlated with the number of absent RPMs and BMMs in LXR-deficient mice (Figs. 20C, and 21B), therefore establishing that $CD11b^{lo}F4/80^{hi}CD163^+$ RPMs and BMMs constitute a different subpopulation, whose development and/or survival is under the control of LXRα regulation. Our GFP reporter mouse supported these results; both WT/WT and WT/GFP mice presented a $CD11b^{lo}GFP^{hi}CD163^+$ subpopulation within a complete RPM compartment, but this subset was absent in GFP/GFP (LXRα-null) mice (Figs. 22A, C, D and 23).

The question remained of whether LXRα additionally controlled the expression of CD163 receptor as a transcription factor. In all these mouse models, the expression of LXRα was constitutively impaired since the embryonic development, so we next analyzed the splenic RPM population in a CD64CRE;$LXR^{fl/fl}$ mouse model (Fig. 7E, Materials and methods), that only lost LXRα expression when CD64 expression was activated (this is, mostly in mature macrophages[198]). These mice completely lacked CD163 expression, however presenting a full RPM compartment, whose total cell numbers were equivalent to their controls ($LXR^{fl/fl}$) (Fig. 27A-E). This probed that, additionally to the correct development of the full RPM compartment, LXRα transcriptional activity also controlled the expression of CD163 receptor. Given the parallelism described between the red pulp and the bone marrow resident macrophage populations, it seems reasonable to speculate

that LXRα nuclear receptor could control both the cell development and the surface receptor expression in both macrophage subsets, but further analysis is necessary to establish this idea.

8. CD11b^{lo}F4/80^{hi}CD163^{+} red pulp macrophages constitute a subpopulation with iron-recycling functions

Proper iron absorption, processing and recycling are ensured by a complex and intricate mechanism, where different cells and proteins are implicated[77]. It is therefore conceivable that defects in transcriptional regulation in cells implicated in iron recycling would in fact affect iron metabolism at a wider level, and have pathological consequences[75,100]. Transcriptional analysis of sorted WT RPMs showed that many of these key genes involved in iron recycling are significantly up-regulated in CD163^{+} macrophages, compared to the CD163^{-} macrophage subset (Fig. 29A, B). Importantly, a great portion of the transcriptional regulation in CD163^{+} macrophages (~2,000 genes) is under the regulation of LXRα activity. These genes include the heme catabolic enzyme *Hmox1* (HO-1), iron cell exporter *Slc40a1* (FPN-1) and iron endosomic exporter *Slc11a1* (NRAMP-1) (Fig. 29B), three of the most important genes involved in iron metabolism (see Introduction, **1.4.2.**). Knockout mouse models for all these genes suffer from some level of anemia, among other symptoms, such as macrophage ferroptosis and tissue fibrosis[95,97,99], so their regulation becomes of great importance to maintain iron homeostasis.

HO-1 activity is essential for iron processing[77]. As was previously mentioned (see Introduction **1.4.2.**) HO-1-deficient mice suffer from severe anemia, as they are not able to catabolize heme into biliverdin, CO and Fe^{2+}. Excessive heme accumulation within macrophages causes ferroptosis in RPMs, KCs and BMMs, so excess of free iron needs to be cleared by kidney macrophages[97]. Surprisingly, *Hmox1*$^{-/-}$ mice have been described to present higher CD163 mRNA transcription levels in the kidneys than WT mice, presumably as an attempt to withdraw free Hb from the microenvironment[97]. Additionally, ferroportin deficiency in macrophages in *Fpn1*$^{LysM/LysM}$ mice affects different iron parameters, including diminished RBC counts, Hb concentration and Tf saturation, derived from their iron recycling impairment. Even though these mice presented only a mild form of anemia under homeostasis, stress conditions such as PHZ treatment, or iron-deficient diet aggravated their anemic phenotype and ultimately led to increased inflammatory responses[95]. NRAMP-1 (known as *Scl11a1*) expression in macrophages has been described to increase erythrophagocytosis efficiency *in vitro*. In fact, NRAMP1-expressing macrophages were found to phagocytose almost double RBCs than their *Nramp1-/-* counterparts[98,99]. Consequently, NRAMP-1 over-expression is linked to a great up-regulation of HO-1 (in order to process all the ingested heme) and FPN-1 (to allow its liberation from the cell)[98,99].

Importantly, the expression of these three genes has been described to be driven by the presence of heme in the cells by different studies[96,97,99]. Macrophages adjust to stress conditions in order to be able to withdraw the different free iron forms (Fe^{2+}, heme or Hb) from the environment, and they store it within their cytoplasm bounded to ferroproteins (like FTN) that protect cell integrity. Free iron is highly toxic for the tissues, due to its potent oxidative activity, which can affect different

substrates (like LDL molecules) and promote the generation of reactive oxygen species (ROS)[220]. In our LXR-deficient mice, despite the significant iron accumulation, the aforementioned genes, and many others, continue to be markedly down-regulated, meaning that LXR must play an important role in the regulation of iron metabolism.

In addition, the expression of several other heme metabolic enzymes is also highly modulated by the absence of LXRα, such as *Blvra*, which encodes the Biliverdin reductase A, in charge of the reduction of the biliverdin derived from heme degradation, into bilirrubin, in the cytosol[221,222]; *Alas1*, encoding 5'-Aminolevulinate Synthase 1, one of the key enzymes in the *de novo* synthesis of heme in the mitochondrion[221,222]; other solute carriers like *Slc48a1*, encoding the phagolysosome heme exporter HRG-1[89]; *Hebp1*, Heme binding protein 1, which can bind to free porphyrinogens or heme with high affinity in order to avoid their toxicity and ensure cell integrity[77]; the transferrin receptor gene, *Trf*[76]*;* the hereditary hemochromatosis protein (HFE)[75], a described regulator of hepcidin transcription (Fig. 29B). All these genes are significantly up-regulated in WT CD163-expressing RPMs, meaning that their expression is somehow stimulated by LXRα transcriptional activity. However, LXRα$^{-/-}$ CD163^{-} RPMs express these genes to the same extent as their WT counterparts (Fig. 29B). In fact, for some of them, their expression is potentiated in LXRα$^{-/-}$ CD163- RPMs, probably in an attempt to over-compensate for the lack of a CD163^{+} RPM subpopulation. This suggests that the down-regulation of this myriad of iron-related genes could be linked to the absence of the whole CD163-expressing macrophage subset, rather than be directly regulated by LXRα. In the search of new LXRα specific targets among all these iron-related genes, we were able to distinguish two, *Ncoa4* and *Aco1* (Aconitase-1, or IRP1), whose expression was also impaired in LXRα$^{-/-}$ CD163^{-} RPMs compared to their WT CD163^{-} RPM counterparts, suggesting that they might be under a more close LXRα regulation (Fig. 29B). Future studies employing LXR ChIP-seq (Chromatin Immunoprecipitation Sequencing) approaches would help us discern between direct or indirect regulated genes by LXR.

NCOA4 protein is a key regulator of iron metabolism, as it mediates the degradation of ferritin (ferritinophagy)[223,224]. In other words, NCOA4 promotes iron release upon demand for heme synthesis in the mitochondrion, thus having a key role in erythropoiesis[224]. *Ncoa4*$^{-/-}$ mice display iron accumulation in the spleen and the liver, increased serum ferritin levels and a mild microcytic hypochromic anemia, derived from inefficient erythropoiesis due to insufficient iron release[225]. The expression of *Ncoa4* gene in WT mice is significantly higher in CD163-expressing RPMs than in the CD163^{-} RPM subset, but, unlike the iron-related genes mentioned above, LXRα$^{-/-}$ CD163^{-} RPMs present a reduced expression compared to their WT counterparts (Fig. 29B).

In addition, as was previously described (see Introduction **1.4.2.**), the IRP/IRE mechanism modulates the transcription of many different iron-related genes, like TfR, FPN-1 or ALAS-1[103,226]. Thus, a transcriptional regulation of IRP1 expression mediated by LXRα could offer a plausible explanation to the general down-regulation of the transcription of the iron metabolic machinery.

9. Possible implications of LXRα deficiency in bone marrow erythropoiesis

On the other hand, it is reasonable to evaluate the possibility that the absence of LXRα could imply the reduction of the number of erythroblastic islands (EBIs) in the bone marrow and the spleen. EBIs in the red pulp of the spleen become of great importance during stress, or when erythropoiesis in the bone marrow is compromised[111]. In that scenario, extramedullary hematopoiesis (EMH) takes place[148]. At the steady state, adult splenic erythropoiesis in mice has a minimal contribution to the total RBC count, but under hypoxic conditions or anemia, the spleen undertakes the role of the main erythropoietic organ[111]. The presence of EBIs in the red pulp of the spleen has been confirmed in the past[227,228], but currently, the net proportion of resident macrophages that are part of this specialized structure, both in the murine spleen and bone marrow, remains to be revealed. CD163 has also been described as an adhesion molecule present in BM "nursing" macrophages[129], and our current data describes the existence of a CD163-expressing BMM subset that constitutes around the 50% of the total BMM population (Fig. 21A, B), but further analysis is required to acknowledge the proportion of those CD163^{+} macrophages that actually conform the EBIs in both the spleen and the bone marrow. We can state, however, that the absence of LXRα entails the depletion of the totality of CD163-expressing macrophages in the spleen (Fig. 20A-C), and the majority of them in the bone marrow (Fig. 21A, B), probably reducing the number of EBIs in these two locations, and thus handicapping erythropoiesis.

Additional evidence supports this hypothesis. The reported absence of CD169^{+} macrophages in the marginal zone of the spleen of LXRα$^{-/-}$ mice[63], and the parallelism between the splenic red pulp macrophage and the bone marrow macrophage populations established by Murphy and colleagues[101], strongly suggest that the CD169^{+} bone marrow macrophage population could also be impaired in LXRα-deficient mice (Fig. 21A, B), or possibly belong within the CD163^{+}-macrophage missing subset. The absence of these two receptors would directly affect the correct assembly of the EBI structure and the efficiency of the erythroblasts proliferation and maturation[129,131]. Further analysis is needed to determine the exact extent of the influence of LXRα absence in bone marrow erythropoiesis.

Concluding remarks

In conclusion, the present work reveals the existence of two previously unrecognized macrophage subsets within the RPM and BMM compartments (Figs 20A-C and 21A, B). The two RPM subsets residing in the spleen present particular genetic programs which probably determine their functions in homeostasis or stress conditions. One of these subsets is dependent on LXRα transcriptional regulation (CD163^{+}) and presumably exerts greater abilities for phagocytosis and iron-recycling. The second subset within the RPM compartment (CD163^{-}) still develops in the absence of LXRα (Fig. 29A, B), but both require the expression of SPI-C transcription factor for their differentiation *in vivo*[64].

Discussion

We designed a working model that could explain how these two RPM subsets participate in RPM biology in the spleen (Fig. 30A-C). RPMs first develop from embryonic progenitors during development[36]. When macrophage progenitors seed the spleen anlagen, they present high expression of SPI-C, LXRα, IRF8[66], among other transcription markers that are yet to be described. Once the spleen architecture is properly acquired, RPM might divide into two different subsets: one, $CD11b^{lo}F4/80^{hi}CD163^{+}TIM4^{+}$, which expresses high levels of LXRα and is mostly in charge of senescent RBC and Hb/heme phagocytosis, and thus iron recycling under homeostatic conditions; and another one, $CD11b^{lo}F4/80^{hi}CD163^{-}TIM4^{+}$, that also expresses LXRα but to a lesser extent, and carries out other functions, such as oxidative phosphorylation and ATP synthesis, and other immune related functions (according to our transcriptional analysis data) (Fig. 29A). Once in adulthood, the bone marrow is in charge of supplying the tissues with proper replacement for the macrophage compartment if needed, under any stress situation. When iron concentration increases in the tissues, this triggers *Spic* transcription program and circulating monocytes differentiate, through an intermediate pre-RPM state[101], into mature RPM. These mature RPMs might then subdivide into $CD163^{+}$ RPMs, with high expression of LXRα, and $CD163^{-}$ RPMs, which express LXRα to a lesser extent. Our $LXR\alpha^{-/-}$ mouse model presents a RPM population reduction (Fig. 11A-C) that creates a partial niche availability. We hypothesize that these mice accumulate bone marrow derive monocytes that try to fulfill that niche, but are not able to due to LXRα absence. It would be of great interest to test whether the SPI-C-expressing pre-RPMs previously described by Haldar *et al.* (2014) under heme accumulation[101], correlate with the expanded LXRα-expressing monocytes we observed after an hemolysis challenge (Fig. 22A, B), and whether or not these monocytes fully resemble an RPM phenotype, or rather just functionally adapt to the task until homeostatic conditions are restored, and then disappear[211].

Another possibility is that the well established macrophage plasticity[60] allows RPMs to interchange phenotypes within the red pulp compartment, and modify their CD163 expression upon need. This could be of great interest in the case of the BMM population, in the context of the EBI, and how it affects erythropoiesis. The accumulation of senescent RBCs in the red pulp of the spleen (Fig. 16A, B) in $LXR\alpha^{-/-}$ mice can be a consequence of the reduced RPM population, or could also be partly due to an erythrophagocytosis defect of the remaining RPMs. This accumulation culminates in an iron increased concentration, that disrupts the iron cycle and thus affects BM erythropoiesis. All these effects are not severe in young individuals, but become more evident as the mice age (Fig. 16A-D).

Understanding the dynamics of these two resident macrophage compartments would help enlighten the specifics of iron metabolism, and consequently throw some insight into processes like erythropoiesis and its related pathologies[84,229,230] or immune defence against infectious diseases[109]. Our results suggest a possible clinical application for LXRα regulation in the context of many iron-related conditions.

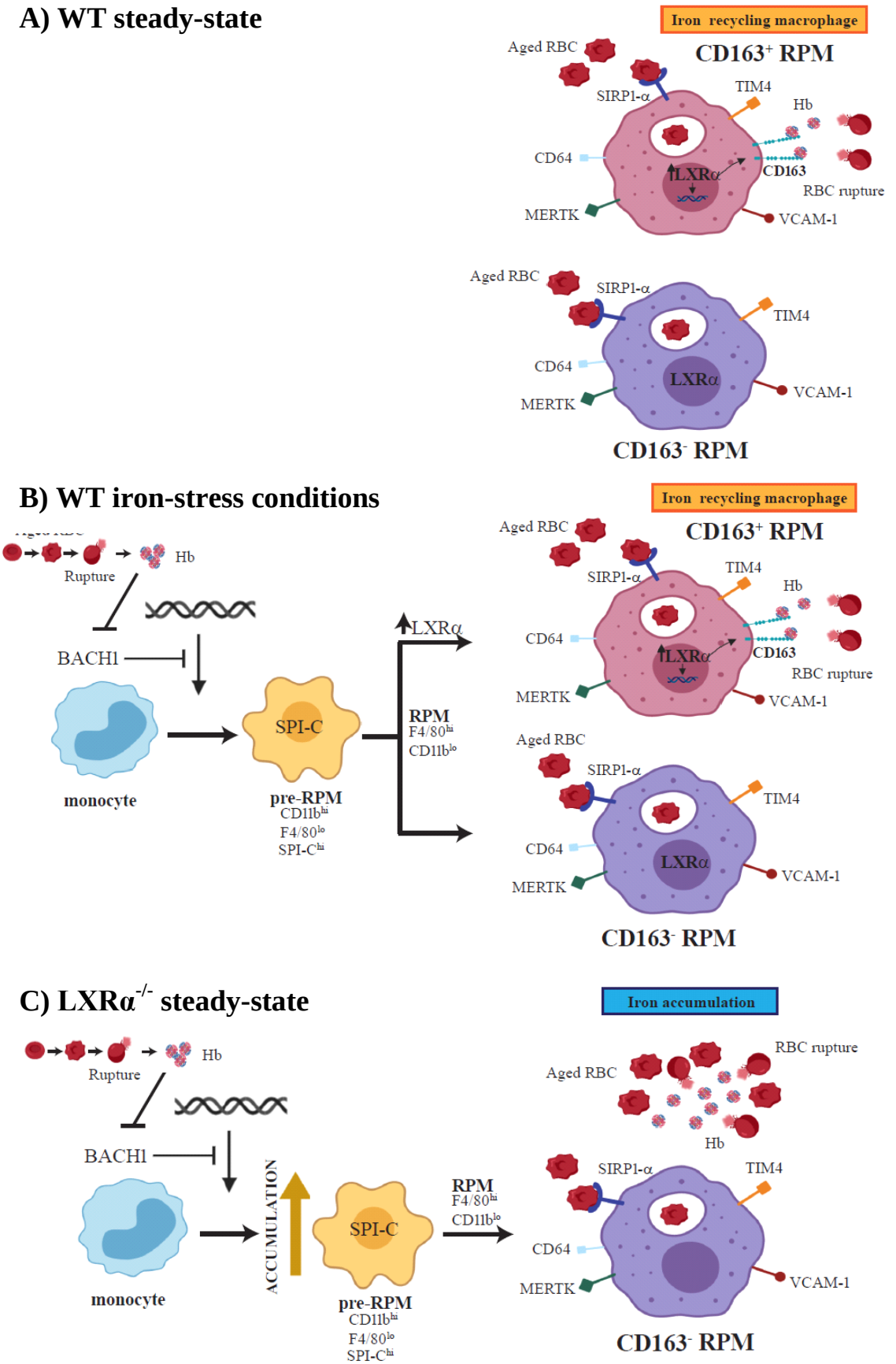

Figure 30. Working model of the possible role of LXRα in the generation of the RPM compartment in mouse spleen, and the regulation of RBC clearance and iron recycling. **A)** WT steady-state conditions. **B)** WT mouse spleen during an iron-stress situation. **C)** LXRα$^{-/-}$ mouse spleen at steady-state situation, where the CD163-expressin subset of the RPM compartment is absent.

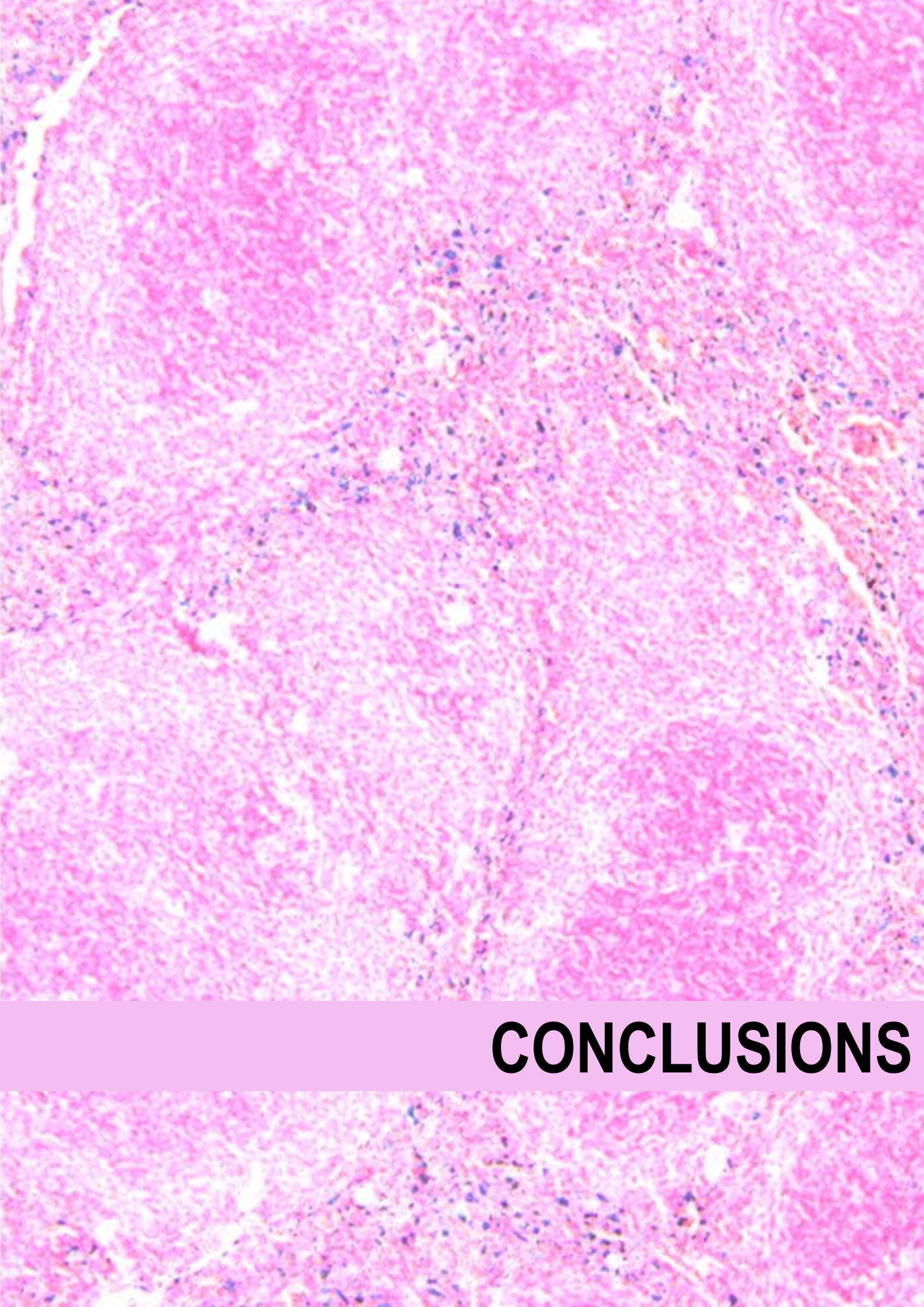

CONCLUSIONS

Conclusions/Conclusiones

1. **LXRα plays an important role in the correct development of the red pulp and bone marrow macrophage compartments. LXR-deficient mice present reduced CD11b^{lo}F4/80^{hi} Red Pulp and Bone Marrow Macrophage populations, and increased CD11b^{hi}F4/8^{lo}SSC^{lo} splenic and bone marrow monocyte numbers.**

2. **LXR-deficient hematopoietic cells present defective CD11b^{lo}F4/80^{hi} Red Pulp and Bone Marrow Macrophage repopulation potential after bone marrow transplant, while showing a tendency to differentiate into CD11b^{hi}F4/8^{lo}SSC^{lo} bone marrow-derived monocytes. These monocytes accumulate in the spleen and bone marrow of transplanted mice in the same way as in LXR-deficient mice.**

3. **The deficiency of LXRα, affects the expression of several iron recycling-related genes, and results in impaired iron metabolism. LXR-deficient mice present marked iron depositions and accumulate unengulfed erythrocytes in the red pulp of the spleen. Conversely, these mice show lower iron levels and total Red Blood Cells frequencies in the bone marrow than Wild Type mice.**

4. **Our results suggest that, as a consequence of defective iron recycling, the process of generating new erythrocytes is compromised in LXR-deficient mice, which present erythroblasts accumulating in the earlier stages of maturation in the bone marrow.**

5. **LXRα controls the development of a subpopulation of resident Red Pulp Macrophages, characterized by the expression of CD163 and TIM4, that has a very specific transcriptional profile, with very well defined associated biological functions, that include iron recycling and immune system activation.**

6. **Our work also highlights the generation of two new mouse models for the analysis of LXRα signaling; one LXRα-DTR model to deplete LXRα^{+} cells, and a second LXRα-GFP model, that allows the visualization of LXRα^{+} cells through GFP expression *in vivo* or *in vitro.***

Conclusions/Conclusiones

1. **LXRα juega un papel importante en el correcto desarrollo de las poblaciones de macrófagos residentes de la pulpa roja del bazo y la médula ósea. Los ratones deficientes en LXR presentan una reducción en estas poblaciones de macrófagos (CD11b^{lo}F4/80^{hi}), y un elevado número de monocitos (CD11b^{hi}F4/8^{lo}SSC^{lo}) en estos tejidos.**

2. **Las células hematopoyéticas deficientes en LXR no son capaces de reconstituir las poblaciones de macrófagos residentes de la pulpa roja del bazo y la médula ósea (CD11b^{lo}F4/80^{hi}) tras un trasplante de médula, mientras que son propensas genéticamente a diferenciarse a monocitos (CD11b^{hi}F4/8^{lo}SSC^{lo}), que se acumulan en los bazos y las médulas de los ratones trasplantados de la misma forma que lo hacen en los ratones deficientes en LXR.**

3. **La deficiencia de LXRα, afecta a la expresión de varios genes relacionados con el reciclaje del hierro, y tiene como resultado un fallo en el metabolismo del hierro. Los ratones deficientes en LXR presentan grandes depósitos de hierro y acumulan eritrocitos en la pulpa roja del bazo. Por el contrario, estos ratones muestran niveles más bajos de hierro en la médula ósea y un porcentaje menor de eritrocitos totales comparado con los niveles de los ratones control.**

4. **Nuestros resultados sugieren que, como consecuencia de un reciclaje de hierro defectuoso, la generación de nuevos eritrocitos está comprometida en los ratones deficientes en LXR, los cuales presentan acumulación de eritroblastos en las primeras etapas de maduración en la médula ósea.**

5. **LXRα controla el desarrollo de una subpoblación de macrófagos de la pulpa roja del bazo caracterizada por la expresión de los receptores CD163 y TIM4, los cuales tienen un perfil transcripcional muy específico, al que se le asocian funciones biológicas muy bien definidas como el procesamiento y reciclaje del hierro y el procesamiento de las respuestas inmunes.**

6. **Nuestro trabajo ha permitido la generación de dos nuevos modelos de ratón para el análisis de la señalización de LXRα; el primero, LXRα-DTR, elimina las células que expresan LXRα de forma selectiva, y el segundo, LXRα-GFP, permite la visualización de las células LXRα^{+} mediante la expresión de la proteína verde fluorescente (GFP), tanto *in vivo* como *in vitro*.**

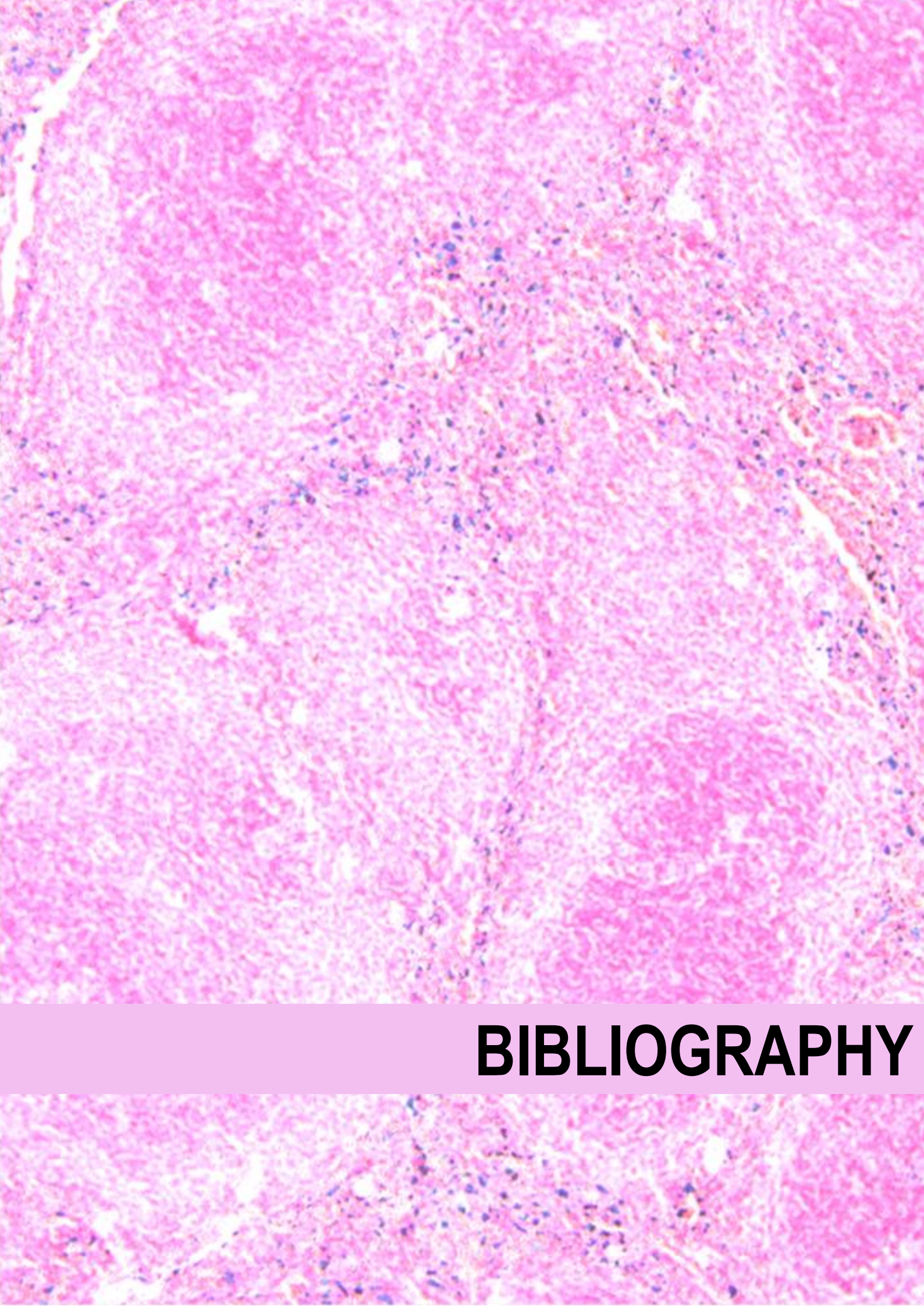

BIBLIOGRAPHY

Bibliography

1. Kennedy MA. A Brief Review of the Basics of Immunology: The Innate and Adaptive Response. *Vet Clin North Am Small Anim Pract*. 2010;40(3):369-379. doi:10.1016/j.cvsm.2010.01.003

2. Kaczmarek A, Vandenabeele P, Krysko D V. Necroptosis: The Release of Damage-Associated Molecular Patterns and Its Physiological Relevance. *Immunity*. 2013;38(2):209-223. doi:10.1016/j.immuni.2013.02.003

3. Ma J, Chen T, Mandelin J, et al. Regulation of macrophage activation. *Cell Mol Life Sci*. 2003;60(11):2334-2346. doi:10.1007/s00018-003-3020-0

4. Martinez FO, Gordon S. The M1 and M2 paradigm of macrophage activation: time for reassessment. *F1000Prime Rep*. 2014;6(March):1-13. doi:10.12703/P6-13

5. Orecchioni M, Ghosheh Y, Pramod AB, Ley K. Macrophage Polarization: Different Gene Signatures in M1(LPS+) vs. Classically and M2(LPS–) vs. Alternatively Activated Macrophages. *Front Immunol*. 2019;10(MAY):1-14. doi:10.3389/fimmu.2019.01084

6. Ravichandran KS, Lorenz U. Engulfment of apoptotic cells: signals for a good meal. *Nat Rev Immunol*. 2007;7(12):964-974. doi:10.1038/nri2214

7. Miyanishi M, Tada K, Koike M, Uchiyama Y, Kitamura T, Nagata S. Identification of Tim4 as a phosphatidylserine receptor. *Nature*. 2007;450(7168):435-439. doi:10.1038/nature06307

8. Lemke G, Rothlin C V. Immunobiology of the TAM receptors. *Nat Rev Immunol*. 2008;8(5):327-336. doi:10.1038/nri2303

9. Botto M, Dell' Agnola C, Bygrave AE, et al. Homozygous C1q deficiency causes glomerulonephritis associated with multiple apoptotic bodies. *Nat Genet*. 1998;19(1):56-59. doi:10.1038/ng0598-56

10. Ishimoto Y, Ohashi K, Mizuno K, Nakano T. Promotion of the Uptake of PS Liposomes and Apoptotic Cells by a Product of Growth Arrest-Specific Gene, gas6. *J Biochem*. 2000;127(3):411-417. doi:10.1093/oxfordjournals.jbchem.a022622

11. Hanayama R, Tanaka M, Miwa K, Shinohara A, Iwamatsu A, Nagata S. Identification of a factor that links apoptotic cells to phagocytes. *Nature*. 2002;417(6885):182-187. doi:10.1038/417182a

12. Fadok VA, Bratton DL, Konowal A, Freed PW, Westcott JY, Henson PM. Macrophages that have ingested apoptotic cells in vitro inhibit proinflammatory cytokine production through autocrine/paracrine mechanisms involving TGF-beta, PGE2, and PAF. *J Clin Invest*. 1998;101(4):890-898. doi:10.1172/JCI1112

13. Li MO, Flavell RA. TGF-β: A Master of All T Cell Trades. *Cell*. 2008;134(3):392-404. doi:10.1016/j.cell.2008.07.025

14. Savill J, Dransfield I, Gregory C, Haslett C. A blast from the past: clearance of apoptotic cells regulates immune responses. *Nat Rev Immunol*. 2002;2(12):965-975. doi:10.1038/nri957

15. Wermeling F, Karlsson MCI, McGaha TL. An anatomical view on macrophages in tolerance. *Autoimmun Rev*. 2009;9(1):49-52. doi:10.1016/j.autrev.2009.03.004

16. Lavin Y, Winter D, Blecher-Gonen R, et al. Tissue-Resident Macrophage Enhancer Landscapes Are Shaped by the Local Microenvironment. *Cell*. 2014;159(6):1312-1326. doi:10.1016/j.cell.2014.11.018

17. Koh TJ, DiPietro LA. Inflammation and wound healing: the role of the macrophage. *Expert Rev Mol Med*. 2011;13(1):e23. doi:10.1017/S1462399411001943

18. Krzyszczyk P, Schloss R, Palmer A, Berthiaume F. The Role of Macrophages in Acute and Chronic Wound Healing and Interventions to Promote Pro-wound Healing Phenotypes. *Front Physiol*.

2018;9(MAY):1-22. doi:10.3389/fphys.2018.00419

19. Paolicelli RC, Bolasco G, Pagani F, et al. Synaptic Pruning by Microglia Is Necessary for Normal Brain Development. *Science (80-)*. 2011;333(6048):1456-1458. doi:10.1126/science.1202529

20. Virolainen M. Hematopoietic origin of macrophages as studied by chromosome markers in mice. 1968:943-952.

21. van Furth, Ralph; Diesselhoff-den Dulk MMC. The kinetics of promonocytes and monocytes in the bone marrow. 1970:813-828.

22. Auffray C, Sieweke MH, Geissmann F. Blood Monocytes: Development, Heterogeneity, and Relationship with Dendritic Cells. *Annu Rev Immunol*. 2009;27(1):669-692. doi:10.1146/annurev.immunol.021908.132557

23. Merad M, Manz MG, Karsunky H, et al. Langerhans cells renew in the skin throughout life under steady-state conditions. *Nat Immunol*. 2002;3(12):1135-1141. doi:10.1038/ni852

24. Ajami B, Bennett JL, Krieger C, Tetzlaff W, Rossi FM V. Local self-renewal can sustain CNS microglia maintenance and function throughout adult life. *Nat Neurosci*. 2007;10(12):1538-1543. doi:10.1038/nn2014

25. Ginhoux F, Greter M, Leboeuf M, et al. Fate Mapping Analysis Reveals That Adult Microglia Derive from Primitive Macrophages. *Science (80-)*. 2010;330(6005):841-845. doi:10.1126/science.1194637

26. Guilliams M, De Kleer I, Henri S, et al. Alveolar macrophages develop from fetal monocytes that differentiate into long-lived cells in the first week of life via GM-CSF. *J Exp Med*. 2013;210(10):1977-1992. doi:10.1084/jem.20131199

27. Hashimoto D, Chow A, Noizat C, et al. Tissue-Resident Macrophages Self-Maintain Locally throughout Adult Life with Minimal Contribution from Circulating Monocytes. *Immunity*. 2013;38(4):792-804. doi:10.1016/j.immuni.2013.04.004

28. Davies LC, Rosas M, Smith PJ, Fraser DJ, Jones SA, Taylor PR. A quantifiable proliferative burst of tissue macrophages restores homeostatic macrophage populations after acute inflammation. *Eur J Immunol*. 2011;41(8):2155-2164. doi:10.1002/eji.201141817

29. Jenkins SJ, Ruckerl D, Cook PC, et al. Local Macrophage Proliferation, Rather than Recruitment from the Blood, Is a Signature of TH2 Inflammation. *Science (80-)*. 2011;332(6035):1284-1288. doi:10.1126/science.1204351

30. Yona S, Kim K-W, Wolf Y, et al. Fate Mapping Reveals Origins and Dynamics of Monocytes and Tissue Macrophages under Homeostasis. *Immunity*. 2013;38(1):79-91. doi:10.1016/j.immuni.2012.12.001

31. Romani N, Schuler G, Fritsch P. Ontogeny of Ia-Positive and Thy-1-Positive Leukocytes of Murine Epidermis. *J Invest Dermatol*. 1986;86(2):129-133. doi:10.1111/1523-1747.ep12284135

32. Takahashi K, Naito M. Development, differentiation, and proliferation of macrophages in the rat yolk sac. *Tissue Cell*. 1993;25(3):351-362. doi:10.1016/0040-8166(93)90077-X

33. Mizoguchi S, Takahashi K, Takeya M, Naito M, Morioka T. Development, differentiation, and proliferation of epidermal Langerhans cells in rat ontogeny studied by a novel monoclonal antibody against epidermal Langerhans cells, RED-1. *J Leukoc Biol*. 1992;52(1):52-61. doi:10.1002/jlb.52.1.52

34. Orkin SH, Zon LI. Hematopoiesis: An Evolving Paradigm for Stem Cell Biology. *Cell*. 2008;132(4):631-644. doi:10.1016/j.cell.2008.01.025

35. Hoeffel G, Ginhoux F. Ontogeny of Tissue-Resident Macrophages. *Front Immunol*. 2015;6(SEP).

doi:10.3389/fimmu.2015.00486

36. Ginhoux F, Guilliams M. Tissue-Resident Macrophage Ontogeny and Homeostasis. *Immunity*. 2016;44(3):439-449. doi:10.1016/j.immuni.2016.02.024

37. Tober J, Koniski A, McGrath KE, et al. The megakaryocyte lineage originates from hemangioblast precursors and is an integral component both of primitive and of definitive hematopoiesis. *Blood*. 2007;109(4):1433-1441. doi:10.1182/blood-2006-06-031898

38. Palis J, Robertson S, Kennedy M, Wall C, Keller G. Development of erythroid and myeloid progenitors in the yolk sac and embryo proper of the mouse. *Development*. 1999;126(22):5073-5084.

39. Naito M, Yamamura F, Nishikawa S, Takahashi K. Development, Differentiation, and Maturation of Fetal Mouse Yolk Sac Macrophages in Cultures. *J Leukoc Biol*. 1989;46(1):1-10. doi:10.1002/jlb.46.1.1

40. Takahashi K, Yamamura F, Naito M. Differentiation, Maturation, and Proliferation of Macrophages in the Mouse Yolk Sac: A Light-Microscopic, Enzyme-Cytochemical, Immunohistochemical, and Ultrastructural Study. *J Leukoc Biol*. 1989;45(2):87-96. doi:10.1002/jlb.45.2.87

41. Morioka Y, Naito M, Sato T, Takahashi K. Immunophenotypic and ultrastructural heterogeneity of macrophage differentiation in bone marrow and fetal hematopoiesis of mouse in vitro and in vivo. *J Leukoc Biol*. 1994;55(5):642-651. doi:10.1002/jlb.55.5.642

42. Frame JM, McGrath KE, Palis J. Erythro-myeloid progenitors: "Definitive" hematopoiesis in the conceptus prior to the emergence of hematopoietic stem cells. *Blood Cells, Mol Dis*. 2013;51(4):220-225. doi:10.1016/j.bcmd.2013.09.006

43. Bertrand JY, Kim AD, Violette EP, Stachura DL, Cisson JL, Traver D. Definitive hematopoiesis initiates through a committed erythromyeloid progenitor in the zebrafish embryo. *Development*. 2007;134(23):4147-4156. doi:10.1242/dev.012385

44. Hoeffel G, Chen J, Lavin Y, et al. C-Myb+ Erythro-Myeloid Progenitor-Derived Fetal Monocytes Give Rise to Adult Tissue-Resident Macrophages. *Immunity*. 2015;42(4):665-678. doi:10.1016/j.immuni.2015.03.011

45. Sumner R, Crawford A, Mucenski M, Frampton J. Initiation of adult myelopoiesis can occur in the absence of c-Myb whereas subsequent development is strictly dependent on the transcription factor. *Oncogene*. 2000;19(30):3335-3342. doi:10.1038/sj.onc.1203660

46. Palis J, Yoder MC. Yolk-sac hematopoiesis: the first blood cells of mouse and man. *Exp Hematol*. 2001;29(8):927-936. doi:0301-472X(01)00669-5

47. Godin I, Cumano A. The hare and the tortoise: an embryonic haematopoietic race. *Nat Rev Immunol*. 2002;2(8):593-604. doi:10.1038/nri857

48. Kieusseian A, de la Grange PB, Burlen-Defranoux O, Godin I, Cumano A. Immature hematopoietic stem cells undergo maturation in the fetal liver. *Development*. 2012;139(19):3521-3530. doi:10.1242/dev.079210

49. Samokhvalov IM, Samokhvalova NI, Nishikawa S. Cell tracing shows the contribution of the yolk sac to adult haematopoiesis. *Nature*. 2007;446(7139):1056-1061. doi:10.1038/nature05725

50. Tober J, Yzaguirre AD, Piwarzyk E, Speck NA. Distinct temporal requirements for Runx1 in hematopoietic progenitors and stem cells. *Development*. 2013;140(18):3765-3776. doi:10.1242/dev.094961

51. Gomez Perdiguero E, Klapproth K, Schulz C, et al. Tissue-resident macrophages originate from yolk-sac-derived erythro-myeloid progenitors. *Nature*. 2015;518(7540):547-551. doi:10.1038/nature13989

Bibliography

52. Schulz C, Perdiguero EG, Chorro L, et al. A Lineage of Myeloid Cells Independent of Myb and Hematopoietic Stem Cells. *Science (80-)*. 2012;336(6077):86-90. doi:10.1126/science.1219179

53. McKercher SR, Torbett BE, Anderson KL, et al. Targeted disruption of the PU.1 gene results in multiple hematopoietic abnormalities. *EMBO J*. 1996;15(20):5647-5658. doi:10.1002/j.1460-2075.1996.tb00949.x

54. Kierdorf K, Erny D, Goldmann T, et al. Microglia emerge from erythromyeloid precursors via Pu.1- and Irf8-dependent pathways. *Nat Neurosci*. 2013;16(3):273-280. doi:10.1038/nn.3318

55. van de Laar L, Saelens W, De Prijck S, et al. Yolk Sac Macrophages, Fetal Liver, and Adult Monocytes Can Colonize an Empty Niche and Develop into Functional Tissue-Resident Macrophages. *Immunity*. 2016;44(4):755-768. doi:10.1016/j.immuni.2016.02.017

56. Zigmond E, Varol C, Farache J, et al. Ly6Chi Monocytes in the Inflamed Colon Give Rise to Proinflammatory Effector Cells and Migratory Antigen-Presenting Cells. *Immunity*. 2012;37(6):1076-1090. doi:10.1016/j.immuni.2012.08.026

57. Tamoutounour S, Guilliams M, Montanana Sanchis F, et al. Origins and Functional Specialization of Macrophages and of Conventional and Monocyte-Derived Dendritic Cells in Mouse Skin. *Immunity*. 2013;39(5):925-938. doi:10.1016/j.immuni.2013.10.004

58. Epelman S, Lavine KJ, Beaudin AE, et al. Embryonic and Adult-Derived Resident Cardiac Macrophages Are Maintained through Distinct Mechanisms at Steady State and during Inflammation. *Immunity*. 2014;40(1):91-104. doi:10.1016/j.immuni.2013.11.019

59. Molawi K, Wolf Y, Kandalla PK, et al. Progressive replacement of embryo-derived cardiac macrophages with age. *J Exp Med*. 2014;211(11):2151-2158. doi:10.1084/jem.20140639

60. Bonnardel J, Guilliams M. Developmental control of macrophage function. *Curr Opin Immunol*. 2018;50:64-74. doi:10.1016/j.coi.2017.12.001

61. Price JG, Idoyaga J, Salmon H, et al. CDKN1A regulates Langerhans cell survival and promotes Treg cell generation upon exposure to ionizing irradiation. *Nat Immunol*. 2015;16(10):1060-1068. doi:10.1038/ni.3270

62. Mass E, Ballesteros I, Farlik M, et al. Specification of tissue-resident macrophages during organogenesis. *Science (80-)*. 2016;353(6304):aaf4238-aaf4238. doi:10.1126/science.aaf4238

63. A-Gonzalez N, Guillen JA, Gallardo G, et al. The nuclear receptor LXRα controls the functional specialization of splenic macrophages. *Nat Immunol*. 2013;14(8):831-839. doi:10.1038/ni.2622

64. Kohyama M, Ise W, Edelson BT, et al. Role for Spi-C in the development of red pulp macrophages and splenic iron homeostasis. *Nature*. 2009;457(7227):318-321. doi:10.1038/nature07472

65. Gautier EL, Shay T, Miller J, et al. Gene-expression profiles and transcriptional regulatory pathways that underlie the identity and diversity of mouse tissue macrophages. *Nat Immunol*. 2012;13(11):1118-1128. doi:10.1038/ni.2419

66. A-Gonzalez N, Castrillo A. Origin and specialization of splenic macrophages. *Cell Immunol*. 2018;330(October 2017):151-158. doi:10.1016/j.cellimm.2018.05.005

67. Mebius RE, Kraal G. Structure and function of the spleen. *Nat Rev Immunol*. 2005;5(8):606-616. doi:10.1038/nri1669

68. Vondenhoff MFR, Desanti GE, Cupedo T, et al. Separation of splenic red and white pulp occurs before birth in a LTαβ-independent manner. *J Leukoc Biol*. 2008;84(1):152-161. doi:10.1189/jlb.0907659

69. Kurotaki D, Uede T, Tamura T. Functions and development of red pulp macrophages. *Microbiol Immunol*.

2015;59(2):55-62. doi:10.1111/1348-0421.12228

70. Kurotaki D, Kon S, Bae K, et al. CSF-1–Dependent Red Pulp Macrophages Regulate CD4 T Cell Responses. *J Immunol*. 2011;186(4):2229-2237. doi:10.4049/jimmunol.1001345

71. den Haan JMM, Kraal G. Innate Immune Functions of Macrophage Subpopulations in the Spleen. *J Innate Immun*. 2012;4(5-6):437-445. doi:10.1159/000335216

72. Backer R, Schwandt T, Greuter M, et al. Effective collaboration between marginal metallophilic macrophages and CD8+ dendritic cells in the generation of cytotoxic T cells. *Proc Natl Acad Sci*. 2010;107(1):216-221. doi:10.1073/pnas.0909541107

73. Karlsson MCI, Guinamard R, Bolland S, Sankala M, Steinman RM, Ravetch J V. Macrophages Control the Retention and Trafficking of B Lymphocytes in the Splenic Marginal Zone. *J Exp Med*. 2003;198(2):333-340. doi:10.1084/jem.20030684

74. McGaha TL, Chen Y, Ravishankar B, van Rooijen N, Karlsson MCI. Marginal zone macrophages suppress innate and adaptive immunity to apoptotic cells in the spleen. *Blood*. 2011;117(20):5403-5412. doi:10.1182/blood-2010-11-320028

75. Ganz T, Nemeth E. Hepcidin and iron homeostasis. *Biochim Biophys Acta - Mol Cell Res*. 2012;1823(9):1434-1443. doi:10.1016/j.bbamcr.2012.01.014

76. de Back DZ, Kostova EB, van Kraaij M, van den Berg TK, van Bruggen R. Of macrophages and red blood cells; a complex love story. *Front Physiol*. 2014;5(January). doi:10.3389/fphys.2014.00009

77. Muckenthaler MU, Rivella S, Hentze MW, Galy B. A Red Carpet for Iron Metabolism. *Cell*. 2017;168(3):344-361. doi:10.1016/j.cell.2016.12.034

78. Lutz HU. Innate immune and non-immune mediators of erythrocyte clearance. *Cell Mol Biol (Noisy-le-grand)*. 2004;50(2):107-116.

79. Arese P, Turrini F, Schwarzer E. Band 3/Complement-mediated Recognition and Removal of Normally Senescent and Pathological Human Erythrocytes. *Cell Physiol Biochem*. 2005;16(4-6):133-146. doi:10.1159/000089839

80. Park S-Y, Jung M-Y, Kim H-J, et al. Rapid cell corpse clearance by stabilin-2, a membrane phosphatidylserine receptor. *Cell Death Differ*. 2008;15(1):192-201. doi:10.1038/sj.cdd.4402242

81. Park S-Y, Kim S-Y, Jung M-Y, Bae D-J, Kim I-S. Epidermal Growth Factor-Like Domain Repeat of Stabilin-2 Recognizes Phosphatidylserine during Cell Corpse Clearance. *Mol Cell Biol*. 2008;28(17):5288-5298. doi:10.1128/MCB.01993-07

82. Raymond A, Ensslin MA, Shur BD. SED1/MFG-E8: A Bi-Motif protein that orchestrates diverse cellular interactions. *J Cell Biochem*. 2009;106(6):957-966. doi:10.1002/jcb.22076

83. Lang E, Lang F. Mechanisms and pathophysiological significance of eryptosis, the suicidal erythrocyte death. *Semin Cell Dev Biol*. 2015;39:35-42. doi:10.1016/j.semcdb.2015.01.009

84. Cao A, Galanello R. Beta-thalassemia. *Genet Med*. 2010;12(2):61-76. doi:10.1097/GIM.0b013e3181cd68ed

85. Oldenborg P-A. Role of CD47 as a Marker of Self on Red Blood Cells. *Science (80-)*. 2000;288(5473):2051-2054. doi:10.1126/science.288.5473.2051

86. Fossati-Jimack L, Azeredo da Silveira S, Moll T, et al. Selective Increase of Autoimmune Epitope Expression on Aged Erythrocytes in Mice: Implications in Anti-erythrocyte Autoimmune Responses. *J Autoimmun*. 2002;18(1):17-25. doi:10.1006/jaut.2001.0563

Bibliography

87. Burger P, Hilarius-Stokman P, de Korte D, van den Berg TK, van Bruggen R. CD47 functions as a molecular switch for erythrocyte phagocytosis. *Blood*. 2012;119(23):5512-5521. doi:10.1182/blood-2011-10-386805

88. Korolnek T, Hamza I. Macrophages and iron trafficking at the birth and death of red cells. *Blood*. 2015;125(19):2893-2897. doi:10.1182/blood-2014-12-567776

89. White C, Yuan X, Schmidt PJ, et al. HRG1 Is Essential for Heme Transport from the Phagolysosome of Macrophages during Erythrophagocytosis. *Cell Metab*. 2013;17(2):261-270. doi:10.1016/j.cmet.2013.01.005

90. Quigley JG, Yang Z, Worthington MT, et al. Identification of a Human Heme Exporter that Is Essential for Erythropoiesis. *Cell*. 2004;118(6):757-766. doi:10.1016/j.cell.2004.08.014

91. Keel SB, Doty RT, Yang Z, et al. A Heme Export Protein Is Required for Red Blood Cell Differentiation and Iron Homeostasis. *Science (80-)*. 2008;319(5864):825-828. doi:10.1126/science.1151133

92. Thomsen JH, Etzerodt A, Svendsen P, Moestrup SK. The Haptoglobin-CD163-Heme Oxygenase-1 Pathway for Hemoglobin Scavenging. *Oxid Med Cell Longev*. 2013;2013:1-11. doi:10.1155/2013/523652

93. Kristiansen M, Graversen JH, Jacobsen C, et al. Identification of the haemoglobin scavenger receptor. *Nature*. 2001;409(6817):198-201. doi:10.1038/35051594

94. Delanghe JR, Langlois MR. Hemopexin: a review of biological aspects and the role in laboratory medicine. *Clin Chim Acta*. 2001;312(1-2):13-23. doi:10.1016/S0009-8981(01)00586-1

95. Zhang Z, Zhang F, An P, et al. Ferroportin1 deficiency in mouse macrophages impairs iron homeostasis and inflammatory responses. *Blood*. 2011;118(7):1912-1922. doi:10.1182/blood-2011-01-330324

96. ZHAO G-Y, DI D-H, WANG B, ZHANG P, XU Y-J. Iron regulates the expression of ferroportin 1 in the cultured hFOB 1.19 osteoblast cell line. *Exp Ther Med*. 2014;8(3):826-830. doi:10.3892/etm.2014.1823

97. Kovtunovych G, Eckhaus MA, Ghosh MC, Ollivierre-Wilson H, Rouault TA. Dysfunction of the heme recycling system in heme oxygenase 1-deficient mice: effects on macrophage viability and tissue iron distribution. *Blood*. 2010;116(26):6054-6062. doi:10.1182/blood-2010-03-272138

98. Soe-Lin S, Sheftel AD, Wasyluk B, Ponka P. Nramp1 equips macrophages for efficient iron recycling. *Exp Hematol*. 2008;36(8):929-937. doi:10.1016/j.exphem.2008.02.013

99. Soe-Lin S, Apte SS, Andriopoulos B, et al. Nramp1 promotes efficient macrophage recycling of iron following erythrophagocytosis in vivo. *Proc Natl Acad Sci*. 2009;106(14):5960-5965. doi:10.1073/pnas.0900808106

100. Hentze MW, Muckenthaler MU, Galy B, Camaschella C. Two to Tango: Regulation of Mammalian Iron Metabolism. *Cell*. 2010;142(1):24-38. doi:10.1016/j.cell.2010.06.028

101. Haldar M, Kohyama M, So AY-L, et al. Heme-Mediated SPI-C Induction Promotes Monocyte Differentiation into Iron-Recycling Macrophages. *Cell*. 2014;156(6):1223-1234. doi:10.1016/j.cell.2014.01.069

102. Lunova M, Goehring C, Kuscuoglu D, et al. Hepcidin knockout mice fed with iron-rich diet develop chronic liver injury and liver fibrosis due to lysosomal iron overload. *J Hepatol*. 2014;61(3):633-641. doi:10.1016/j.jhep.2014.04.034

103. Wilkinson N, Pantopoulos K. The IRP/IRE system in vivo: insights from mouse models. *Front Pharmacol*. 2014;5(July):1-15. doi:10.3389/fphar.2014.00176

104. Casarrubea D, Viatte L, Hallas T, et al. Abnormal body iron distribution and erythropoiesis in a novel

mouse model with inducible gain of iron regulatory protein (IRP)-1 function. *J Mol Med*. 2013;91(7):871-881. doi:10.1007/s00109-013-1008-2

105. Soares MP, Weiss G. The Iron age of host–microbe interactions. *EMBO Rep*. 2015;16(11):1482-1500. doi:10.15252/embr.201540558

106. Kraml P. The role of iron in the pathogenesis of atherosclerosis. *Physiol Res*. 2017;66:S55-S67.

107. Wallace DF, Subramaniam VN. Co-factors in liver disease: The role of HFE-related hereditary hemochromatosis and iron. *Biochim Biophys Acta - Gen Subj*. 2009;1790(7):663-670. doi:10.1016/j.bbagen.2008.09.002

108. Friedman A, Galazka-Friedman J, Bauminger ER. Iron as a trigger of neurodegeneration in Parkinson's disease. In: *Handbook of Clinical Neurology*. Vol 83. ; 2007:493-505. doi:10.1016/S0072-9752(07)83023-5

109. Wessling-Resnick M. Iron Homeostasis and the Inflammatory Response. *Annu Rev Nutr*. 2010;30(1):105-122. doi:10.1146/annurev.nutr.012809.104804

110. Arezes J, Jung G, Gabayan V, et al. Hepcidin-Induced Hypoferremia Is a Critical Host Defense Mechanism against the Siderophilic Bacterium Vibrio vulnificus. *Cell Host Microbe*. 2015;17(1):47-57. doi:10.1016/j.chom.2014.12.001

111. Hom J, Dulmovits BM, Mohandas N, Blanc L. The erythroblastic island as an emerging paradigm in the anemia of inflammation. *Immunol Res*. 2015;63(1-3):75-89. doi:10.1007/s12026-015-8697-2

112. Palis J. Primitive and definitive erythropoiesis in mammals. *Front Physiol*. 2014;5(January):1-9. doi:10.3389/fphys.2014.00003

113. Manwani D, Bieker JJ. Chapter 2 The Erythroblastic Island. In: *Maclean's*. Vol 119. ; 2008:23-53. doi:10.1016/S0070-2153(07)00002-6

114. Kingsley PD. Yolk sac-derived primitive erythroblasts enucleate during mammalian embryogenesis. *Blood*. 2004;104(1):19-25. doi:10.1182/blood-2003-12-4162

115. McGrath KE, Kingsley PD, Koniski AD, Porter RL, Bushnell TP, Palis J. Enucleation of primitive erythroid cells generates a transient population of "pyrenocytes" in the mammalian fetus. *Blood*. 2008;111(4):2409-2417. doi:10.1182/blood-2007-08-107581

116. YOKOYAMA T, ETOH T, KITAGAWA H, TSUKAHARA S, KANNAN Y. Migration of Erythroblastic Islands toward the Sinusoid as Erythroid Maturation Proceeds in Rat Bone Marrow. *J Vet Med Sci*. 2003;65(4):449-452. doi:10.1292/jvms.65.449

117. Hanspal M, Smockova Y, Uong Q. Molecular identification and functional characterization of a novel protein that mediates the attachment of erythroblasts to macrophages. *Blood*. 1998;92(8):2940-2950.

118. Rhodes MM, Kopsombut P, Bondurant MC, Price JO, Koury MJ. Adherence to macrophages in erythroblastic islands enhances erythroblast proliferation and increases erythrocyte production by a different mechanism than erythropoietin. *Blood*. 2007;111(3):1700-1708. doi:10.1182/blood-2007-06-098178

119. Qiu C, Olivier EN, Velho M, Bouhassira EE. Globin switches in yolk sac-like primitive and fetal-like definitive red blood cells produced from human embryonic stem cells. *Blood*. 2008;111(4):2400-2408. doi:10.1182/blood-2007-07-102087

120. Chasis JA, Mohandas N. Erythroblastic islands: niches for erythropoiesis. *Blood*. 2008;112(3):470-478. doi:10.1182/blood-2008-03-077883

Bibliography

121. Socolovsky M. Exploring the erythroblastic island. *Nat Med*. 2013;19(4):399-401. doi:10.1038/nm.3156

122. Ulyanova T, Jiang Y, Padilla S, Nakamoto B, Papayannopoulou T. Combinatorial and distinct roles of 5 and 4 integrins in stress erythropoiesis in mice. *Blood*. 2011;117(3):975-985. doi:10.1182/blood-2010-05-283218

123. Hanspal M, Hanspal JS. The association of erythroblasts with macrophages promotes erythroid proliferation and maturation: A 30-kD heparin-binding protein is involved in this contact. *Blood*. 1994;84(10):3494-3504.

124. Soni S, Bala S, Gwynn B, Sahr KE, Peters LL, Hanspal M. Absence of Erythroblast Macrophage Protein (Emp) Leads to Failure of Erythroblast Nuclear Extrusion. *J Biol Chem*. 2006;281(29):20181-20189. doi:10.1074/jbc.M603226200

125. Sadahira, Yoshito; Yoshito, Tadashi; Monobe Y. Very Late Activation Antigen 4-Vascular Cell Adhesion Molecule 1 Interaction Is Involved in the Formation of Erythroblastic Islands By Yoshito Sadahira, Tadashi Yoshino,* and Yasumasa Monobe. 1995;181(January):0-4.

126. Ulyanova T, Padilla SM, Papayannopoulou T. Stage-specific functional roles of integrins in murine erythropoiesis. *Exp Hematol*. 2014;42(5):404-409.e4. doi:10.1016/j.exphem.2014.01.007

127. Lee G, Lo A, Short SA, et al. Targeted gene deletion demonstrates that the cell adhesion molecule ICAM-4 is critical for erythroblastic island formation. *Blood*. 2006;108(6):2064-2071. doi:10.1182/blood-2006-03-006759

128. Barbé E, Damoiseaux JGMC, Döpp EA, Dijkstra CD. Stromal components in rat bone marrow frozen sections compared to long-term rat bone marrow cultures. *Comp Haematol Int*. 1995;5(2):69-78. doi:10.1007/BF00638922

129. Fabriek BO, Polfliet MMJ, Vloet RPM, et al. The macrophage CD163 surface glycoprotein is an erythroblast adhesion receptor. *Blood*. 2007;109(12):5223-5229. doi:10.1182/blood-2006-08-036467

130. Rughetti A, Biffoni M, Pierelli L, et al. Regulated expression of MUC1 epithelial antigen in erythropoiesis. *Br J Haematol*. 2003;120(2):344-352. doi:10.1046/j.1365-2141.2003.04038.x

131. Chow A, Huggins M, Ahmed J, et al. CD169+ macrophages provide a niche promoting erythropoiesis under homeostasis and stress. *Nat Med*. 2013;19(4):429-436. doi:10.1038/nm.3057

132. Chow A, Lucas D, Hidalgo A, et al. Bone marrow CD169 + macrophages promote the retention of hematopoietic stem and progenitor cells in the mesenchymal stem cell niche. *J Exp Med*. 2011;208(2):261-271. doi:10.1084/jem.20101688

133. Leimberg MJ, Prus E, Konijn AM, Fibach E. Macrophages function as a ferritin iron source for cultured human erythroid precursors. *J Cell Biochem*. 2008;103(4):1211-1218. doi:10.1002/jcb.21499

134. Bessis, Marcel C.; Breton-Gorius J. Iron metabolism in the bone marrow as seen by electron microscopy; a critical review. *Blood, J Hematol*. 1962;XIX(6):635-663.

135. Leimberg JM, Konijn AM, Fibach E. Developing human erythroid cells grown in transferrin-free medium utilize iron originating from extracellular ferritin. *Am J Hematol*. 2003;73(3):211-212. doi:10.1002/ajh.10355

136. Chiabrando D, Marro S, Mercurio S, et al. The mitochondrial heme exporter FLVCR1b mediates erythroid differentiation. *J Clin Invest*. 2012;122(12):4569-4579. doi:10.1172/JCI62422

137. Mercurio S, Petrillo S, Chiabrando D, et al. The heme exporter Flvcr1 regulates expansion and differentiation of committed erythroid progenitors by controlling intracellular heme accumulation. *Haematologica*. 2015;100(6):720-729. doi:10.3324/haematol.2014.114488

Bibliography

138. Campbell MR, Karaca M, Adamski KN, Chorley BN, Wang X, Bell DA. Novel Hematopoietic Target Genes in the NRF2-Mediated Transcriptional Pathway. *Oxid Med Cell Longev*. 2013;2013:1-12. doi:10.1155/2013/120305

139. Koury, Stephen T.; Koury, Mark J.; Bondurant, Maurice C.; Caro, Jaime; Graber SE. Quantification of eythropoietin-producing cells in kidneys of mice by in situ hybridization: correlation with hematocrit, renal erythropoietin mRNA, and serum erythropoietin concentration. 1989;74(2):645-651.

140. Yoshida H, Kawane K, Koike M, Mori Y, Uchiyama Y, Nagata S. Phosphatidylserine-dependent engulfment by macrophages of nuclei from erythroid precursor cells. *Nature*. 2005;437(7059):754-758. doi:10.1038/nature03964

141. Fujiwara Y, Browne CP, Cunniff K, Goff SC, Orkin SH. Arrested development of embryonic red cell precursors in mouse embryos lacking transcription factor GATA-1. *Proc Natl Acad Sci*. 1996;93(22):12355-12358. doi:10.1073/pnas.93.22.12355

142. Eggold JT, Rankin EB. Erythropoiesis, EPO, macrophages, and bone. *Bone*. 2019;119:36-41. doi:10.1016/j.bone.2018.03.014

143. Luo B, Jiang M, Yang X, et al. Erythropoietin is a hypoxia inducible factor-induced protective molecule in experimental autoimmune neuritis. *Biochim Biophys Acta - Mol Basis Dis*. 2013;1832(8):1260-1270. doi:10.1016/j.bbadis.2013.04.015

144. Luo B, Wang J, Liu Z, et al. Phagocyte respiratory burst activates macrophage erythropoietin signalling to promote acute inflammation resolution. *Nat Commun*. 2016;7(1):12177. doi:10.1038/ncomms12177

145. Tamura T, Aoyama M, Ukai S, Kakita H, Sobue K, Asai K. Neuroprotective erythropoietin attenuates microglial activation, including morphological changes, phagocytosis, and cytokine production. *Brain Res*. 2017;1662:65-74. doi:10.1016/j.brainres.2017.02.023

146. Lifshitz L, Tabak G, Gassmann M, Mittelman M, Neumann D. Macrophages as novel target cells for erythropoietin. *Haematologica*. 2010;95(11):1823-1831. doi:10.3324/haematol.2010.025015

147. Kim J, Cha Y-N, Surh Y-J. A protective role of nuclear factor-erythroid 2-related factor-2 (Nrf2) in inflammatory disorders. *Mutat Res Mol Mech Mutagen*. 2010;690(1-2):12-23. doi:10.1016/j.mrfmmm.2009.09.007

148. Johns JL, Christopher MM. Extramedullary Hematopoiesis: A New Look at the Underlying Stem Cell Niche, Theories of Development, and Occurrence in Animals. *Vet Pathol*. 2012;49(3):508-523. doi:10.1177/0300985811432344

149. Platzbecker U, Prange-krex G, Bornhäuser M, et al. Spleen enlargement in healthy donors during G–CSF mobilization of PBPCs. 2001;41(February):184-189.

150. Crosby WH. Normal functions of the spleen relative to red blood cells: a review. *Am Soc Hematol*. 1958:399-408.

151. Jacobsen RN, Forristal CE, Raggatt LJ, et al. Mobilization with granulocyte colony-stimulating factor blocks medullar erythropoiesis by depleting F4/80+VCAM1+CD169+ER-HR3+Ly6G+ erythroid island macrophages in the mouse. *Exp Hematol*. 2014;42(7):547-561.e4. doi:10.1016/j.exphem.2014.03.009

152. Morrison SJ, Shah NM, Anderson DJ. Regulatory Mechanisms in Stem Cell Biology. *Cell*. 1997;88(3):287-298. doi:10.1016/S0092-8674(00)81867-X

153. Olefsky JM. Nuclear Receptor Minireview Series. *J Biol Chem*. 2001;276(40):36863-36864. doi:10.1074/jbc.R100047200

154. Glass CK, Ogawa S. Combinatorial roles of nuclear receptors in inflammation and immunity. *Nat Rev*

Immunol. 2006;6(1):44-55. doi:10.1038/nri1748

155. Willy PJ, Umesono K, Ong ES, Evans RM, Heyman RA, Mangelsdorf DJ. LXR, a nuclear receptor that defines a distinct retinoid response pathway. *Genes Dev*. 1995;9(9):1033-1045. doi:10.1101/gad.9.9.1033

156. Umesono K, Murakami KK, Thompson CC, Evans RM. Direct repeats as selective response elements for the thyroid hormone, retinoic acid, and vitamin D3 receptors. *Cell*. 1991;65(7):1255-1266. doi:10.1016/0092-8674(91)90020-Y

157. Glass CK, Saijo K. Nuclear receptor transrepression pathways that regulate inflammation in macrophages and T cells. *Nat Rev Immunol*. 2010;10(5):365-376. doi:10.1038/nri2748

158. Ghisletti S, Huang W, Ogawa S, et al. Parallel SUMOylation-Dependent Pathways Mediate Gene- and Signal-Specific Transrepression by LXRs and PPARγ. *Mol Cell*. 2007;25(1):57-70. doi:10.1016/j.molcel.2006.11.022

159. Pascual G, Fong AL, Ogawa S, et al. A SUMOylation-dependent pathway mediates transrepression of inflammatory response genes by PPAR-γ. *Nature*. 2005;437(7059):759-763. doi:10.1038/nature03988

160. Apfel R, Benbrook D, Lernhardt E, Ortiz MA, Salbert G, Pfahl M. A novel orphan receptor specific for a subset of thyroid hormone-responsive elements and its interaction with the retinoid/thyroid hormone receptor subfamily. *Mol Cell Biol*. 1994;14(10):7025-7035. doi:10.1128/MCB.14.10.7025

161. Teboul M, Enmark E, Li Q, Wikstrom AC, Pelto-Huikko M, Gustafsson JA. OR-1, a member of the nuclear receptor superfamily that interacts with the 9-cis-retinoic acid receptor. *Proc Natl Acad Sci*. 1995;92(6):2096-2100. doi:10.1073/pnas.92.6.2096

162. Viennois E, Mouzat K, Dufour J, Morel L, Lobaccaro J-M, Baron S. Selective liver X receptor modulators (SLiMs): What use in human health? *Mol Cell Endocrinol*. 2012;351(2):129-141. doi:10.1016/j.mce.2011.08.036

163. Zuercher WJ, Buckholz RG, Campobasso N, et al. Discovery of Tertiary Sulfonamides as Potent Liver X Receptor Antagonists. *J Med Chem*. 2010;53(8):3412-3416. doi:10.1021/jm901797p

164. Hong C, Tontonoz P. Coordination of inflammation and metabolism by PPAR and LXR nuclear receptors. *Curr Opin Genet Dev*. 2008;18(5):461-467. doi:10.1016/j.gde.2008.07.016

165. Repa JJ, Mangelsdorf DJ. The Role of Orphan Nuclear Receptors in the Regulation of Cholesterol Homeostasis. *Annu Rev Cell Dev Biol*. 2000;16(1):459-481. doi:10.1146/annurev.cellbio.16.1.459

166. Janowski, Bethany A.; Willy, Patricia J.; Devi, Thota Rama; Falck, J. R.; Mangelsdorf DJ. An oxysterol signalling pathway mediated by the nuclear receptor LXR alpha. 1996:728-731.

167. Lehmann JM, Kliewer SA, Moore LB, et al. Activation of the Nuclear Receptor LXR by Oxysterols Defines a New Hormone Response Pathway. *J Biol Chem*. 1997;272(6):3137-3140. doi:10.1074/jbc.272.6.3137

168. Peet DJ, Turley SD, Ma W, et al. Cholesterol and Bile Acid Metabolism Are Impaired in Mice Lacking the Nuclear Oxysterol Receptor LXRalpha. *Cell Press*. 1998;93:693-704.

169. Castrillo A, Tontonoz P. NUCLEAR RECEPTORS IN MACROPHAGE BIOLOGY: At the Crossroads of Lipid Metabolism and Inflammation. *Annu Rev Cell Dev Biol*. 2004;20(1):455-480. doi:10.1146/annurev.cellbio.20.012103.134432

170. Venkateswaran A, Laffitte BA, Joseph SB, et al. Control of cellular cholesterol efflux by the nuclear oxysterol receptor LXRalpha. *Proc Natl Acad Sci*. 2000;97(22):12097-12102. doi:10.1073/pnas.200367697

Bibliography

171. Repa JJ, Berge KE, Pomajzl C, Richardson JA, Hobbs H, Mangelsdorf DJ. Regulation of ATP-binding Cassette Sterol Transporters ABCG5 and ABCG8 by the Liver X Receptors α and β. *J Biol Chem*. 2002;277(21):18793-18800. doi:10.1074/jbc.M109927200

172. Laffitte BA, Joseph SB, Walczak R, et al. Autoregulation of the Human Liver X Receptor alpha Promoter. *Mol Cell Biol*. 2001;21(22):7558-7568. doi:10.1128/MCB.21.22.7558-7568.2001

173. Mak PA, Laffitte BA, Desrumaux C, et al. Regulated Expression of the Apolipoprotein E/C-I/C-IV/C-II Gene Cluster in Murine and Human Macrophages. *J Biol Chem*. 2002;277(35):31900-31908. doi:10.1074/jbc.M202993200

174. Schultz JR. Role of LXRs in control of lipogenesis. *Genes Dev*. 2000;14(22):2831-2838. doi:10.1101/gad.850400

175. Zelcer N, Hong C, Boyadjian R, Tontonoz P. LXR Regulates Cholesterol Uptake Through Idol-Dependent Ubiquitination of the LDL Receptor. *Science (80-)*. 2009;325(5936):100-104. doi:10.1126/science.1168974

176. Calkin AC, Tontonoz P. Transcriptional integration of metabolism by the nuclear sterol-activated receptors LXR and FXR. *Nat Rev Mol Cell Biol*. 2012;13(4):213-224. doi:10.1038/nrm3312

177. Repa JJ, Liand G, Ou J, et al. Regulation of mouse sterol regulatory element-binding protein-1c gene (SREBP-1c) by oxysterol receptors, LXRalpha and LXRbeta. *Genes Dev*. 2000;14(22):2819-2830. doi:10.1101/gad.844900

178. Joseph SB, Laffitte BA, Patel PH, et al. Direct and Indirect Mechanisms for Regulation of Fatty Acid Synthase Gene Expression by Liver X Receptors. *J Biol Chem*. 2002;277(13):11019-11025. doi:10.1074/jbc.M111041200

179. Tangirala RK, Bischoff ED, Joseph SB, et al. Identification of macrophage liver X receptors as inhibitors of atherosclerosis. *Proc Natl Acad Sci*. 2002;99(18):11896-11901. doi:10.1073/pnas.182199799

180. Schuster GU, Parini P, Wang L, et al. Accumulation of Foam Cells in Liver X Receptor-Deficient Mice. *Circulation*. 2002;106(9):1147-1153. doi:10.1161/01.CIR.0000026802.79202.96

181. Calkin AC, Tontonoz P. Liver X Receptor Signaling Pathways and Atherosclerosis. *Arterioscler Thromb Vasc Biol*. 2010;30(8):1513-1518. doi:10.1161/ATVBAHA.109.191197

182. Terasaka N, Hiroshima A, Koieyama T, et al. T-0901317, a synthetic liver X receptor ligand, inhibits development of atherosclerosis in LDL receptor-deficient mice. *FEBS Lett*. 2003;536(1-3):6-11. doi:10.1016/S0014-5793(02)03578-0

183. Bradley MN, Hong C, Chen M, et al. Ligand activation of LXRβ reverses atherosclerosis and cellular cholesterol overload in mice lacking LXRα and apoE. *J Clin Invest*. 2007;117(8):2337-2346. doi:10.1172/JCI31909

184. Bischoff ED, Daige CL, Petrowski M, et al. Non-redundant roles for LXR and LXR in atherosclerosis susceptibility in low density lipoprotein receptor knockout mice. *J Lipid Res*. 2010;51(5):900-906. doi:10.1194/jlr.M900096

185. Teupser D, Persky AD, Breslow JL. Induction of Atherosclerosis by Low-Fat, Semisynthetic Diets in LDL Receptor–Deficient C57BL/6J and FVB/NJ Mice. *Arterioscler Thromb Vasc Biol*. 2003;23(10):1907-1913. doi:10.1161/01.ATV.0000090126.34881.B1

186. Joseph SB, Castrillo A, Laffitte BA, Mangelsdorf DJ, Tontonoz P. Reciprocal regulation of inflammation and lipid metabolism by liver X receptors. *Nat Med*. 2003;9(2):213-219. doi:10.1038/nm820

187. Castrillo A, Joseph SB, Marathe C, Mangelsdorf DJ, Tontonoz P. Liver X Receptor-dependent

Repression of Matrix Metalloproteinase-9 Expression in Macrophages. *J Biol Chem*. 2003;278(12):10443-10449. doi:10.1074/jbc.M213071200

188. Terasaka N, Hiroshima A, Ariga A, et al. Liver X receptor agonists inhibit tissue factor expression in macrophages. *FEBS J*. 2005;272(6):1546-1556. doi:10.1111/j.1742-4658.2005.04599.x

189. Fowler AJ, Sheu MY, Schmuth M, et al. Liver X Receptor Activators Display Anti-Inflammatory Activity in Irritant and Allergic Contact Dermatitis Models: Liver-X-Receptor-Specific Inhibition of Inflammation and Primary Cytokine Production. *J Invest Dermatol*. 2003;120(2):246-255. doi:10.1046/j.1523-1747.2003.12033.x

190. Zelcer N, Khanlou N, Clare R, et al. Attenuation of neuroinflammation and Alzheimer's disease pathology by liver x receptors. *Proc Natl Acad Sci*. 2007;104(25):10601-10606. doi:10.1073/pnas.0701096104

191. Joseph SB, Bradley MN, Castrillo A, et al. LXR-Dependent Gene Expression Is Important for Macrophage Survival and the Innate Immune Response. *Cell*. 2004;119(2):299-309. doi:10.1016/j.cell.2004.09.032

192. Korf H, Vander Beken S, Romano M, et al. Liver X receptors contribute to the protective immune response against Mycobacterium tuberculosis in mice. *J Clin Invest*. 2009;119(6):1626-1637. doi:10.1172/JCI35288

193. Castrillo A, Joseph SB, Vaidya SA, et al. Crosstalk between LXR and Toll-like Receptor Signaling Mediates Bacterial and Viral Antagonism of Cholesterol Metabolism. *Mol Cell*. 2003;12(4):805-816. doi:10.1016/S1097-2765(03)00384-8

194. Muñoz LE, Lauber K, Schiller M, Manfredi AA, Herrmann M. The role of defective clearance of apoptotic cells in systemic autoimmunity. *Nat Rev Rheumatol*. 2010;6(5):280-289. doi:10.1038/nrrheum.2010.46

195. A-Gonzalez N, Quintana JA, García-Silva S, et al. Phagocytosis imprints heterogeneity in tissue-resident macrophages. *J Exp Med*. 2017;214(5):1281-1296. doi:10.1084/jem.20161375

196. A-Gonzalez N, Bensinger SJ, Hong C, et al. Apoptotic Cells Promote Their Own Clearance and Immune Tolerance through Activation of the Nuclear Receptor LXR. *Immunity*. 2009;31(2):245-258. doi:10.1016/j.immuni.2009.06.018

197. Lemke G, Burstyn-Cohen T. TAM receptors and the clearance of apoptotic cells. *Ann N Y Acad Sci*. 2010;1209(1):23-29. doi:10.1111/j.1749-6632.2010.05744.x

198. Baranska A, Shawket A, Jouve M, et al. Unveiling skin macrophage dynamics explains both tattoo persistence and strenuous removal. *J Exp Med*. 2018;215(4):1115-1133. doi:10.1084/jem.20171608

199. Meredith MM, Liu K, Darrasse-Jeze G, et al. Expression of the zinc finger transcription factor zDC (Zbtb46, Btbd4) defines the classical dendritic cell lineage. *J Exp Med*. 2012;209(6):1153-1165. doi:10.1084/jem.20112675

200. Saito M, Iwawaki T, Taya C, et al. Diphtheria toxin receptor–mediated conditional and targeted cell ablation in transgenic mice. *Nat Biotechnol*. 2001;19(8):746-750. doi:10.1038/90795

201. Liu J, Zhang J, Ginzburg Y, et al. Quantitative analysis of murine terminal erythroid differentiation in vivo:novelmethod to study normal and disordered erythropoiesis. *Blood*. 2013;121(8):43-50. doi:10.1182/blood-2012- 09-456079

202. Wang B, Tontonoz P. Liver X receptors in lipid signalling and membrane homeostasis. *Nat Rev Endocrinol*. 2018;14(8):452-463. doi:10.1038/s41574-018-0037-x

203. Ramón-Vázquez A, de la Rosa JV, Tabraue C, et al. Common and Differential Transcriptional Actions of Nuclear Receptors Liver X Receptors α and β in Macrophages. *Mol Cell Biol*. 2019;39(5):e00376-18. doi:10.1128/MCB.00376-18

Bibliography

204. Teupser D, Kretzschmar D, Tennert C, et al. Effect of Macrophage Overexpression of Murine Liver X Receptor -α (LXR -α) on Atherosclerosis in LDL-Receptor Deficient Mice. *Arterioscler Thromb Vasc Biol*. 2008;28(11):2009-2015. doi:10.1161/ATVBAHA.108.175257

205. van Furth R. The origin and kinetics of mononuclear phagocytes. *J Exp Med*. 1968;128(3):415-435. doi:10.1084/jem.128.3.415

206. Scott CL, T'Jonck W, Martens L, et al. The Transcription Factor ZEB2 Is Required to Maintain the Tissue-Specific Identities of Macrophages. *Immunity*. 2018;49(2):312-325.e5. doi:10.1016/j.immuni.2018.07.004

207. Fainaru O, Woolf E, Lotem J, et al. Runx3 regulates mouse TGF-β-mediated dendritic cell function and its absence results in airway inflammation. *EMBO J*. 2004;23(4):969-979. doi:10.1038/sj.emboj.7600085

208. Okabe Y, Medzhitov R. Tissue-Specific Signals Control Reversible Program of Localization and Functional Polarization of Macrophages. *Cell*. 2014;157(4):832-844. doi:10.1016/j.cell.2014.04.016

209. Schneider C, Nobs SP, Heer AK, et al. Alveolar Macrophages Are Essential for Protection from Respiratory Failure and Associated Morbidity following Influenza Virus Infection. Pekosz A, ed. *PLoS Pathog*. 2014;10(4):e1004053. doi:10.1371/journal.ppat.1004053

210. Chawla A, Barak Y, Nagy L, Liao D, Tontonoz P, Evans RM. PPAR-γ dependent and independent effects on macrophage-gene expression in lipid metabolism and inflammation. *Nat Med*. 2001;7(1):48-52. doi:10.1038/83336

211. Theurl I, Hilgendorf I, Nairz M, et al. On-demand erythrocyte disposal and iron recycling requires transient macrophages in the liver. *Nat Med*. 2016;22(8):945-951. doi:10.1038/nm.4146

212. Marathe C, Bradley MN, Hong C, et al. The Arginase II Gene Is an Anti-inflammatory Target of Liver X Receptor in Macrophages. *J Biol Chem*. 2006;281(43):32197-32206. doi:10.1074/jbc.M605237200

213. Repsold L, Joubert AM. Eryptosis: An Erythrocyte's Suicidal Type of Cell Death. *Biomed Res Int*. 2018;2018:1-10. doi:10.1155/2018/9405617

214. Schaer DJ, Vinchi F, Ingoglia G, Tolosano E, Buehler PW. Haptoglobin, hemopexin, and related defense pathwaysâ€"basic science, clinical perspectives, and drug development. *Front Physiol*. 2014;5(October):1-13. doi:10.3389/fphys.2014.00415

215. Moller HJ, Peterslund NA, Graversen JH, Moestrup SK. Identification of the hemoglobin scavenger receptor/CD163 as a natural soluble protein in plasma. *Blood*. 2002;99(1):378-380. doi:10.1182/blood.V99.1.378

216. Moreno JA, Muñoz-García B, Martín-Ventura JL, et al. The CD163-expressing macrophages recognize and internalize TWEAK. *Atherosclerosis*. 2009;207(1):103-110. doi:10.1016/j.atherosclerosis.2009.04.033

217. Fabriek BO, van Bruggen R, Deng DM, et al. The macrophage scavenger receptor CD163 functions as an innate immune sensor for bacteria. *Blood*. 2009;113(4):887-892. doi:10.1182/blood-2008-07-167064

218. Sulahian TH, Högger P, Wahner AE, et al. HUMAN MONOCYTES EXPRESS CD163, WHICH IS UPREGULATED BY IL-10 AND IDENTICAL TO p155. *Cytokine*. 2000;12(9):1312-1321. doi:10.1006/cyto.2000.0720

219. Etzerodt A, Kjolby M, Nielsen MJ, Maniecki M, Svendsen P, Moestrup SK. Plasma Clearance of Hemoglobin and Haptoglobin in Mice and Effect of CD163 Gene Targeting Disruption. *Antioxid Redox Signal*. 2013;18(17):2254-2263. doi:10.1089/ars.2012.4605

220. Xie Y, Hou W, Song X, et al. Ferroptosis: process and function. *Cell Death Differ*. 2016;23(3):369-379. doi:10.1038/cdd.2015.158

Bibliography

221. Takeda T, Mu A, Tai TT, Kitajima S, Taketani S. Continuous de novo biosynthesis of haem and its rapid turnover to bilirubin are necessary for cytoprotection against cell damage. *Sci Rep*. 2015;5(1):10488. doi:10.1038/srep10488

222. Taketani S. Aquisition, Mobilization and Utilization of Cellular Iron and Heme: Endless Findings and Growing Evidence of Tight Regulation. *Tohoku J Exp Med*. 2005;205(4):297-318. doi:10.1620/tjem.205.297

223. Dowdle WE, Nyfeler B, Nagel J, et al. Selective VPS34 inhibitor blocks autophagy and uncovers a role for NCOA4 in ferritin degradation and iron homeostasis in vivo. *Nat Cell Biol*. 2014;16(11):1069-1079. doi:10.1038/ncb3053

224. Mancias JD, Pontano Vaites L, Nissim S, et al. Ferritinophagy via NCOA4 is required for erythropoiesis and is regulated by iron dependent HERC2-mediated proteolysis. *Elife*. 2015;4(OCTOBER2015):1-19. doi:10.7554/eLife.10308

225. Bellelli R, Federico G, Matte' A, et al. NCOA4 Deficiency Impairs Systemic Iron Homeostasis. *Cell Rep*. 2016;14(3):411-421. doi:10.1016/j.celrep.2015.12.065

226. Goforth JB, Anderson SA, Nizzi CP, Eisenstein RS. Multiple determinants within iron-responsive elements dictate iron regulatory protein binding and regulatory hierarchy. *RNA*. 2010;16(1):154-169. doi:10.1261/rna.1857210

227. Sadahira Y, Mori M, Kimoto T. Isolation and short-term culture of mouse splenic erythroblastic islands. *Cell Struct Funct*. 1990;15(1):59-65. doi:10.1247/csf.15.59

228. Sadahira Y, Yasuda T, Yoshino T, et al. Impaired splenic erythropoiesis in phlebotomized mice injected with CL2MDP-liposome: An experimental model for studying the role of stromal macrophages in erythropoiesis. *J Leukoc Biol*. 2000;68(4):464-470. doi:10.1189/jlb.68.4.464

229. Koka S, Föller M, Lamprecht G, et al. Iron deficiency influences the course of malaria in Plasmodium berghei infected mice. *Biochem Biophys Res Commun*. 2007;357(3):608-614. doi:10.1016/j.bbrc.2007.03.175

230. Ramos P, Casu C, Gardenghi S, et al. Macrophages support pathological erythropoiesis in polycythemia vera and β-thalassemia. *Nat Med*. 2013;19(4):437-445. doi:10.1038/nm.3126